Physical and Electrochemical Properties of Molten LiCl-KCl Salt for Used Fuel Reprocessing

Sean Martin

Dr. Kumar Sridharan (PI), Prof. Todd Allen, Mehran Mohammadian, Jacob Sager, and Dr. Mike Simpson

Contact email: kumar@engr.wisc.edu

2012 International Pyroprocessing Research Conference

Fontana, WI

August 28th, 2012

DEPARTMENT OF Engineering Physics

College of Engineering University of Wisconsin-Madison

Presentation Outline

- Research Motivation
- Electrochemistry ($LaCl_3$, $CeCl_3$, $NdCl_3$, $DyCl_3$, and UCl_3)
  - Experimental Setup
  - Results
- Melting Point Measurements ($LaCl_3$, $CeCl_3$, $NdCl_3$)
  - Differential Scanning Calorimetry
  - Phase Diagrams
- Molten Salt Density Measurements ($LaCl_3$, $CeCl_3$, $NdCl_3$)
- Conclusions

Research Motivation

- What is the concentration of a given element in the molten LiCl-KCl salt at any point during the electrorefining process?
  - Online monitoring using an electrochemical probe
- At what point does the salt need to disposed of or cleaned?
  - How does metal chloride concentration affect the melting point of the electrorefiner salt (500°C operating temperature)
- What is the mass of salt remaining in the electrorefiner after fuel processing is complete?
  - How does metal chloride concentration affect the density of the electrorefiner salt
- Can the separation processes be further optimized to increase the throughput of the electrorefiner?
  - Electrochemical analysis of thermodynamic, transport, and deposition behavior of metal chlorides

Electrochemistry

Chemicals

- LiCl-KCl (55.8 mol% - 44.2 mol%) salt was obtained from INL
- Lanthanide Chloride Concentration Studies
  - $LaCl_3$, $CeCl_3$, $NdCl_3$, and $DyCl_3$ (99.9+%)
- Depleted uranium (III) chloride additions studied at INL

Crushed salt in mason jar

Desiccators

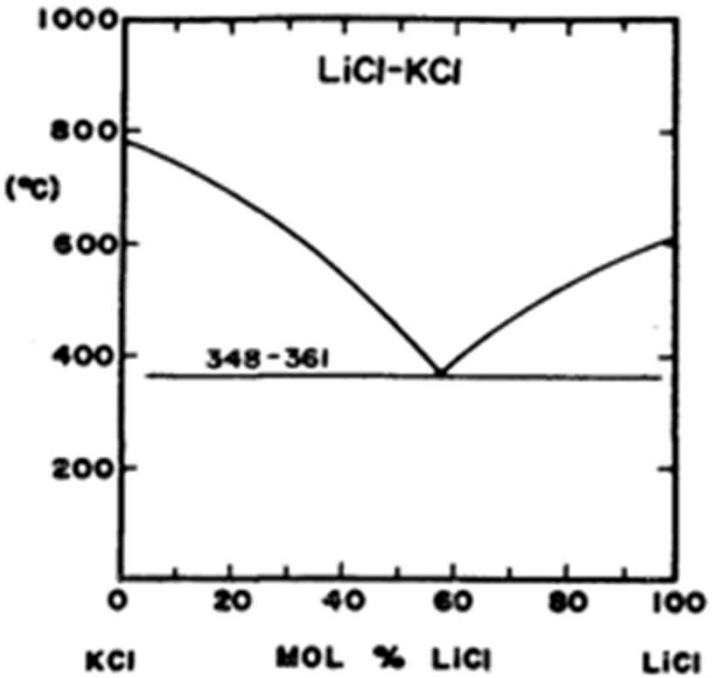

Electrochemistry Equipment - UW

DEPARTMENT OF
Engineering Physics
College of Engineering
University of Wisconsin-Madison

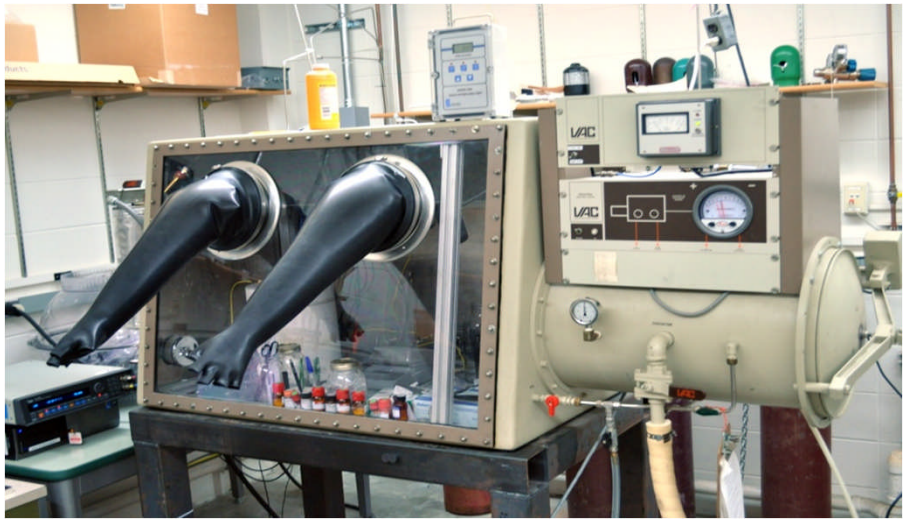

Electrochemistry glovebox

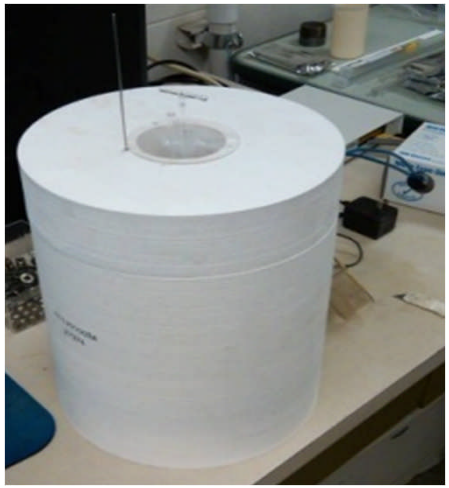

Heater

O_2 meter

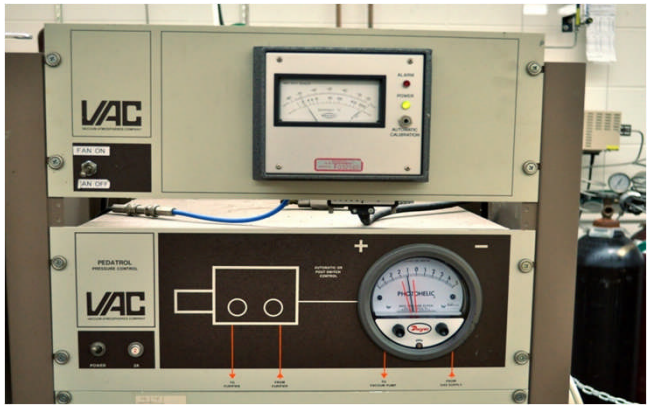

Pressure control system and moisture meter

Potentiostat

Electrochemistry Equipment - INL

Electrochemistry Glovebox

O_2 and H_2O monitoring

Furnace

Located in radiochemistry laboratory at the Center for Advanced Energy Studies (CAES)

Electrochemical Cell Materials

- 3-electrode electrochemical cell, which consists of the following:

Electrode configuration for this work	
Electrode	**Material/Description**
Working Electrode (WE)	2.0 mm 99.95% Tungsten rod
Reference Electrode (RE)	1.0 mm Silver wire in 5 mol% Ag^{+}|Ag solution
Counter Electrode (CE)	3.0 mm glassy carbon rod in contact with the glassy carbon crucible

Crucible	Material Detail	Purpose in electrochemical cell
Glassy Carbon	SIGRADUR GAT19 99.95% Pure	Holds LiCl-KCl eutectic melt for electrochemical measurements
Alumina	99.8% Alumina	Provides a thermal barrier between glassy carbon and stainless steel
Stainless Steel	Grade 316	Welded wire creates a Faraday cage to reduce electronic noise

Electrochemical Setup

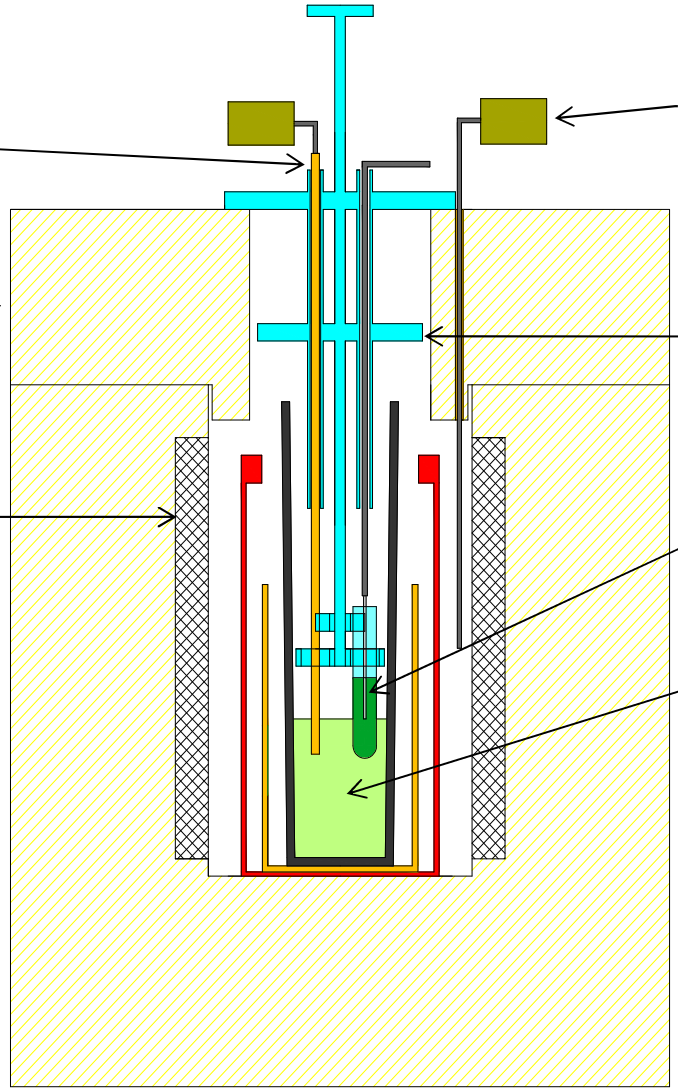

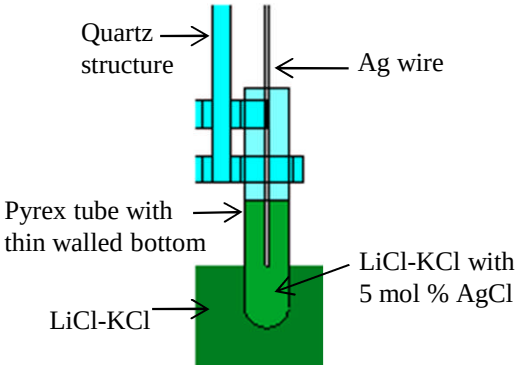

Electrochemical Setup

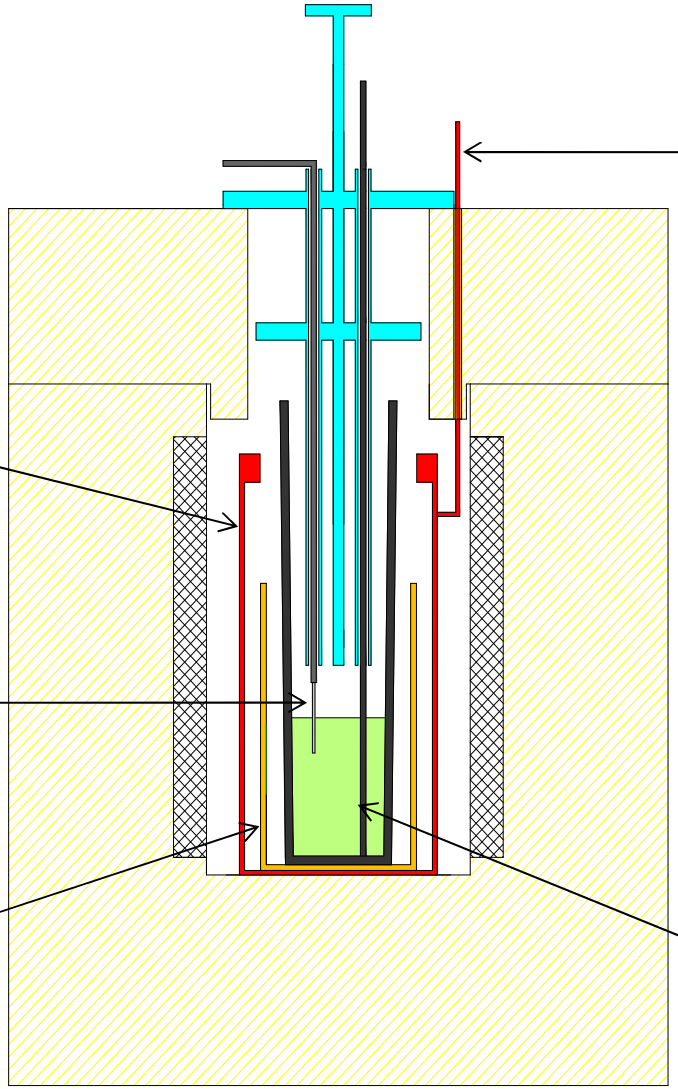

Faraday cage ground for potentiostat

Stainless steel crucible and Faraday cage, grounded to potentiostat ground

Tungsten WE

Alumina secondary crucible

Glassy Carbon CE rod touches GC crucible

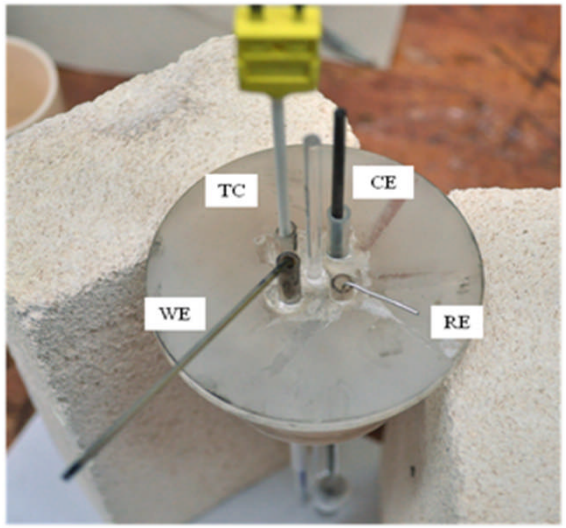

Data Analysis

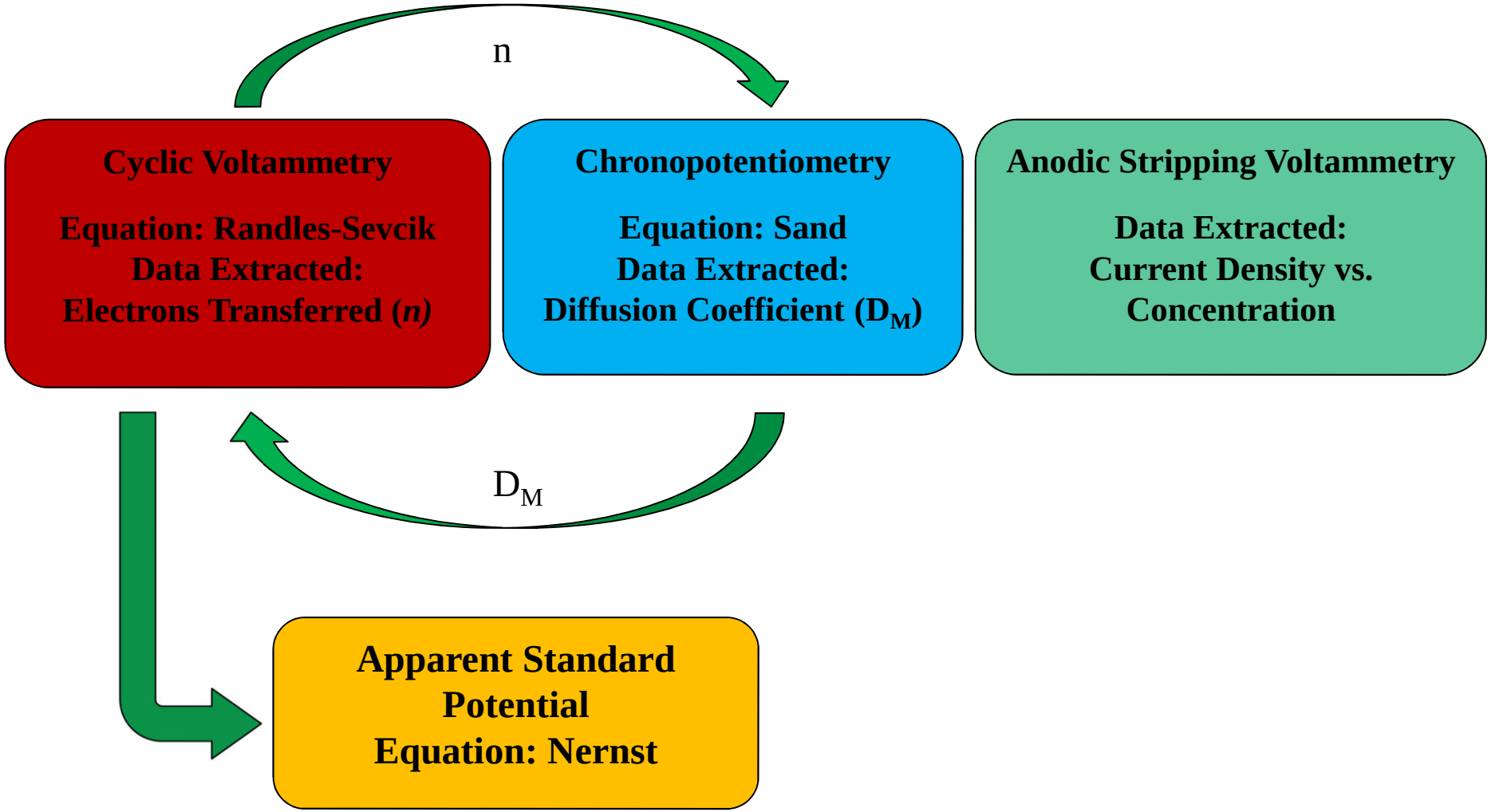

Cyclic Voltammetry

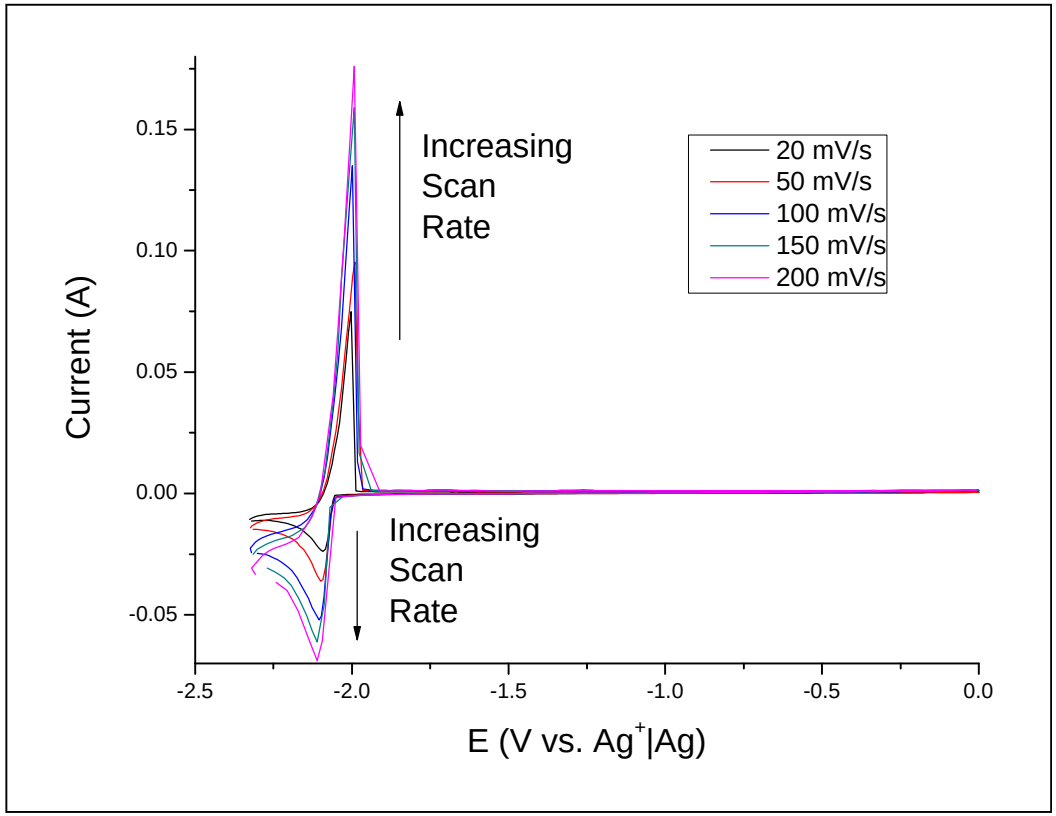

Cyclic voltammograms of 0.99 wt% $LaCl_3$ (X_{LaCl3} =2.27x10^{-3}) in LiCl-KCl with scan rates: 20, 50, 100, 150, and 200 mV/s.

$$\frac{I_{p,c}}{\sqrt{\nu}} = 0.446(nF)^{\frac{3}{2}}(RT)^{-1/2}C_{M^{n+}}D^{1/2}S$$

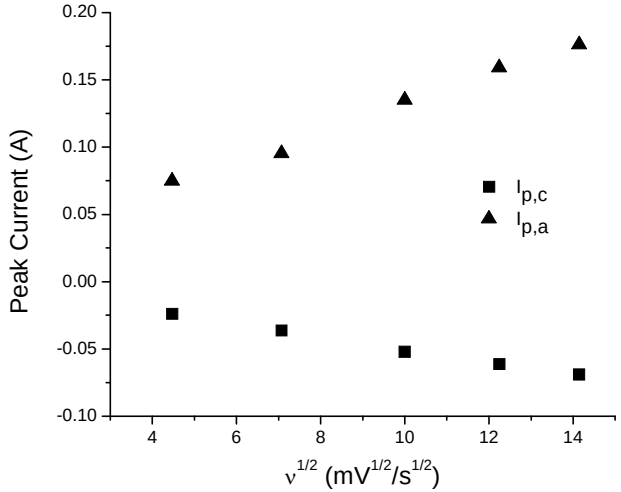

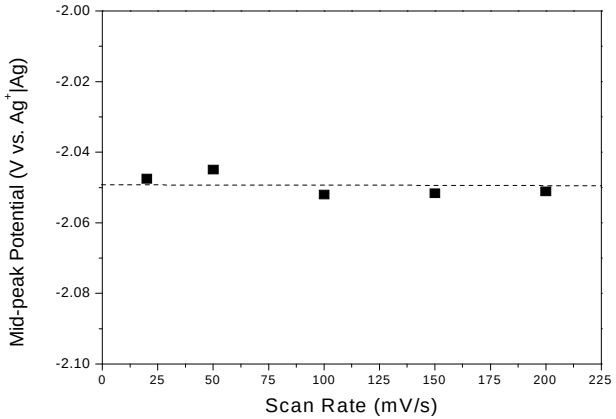

Cyclic Voltammetry

- $LaCl_3$, $CeCl_3$, $NdCl_3$, and $DyCl_3$ investigated at concentrations from 0.1-8 wt%. UCl_3 was investigated at 1 wt%.
- CV was used to determine reversibility and confirm reaction mechanism.

Compound	Reaction Mechanism	Reversibility
$LaCl_3$	$La(III) + 3e^- \leftrightarrow La$	Reversible
$CeCl_3$	$Ce(III) + 3e^- \leftrightarrow Ce$	Reversible
$NdCl_3$	$Nd(III) + e^- \leftrightarrow Nd(II)$ $Nd(II) + 2e^- \leftrightarrow Nd$	Reversible
$DyCl_3$	$Dy(III) + 3e^- \leftrightarrow Dy$	Reversible
UCl_3	$U(IIII) + e^- \leftrightarrow U(III)$ $U(III) + 3e^- \leftrightarrow U$	Reversible Quasi-reversible

Apparent Standard Potentials of $LnCl_x$ in LiCl-KCl at 500°C

DEPARTMENT OF
Engineering Physics
College of Engineering
University of Wisconsin-Madison

Nernst Plot

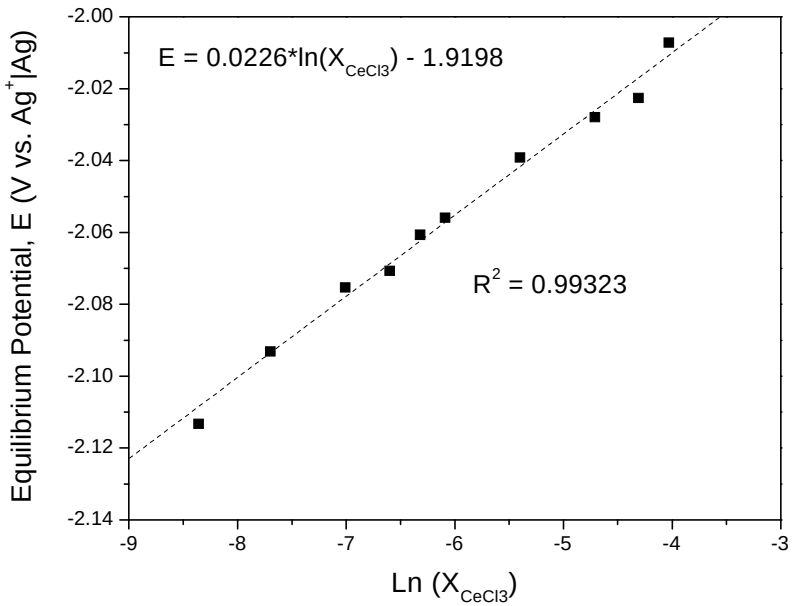

Apparent standard potentials of $LnCl_3$ in LiCl-KCl at 500°C.

Redox Couple	**vs. Ag^+|Ag (V)**	**vs. Cl^-|Cl_2 (V)**	**Lit. vs. Cl^-|Cl_2 (V) ** = 450°C**
La^{3+}|La	-1.959	-3.106	-3.146 **
Ce^{3+}|Ce	-1.920	-3.066	-3.085
Nd^{2+}|Nd	-1.187	-2.964	-3.073**
Nd^{3+}|Nd	-1.935	-3.081	-3.113**
Dy^{3+}|Dy	-1.958	-3.104	-3.150**

Nernst Equation:

$$E_{MCl_x} = \boxed{E^{0\prime}_{MCl_x}} + \frac{RT}{nF} \ln X_{MCl_x}$$

y-intercept

Chronopotentiometry

For a reversible system: $i\sqrt{\tau} = \frac{nF\,C_{M^{n+}}A\sqrt{\pi D_{M^{n+}}}}{2}$ = Constant

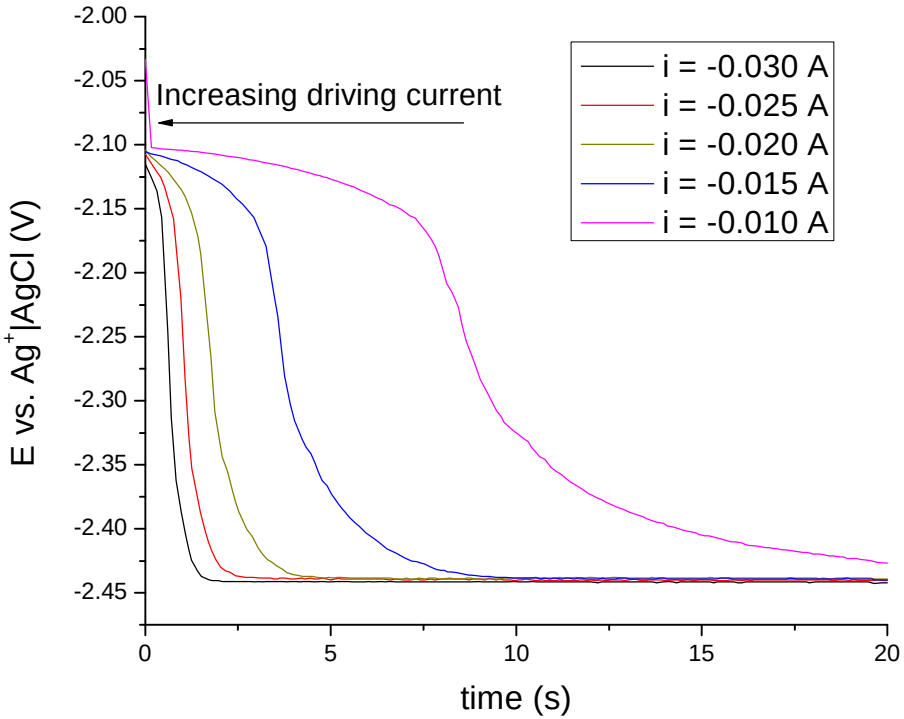

Typical chronopotentiograms of the $LaCl_3$-LiCl-KCl system. Data from $LaCl_3$-LiCl-KCl with $LaCl_3$ concentration of 0.59 wt% (X_{LaCl3} = 1.36x10^{-3}).

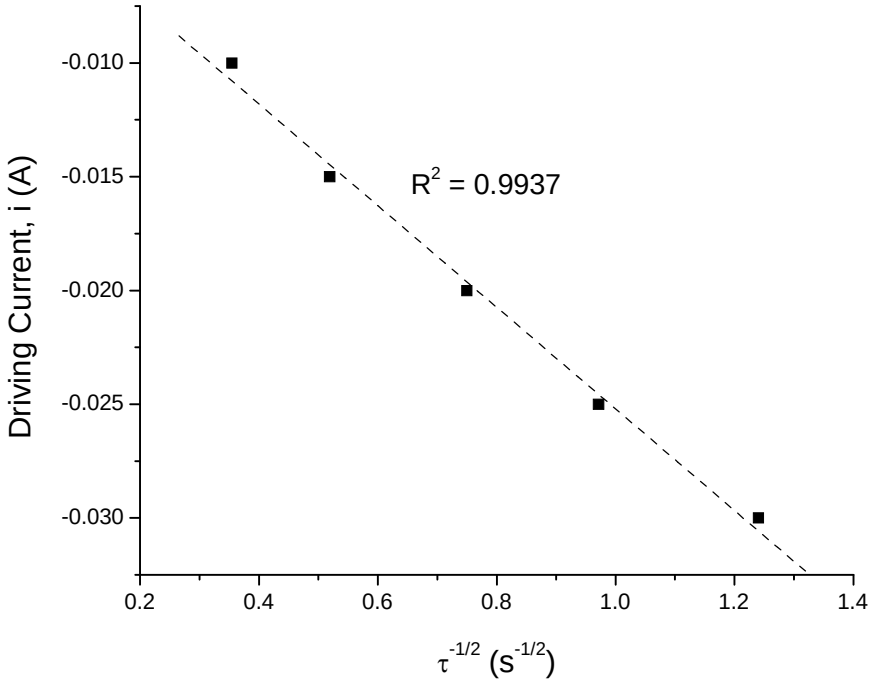

Linear dependency of driving current on t $^{-1/2}$ evidencing reversibility of $LaCl_3$-LiCl-KCl with $LaCl_3$ concentration of 0.59 wt% (X_{LaCl3} = 1.36x10^{-3}).

Dysprosium Ion Diffusion Coefficient

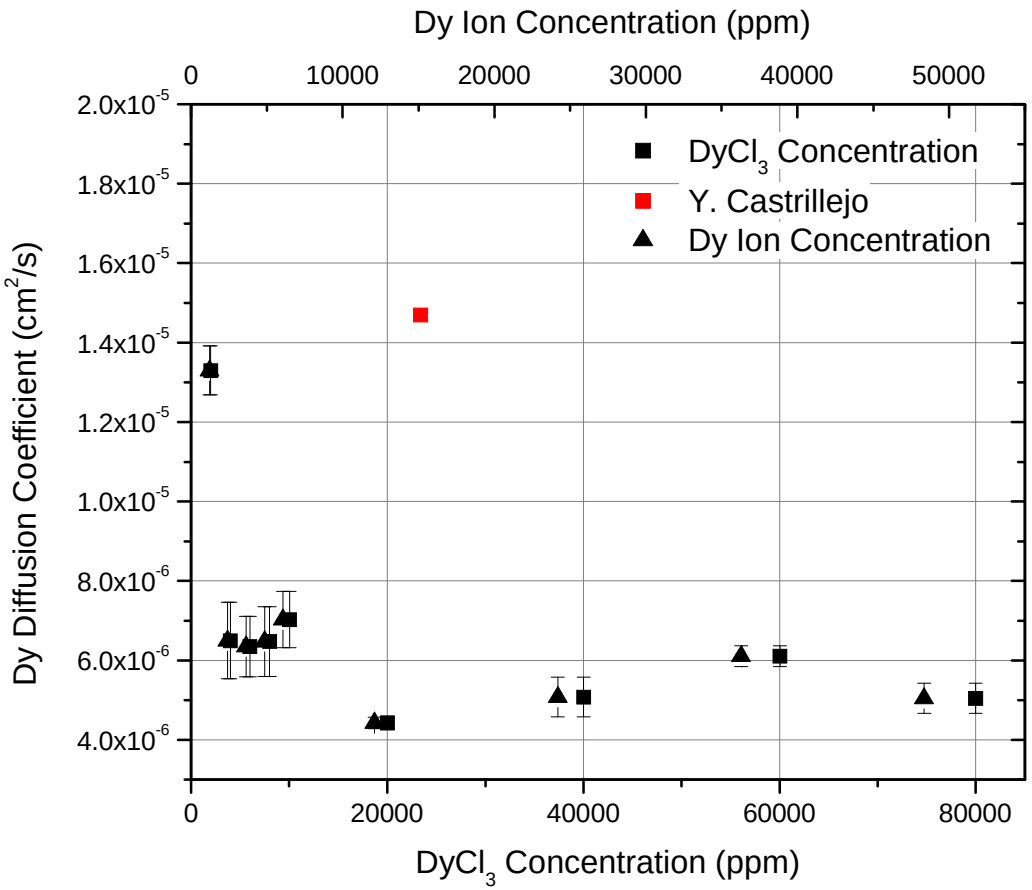

- CP Parameters:
  - 20s @ I = 0A (Equilibrium)
  - 20s @ I = I_d
  - I_d varied for each concentration
  - Diffusion coefficient calculated with the Sand equation for each I_d
  - Average of these diffusion coefficients was plotted
  - Standard deviation used as error

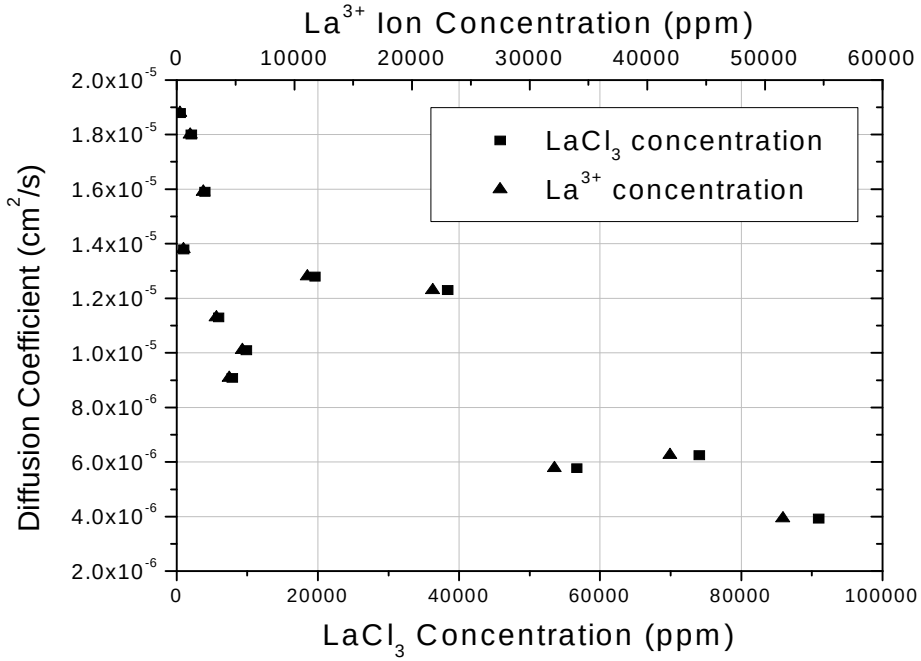

- Similar trends seen with $LaCl_3$, $NdCl_3$, and $CeCl_3$
- Diffusion coefficient drops off inversely with lanthanide chloride concentration
- Possibly due to increasing cation interaction (like charges repelling)

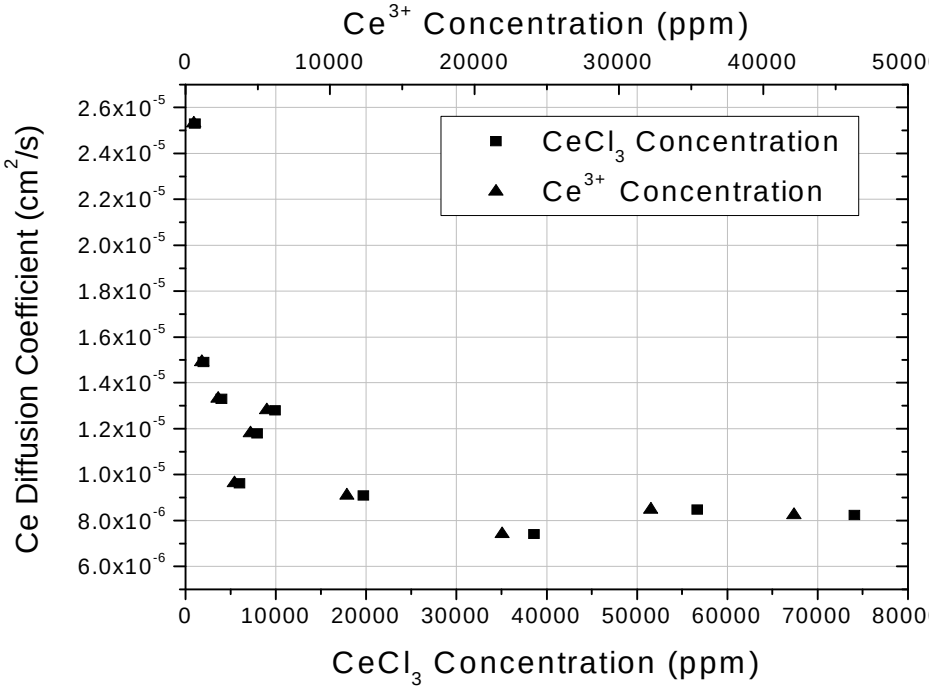

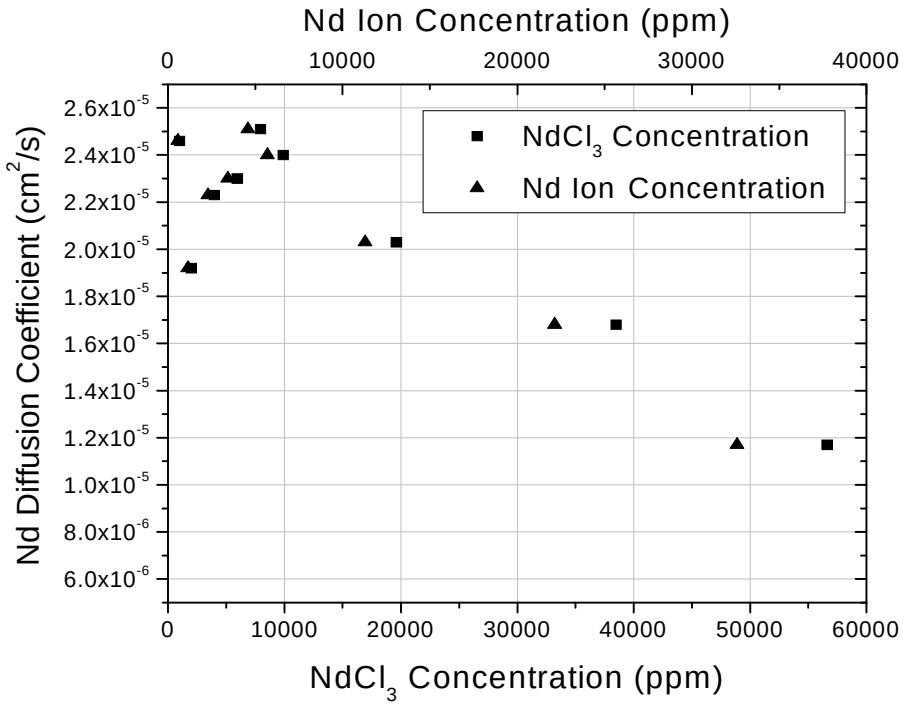

Uranium Ion Diffusion Coefficient

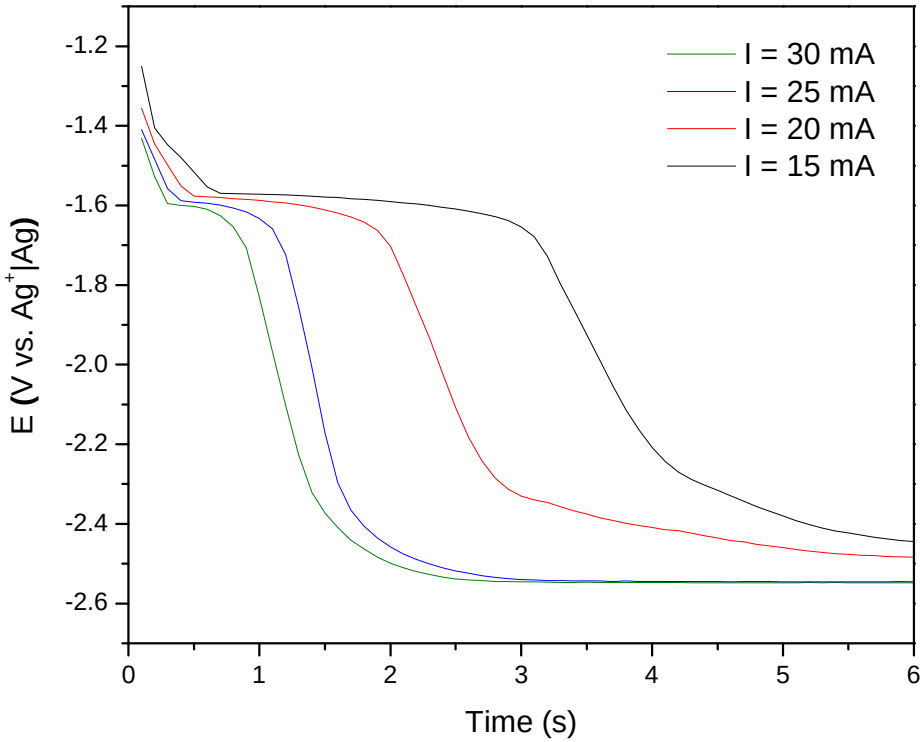

Chronopotentiograms obtained from the UCl_3-LiCl-KCl salt (1 wt% UCl_3) for driving currents of 15, 20, 25, and 30 mA.

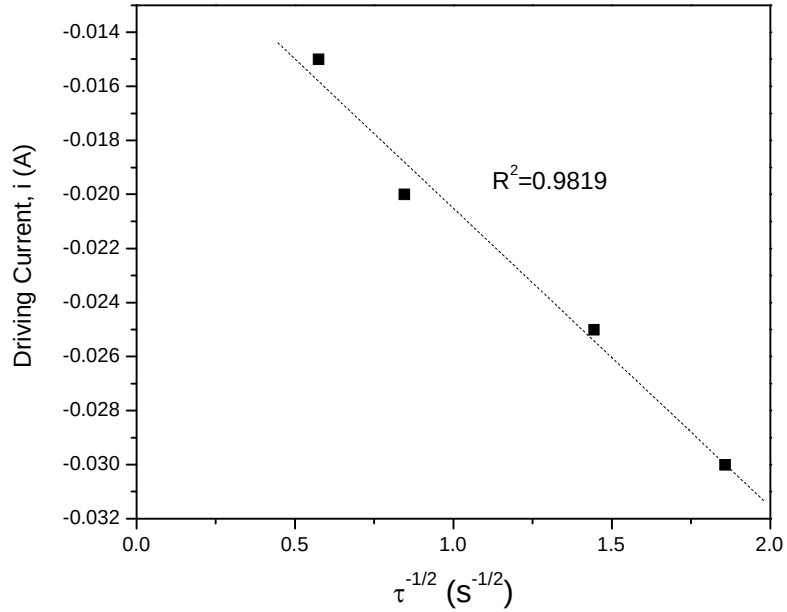

U^{3+} Diffusion Coefficient

- Measured:
  - 7.79×10^{-6} cm^2/s
- Literature:
  - 3.17×10^{-5} to 8.70×10^{-6} cm^2/s

Anodic Stripping Voltammetry

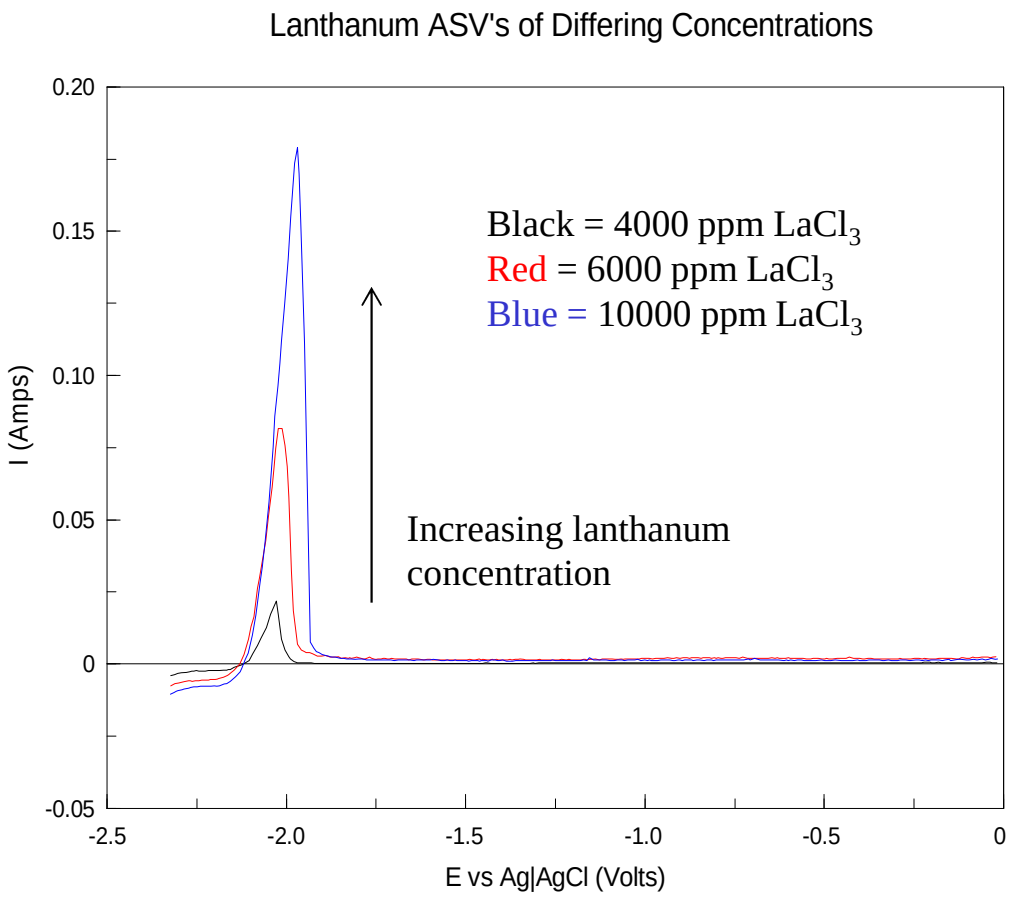

Anodic stripping voltammograms obtained from LiCl-KCl at 500°C containing various concentrations of $LaCl_3$

- ASV Parameters:
  - -2.3 – 0V vs. $Ag^+|Ag$
  - 50 mV/s
  - 60s plating time
  - 10 independent measurements taken
  - Average peak current was calculated
  - Divided through by wetted area of WE
  - Standard deviation of peak current density calculated
- Peak current density increases with concentration
- Scientific basis for salt diagnostic tool

$DyCl_3$ Concentration Determination: ASV Working Curve

DEPARTMENT OF
Engineering Physics
College of Engineering
University of Wisconsin-Madison

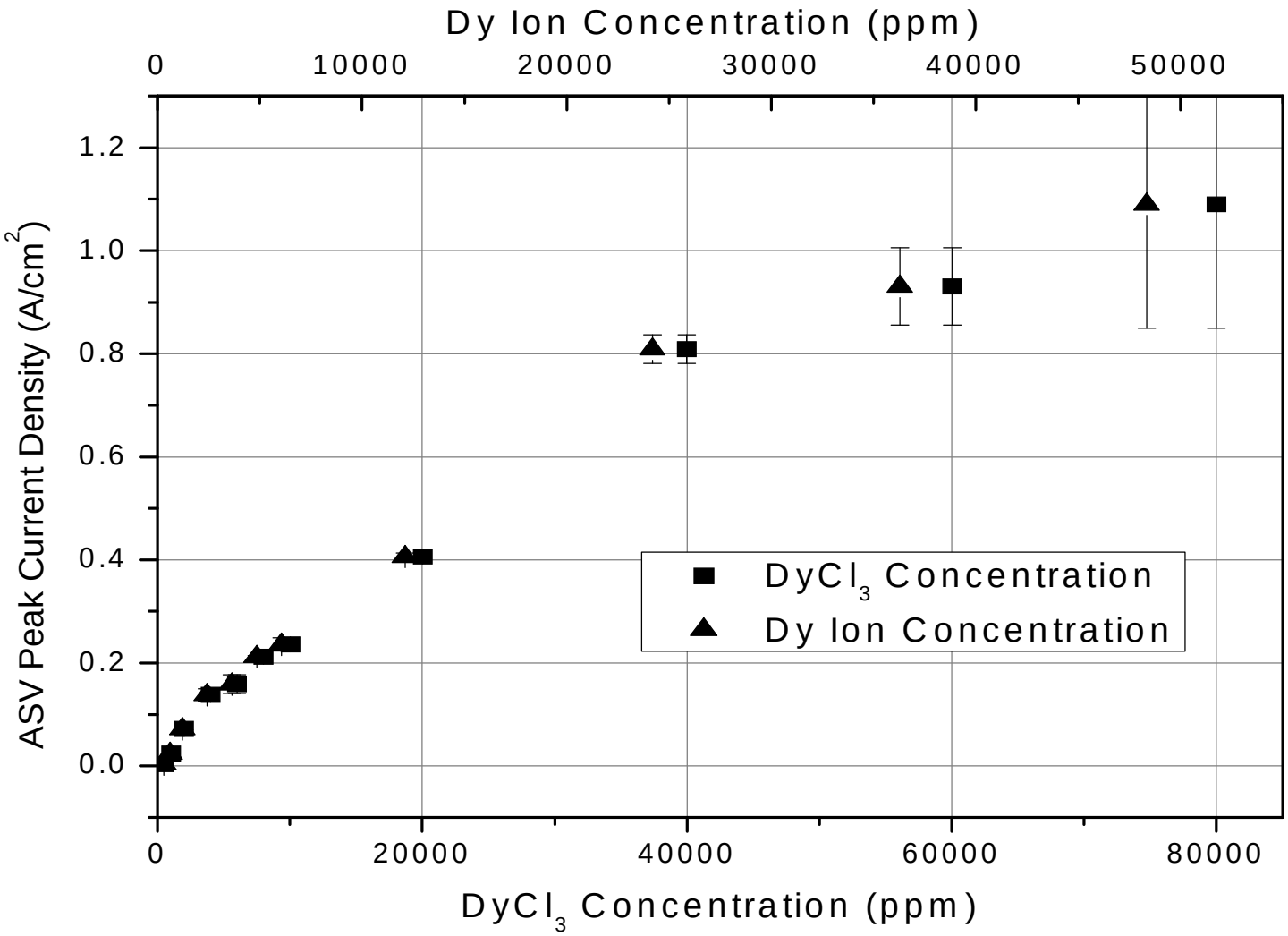

ASV Working Curves

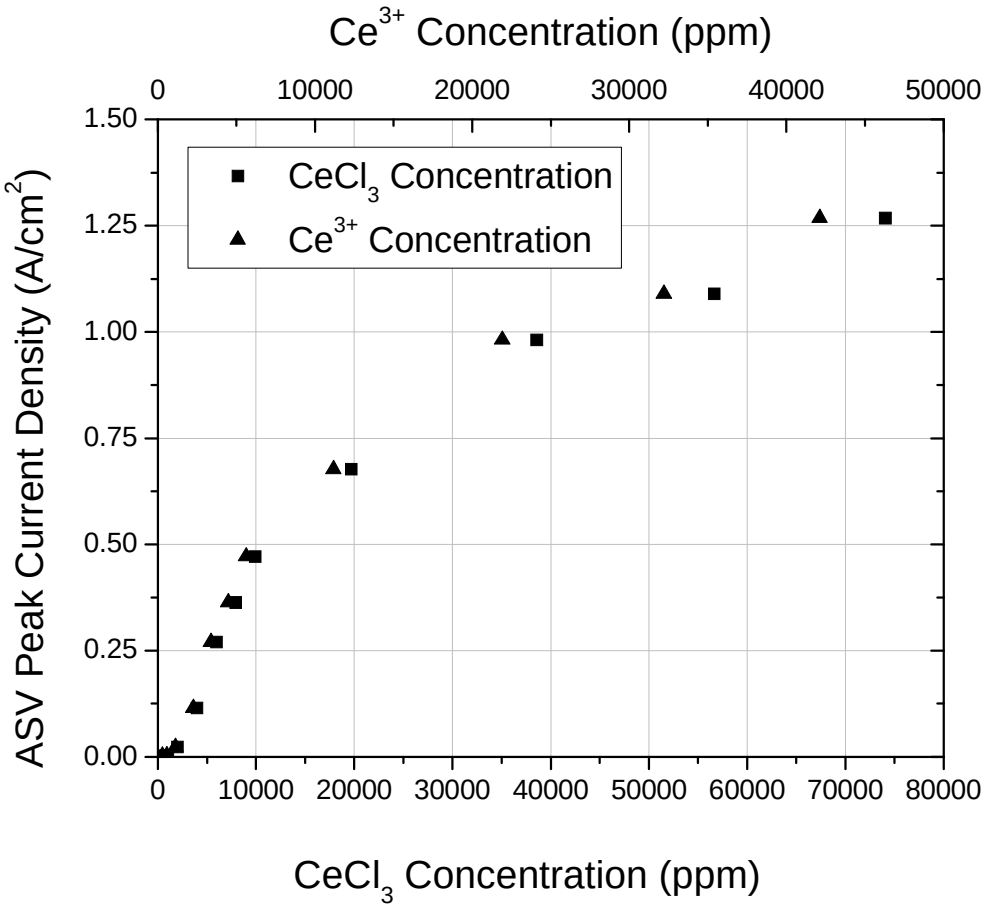

- Similar trends were observed with $LaCl_3$, $CeCl_3$, and $NdCl_3$ additions.
- Slope change near 1 wt% (10,000 ppm) for all elements
- Decreased slope at high concentrations
- Scientific basis for an in situ electrochemical probe

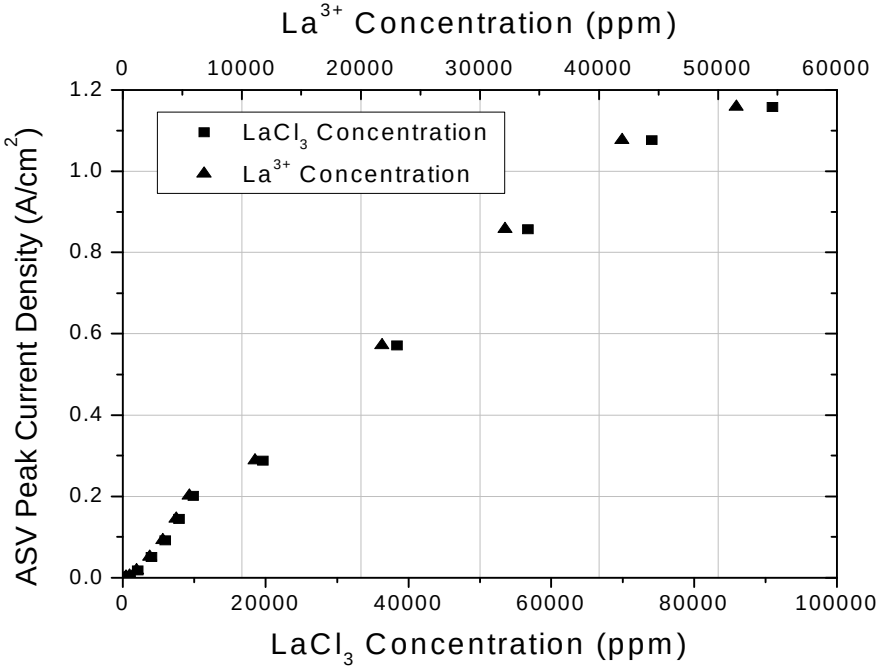

- Similar trends were observed with $LaCl_3$, $CeCl_3$, and $NdCl_3$ additions.
- Slope change near 1 wt% (10,000 ppm) for all elements. Possibly due to surface saturation effects of the WE.
- Decreased slope at high concentrations. Possibly caused by incomplete mixing of the salt. No mechanical mixing is employed.
- These curves serve as the scientific basis for an in situ electrochemical probe to perform online monitoring of fission product concentrations.

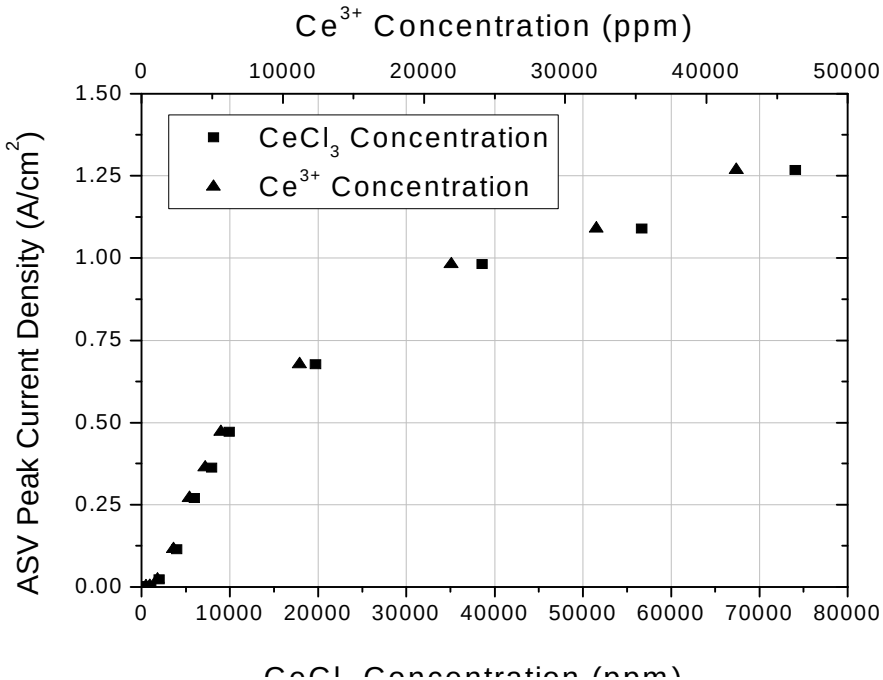

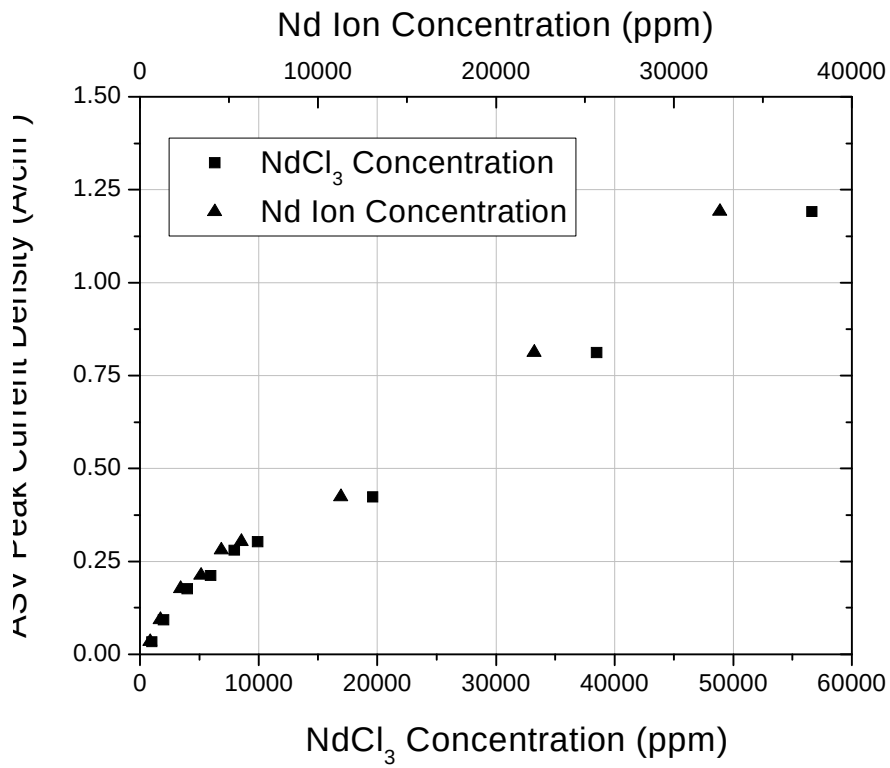

CV: Concentration Determination

- Anodic and cathodic peaks on cyclic voltammograms can also be used to determine the concentration of an analyte in the salt
- Parameters:
  - -2.4 – 0V vs. $Ag^+|Ag$
  - 50 mV/s
  - 3 cycles
  - Record last cycle
  - Divided through by wetted area of WE
- Similar trend compared to ASV concentration curve
- More linear due to the lack of pre-concentration (plating) step

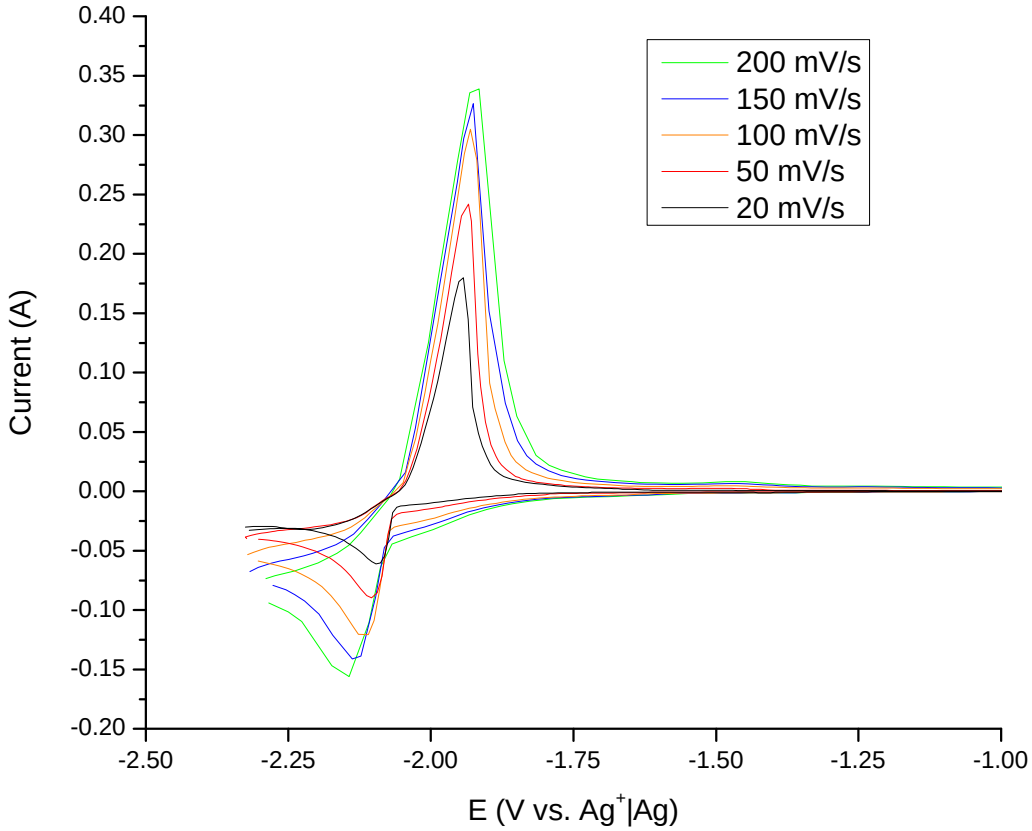

Cyclic voltammograms of 2 wt% $DyCl_3$ in LiCl-KCl at 500°C. -2.4V – 0V vs. 5 mol% $Ag^+|Ag$ RE

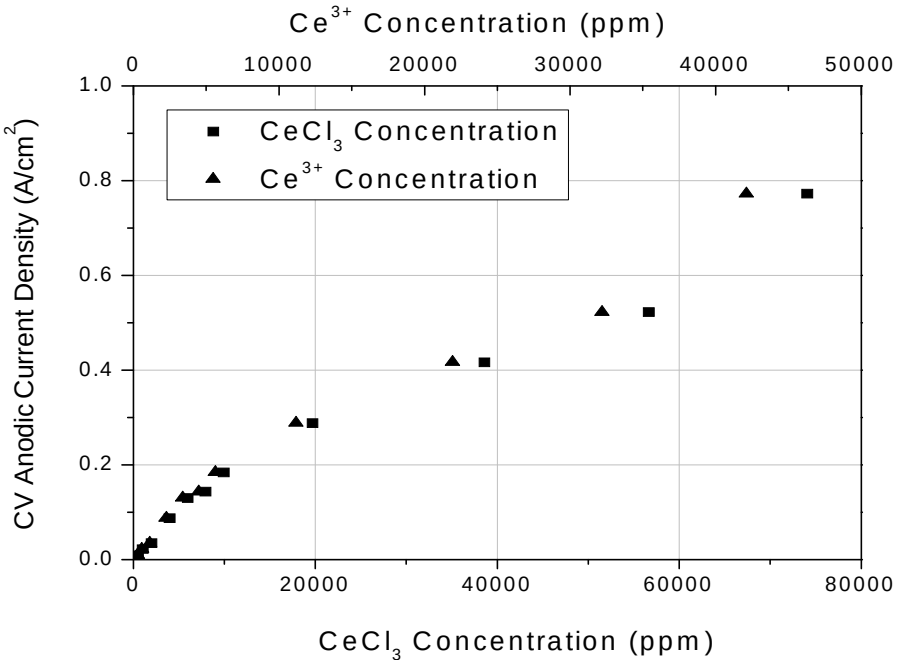
Ce3+ Concentration (ppm)
0
10000
20000
30000
40000
50000
CV Anodic Current Density (A/cm2)
1.0
0.8
0.6
0.4
0.2
0.0
CeCl3 Concentration
Ce3+ Concentration
0
20000
40000
60000
80000
CeCl3 Concentration (ppm)

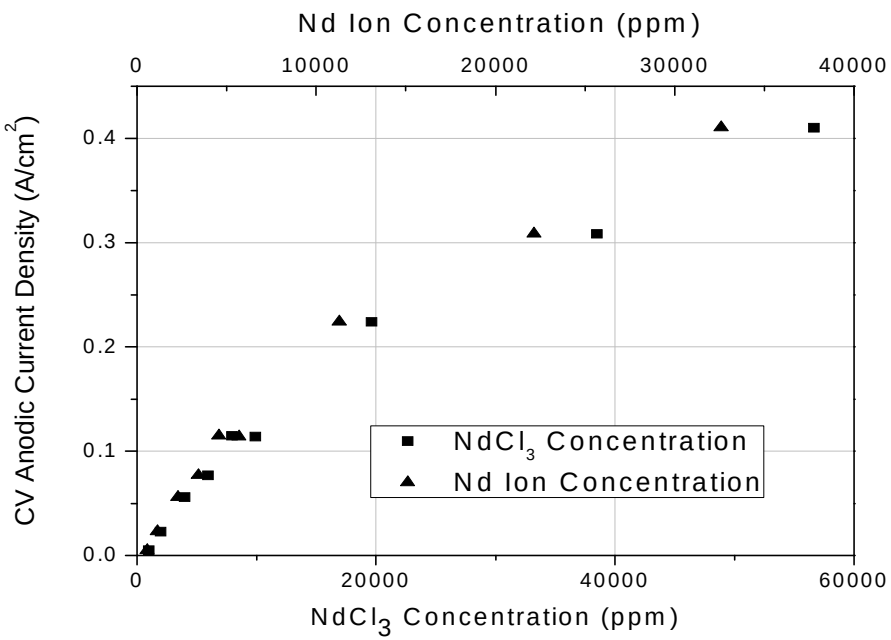
Nd Ion Concentration (ppm)
0
10000
20000
30000
40000
CV Anodic Current Density (A/cm2)
0.4
0.3
0.2
0.1
0.0
NdCl3 Concentration
Nd Ion Concentration
0
20000
40000
60000
NdCl3 Concentration (ppm)

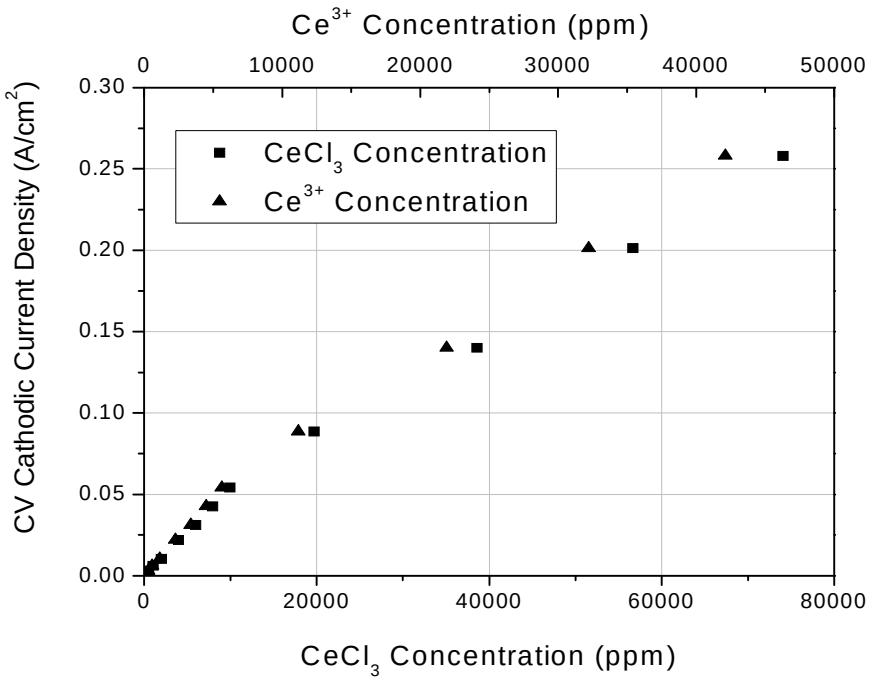
Ce3+ Concentration (ppm)
0
10000
20000
30000
40000
50000
CV Cathodic Current Density (A/cm2)
0.30
0.25
0.20
0.15
0.10
0.05
0.00
CeCl3 Concentration
Ce3+ Concentration
0
20000
40000
60000
80000
CeCl3 Concentration (ppm)

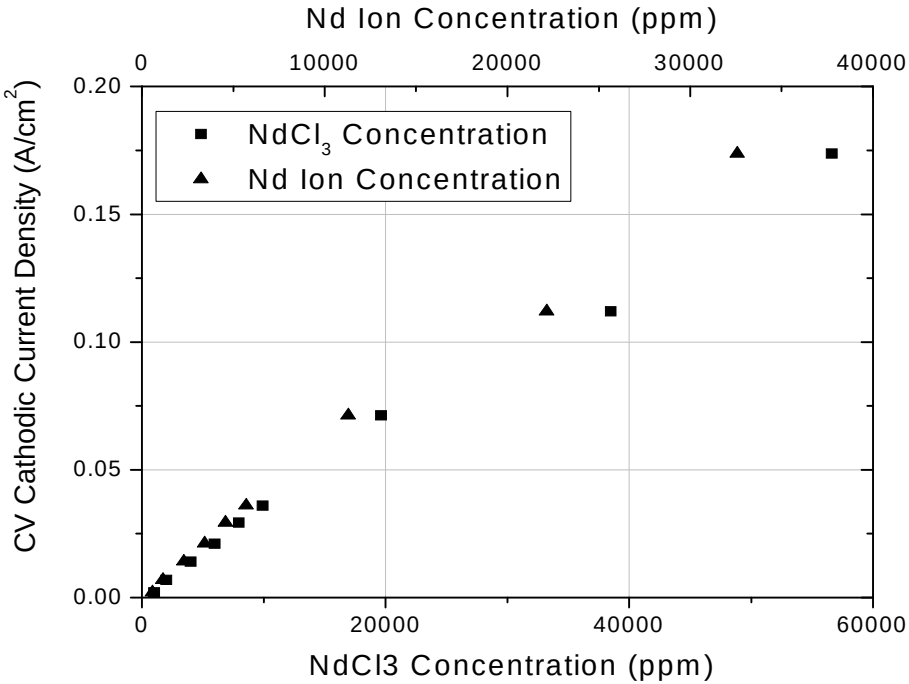
Nd Ion Concentration (ppm)
0
10000
20000
30000
40000
CV Cathodic Current Density (A/cm2)
0.20
0.15
0.10
0.05
0.00
NdCl3 Concentration
Nd Ion Concentration
0
20000
40000
60000
NdCl3 Concentration (ppm)

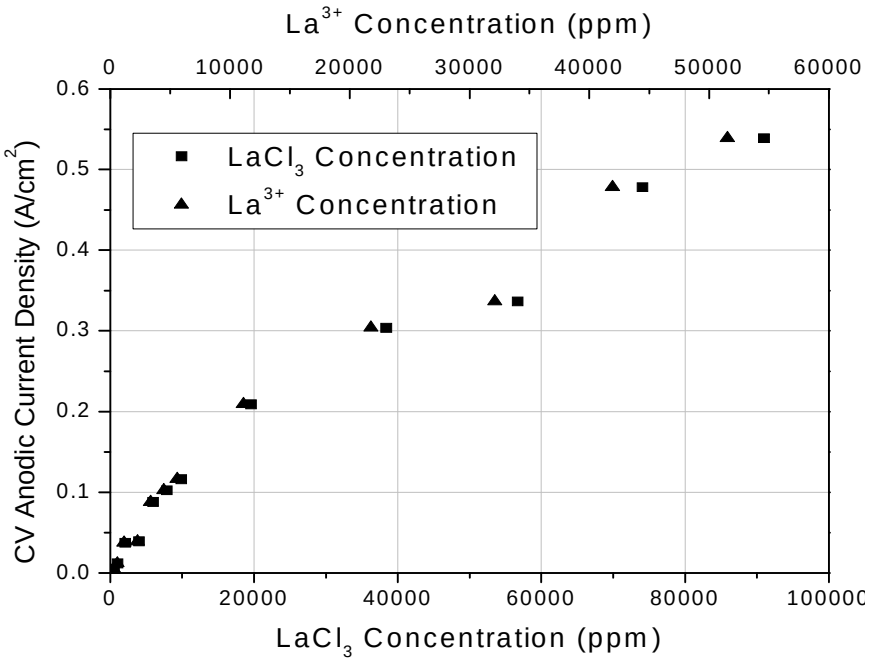
La3+ Concentration (ppm)
0
10000
20000
30000
40000
50000
60000
CV Anodic Current Density (A/cm2)
0.0
0.1
0.2
0.3
0.4
0.5
0.6
LaCl3 Concentration
La3+ Concentration
0
20000
40000
60000
80000
100000
LaCl3 Concentration (ppm)

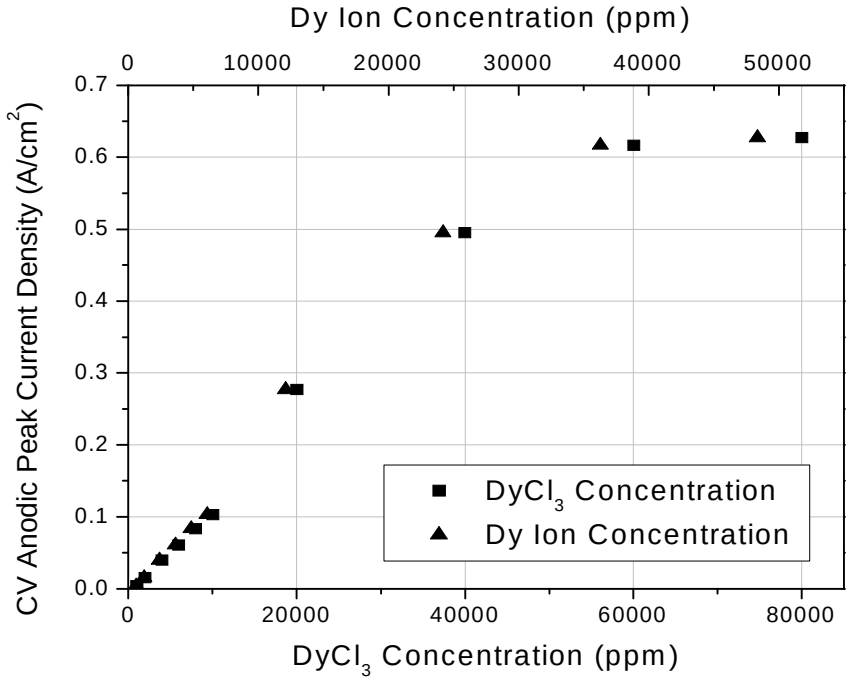
Dy Ion Concentration (ppm)
0
10000
20000
30000
40000
50000
CV Anodic Peak Current Density (A/cm2)
0.0
0.1
0.2
0.3
0.4
0.5
0.6
0.7
DyCl3 Concentration
Dy Ion Concentration
0
20000
40000
60000
80000
DyCl3 Concentration (ppm)

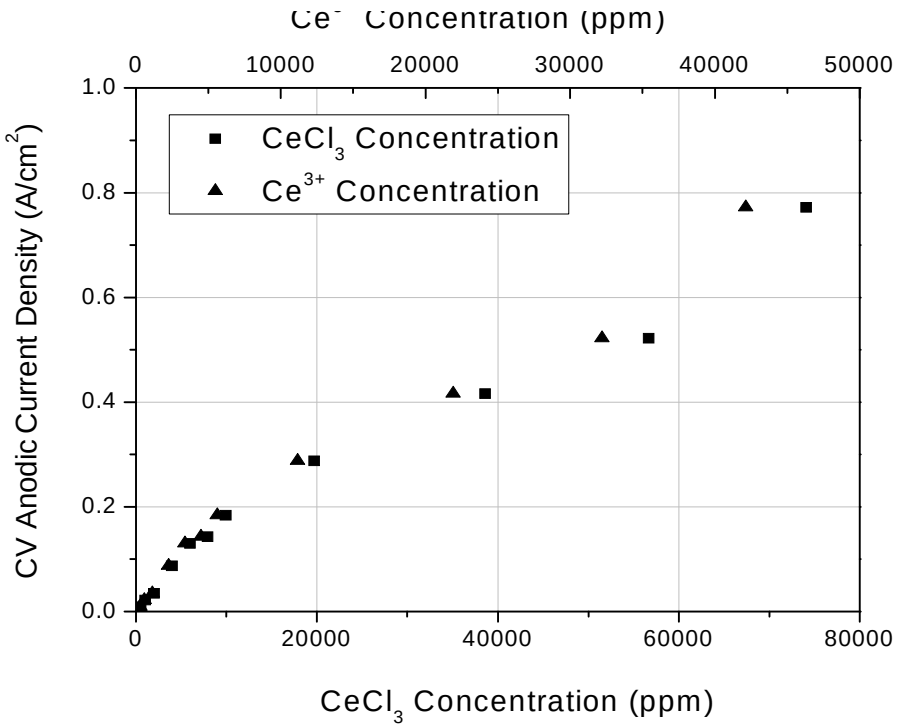
0
10000
20000
30000
40000
50000
CV Anodic Current Density (A/cm2)
0.0
0.2
0.4
0.6
0.8
1.0
CeCl3 Concentration
Ce3+ Concentration
0
20000
40000
60000
80000
CeCl3 Concentration (ppm)

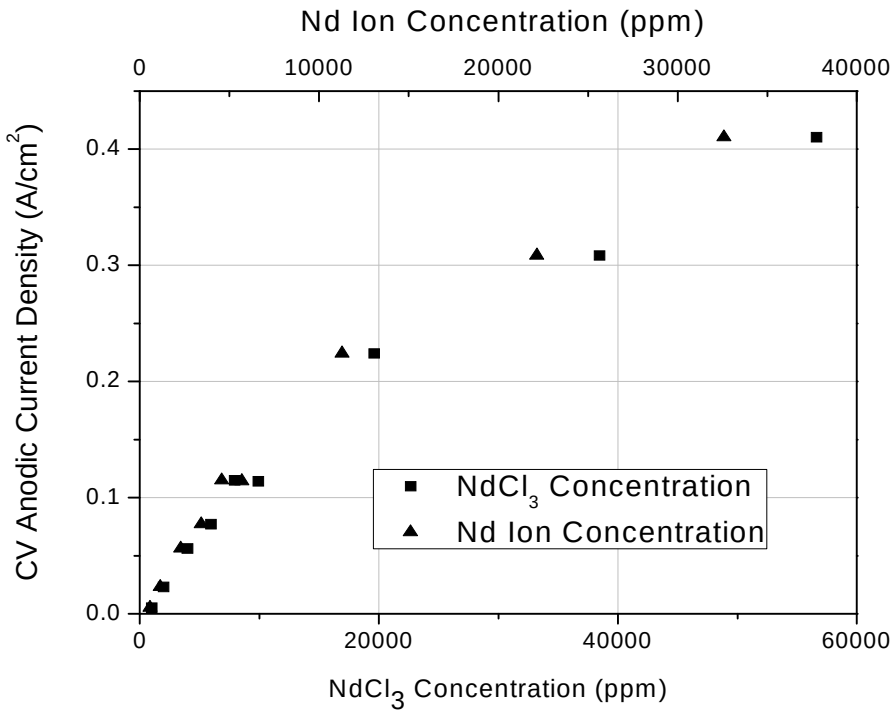
Nd Ion Concentration (ppm)
0
10000
20000
30000
40000
CV Anodic Current Density (A/cm2)
0.0
0.1
0.2
0.3
0.4
NdCl3 Concentration
Nd Ion Concentration
0
20000
40000
60000
NdCl3 Concentration (ppm)

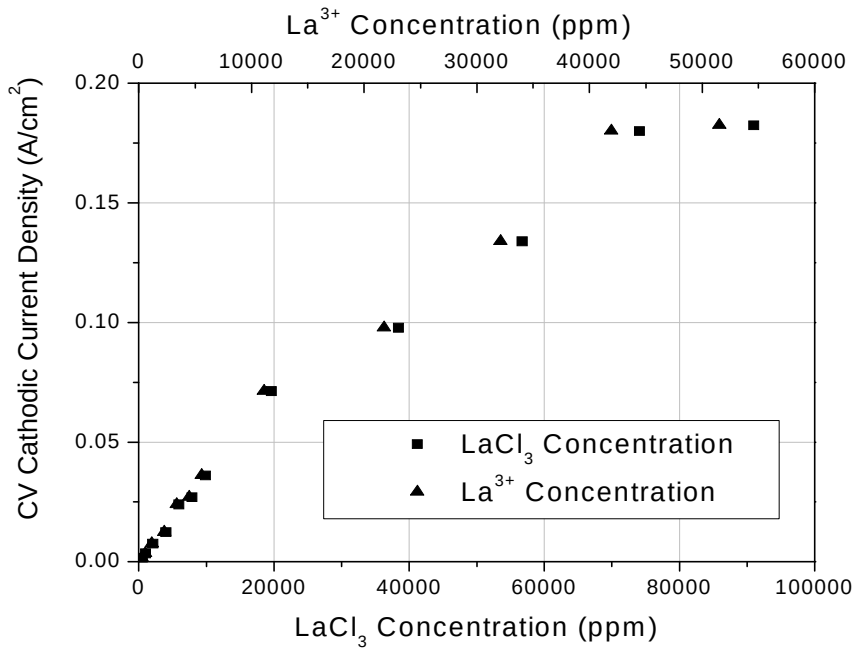
La3+ Concentration (ppm)
0
10000
20000
30000
40000
50000
60000
CV Cathodic Current Density (A/cm2)
0.20
0.15
0.10
0.05
0.00
LaCl3 Concentration
La3+ Concentration
0
20000
40000
60000
80000
100000
LaCl3 Concentration (ppm)

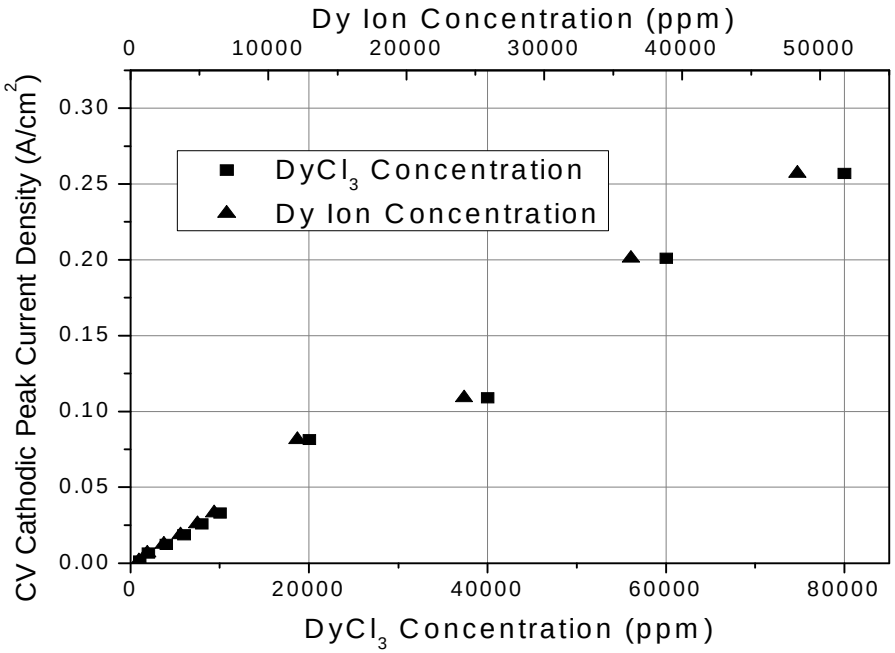
Dy Ion Concentration (ppm)
0
10000
20000
30000
40000
50000
CV Cathodic Peak Current Density (A/cm2)
0.30
0.25
0.20
0.15
0.10
0.05
0.00
DyCl3 Concentration
Dy Ion Concentration
0
20000
40000
60000
80000
DyCl3 Concentration (ppm)

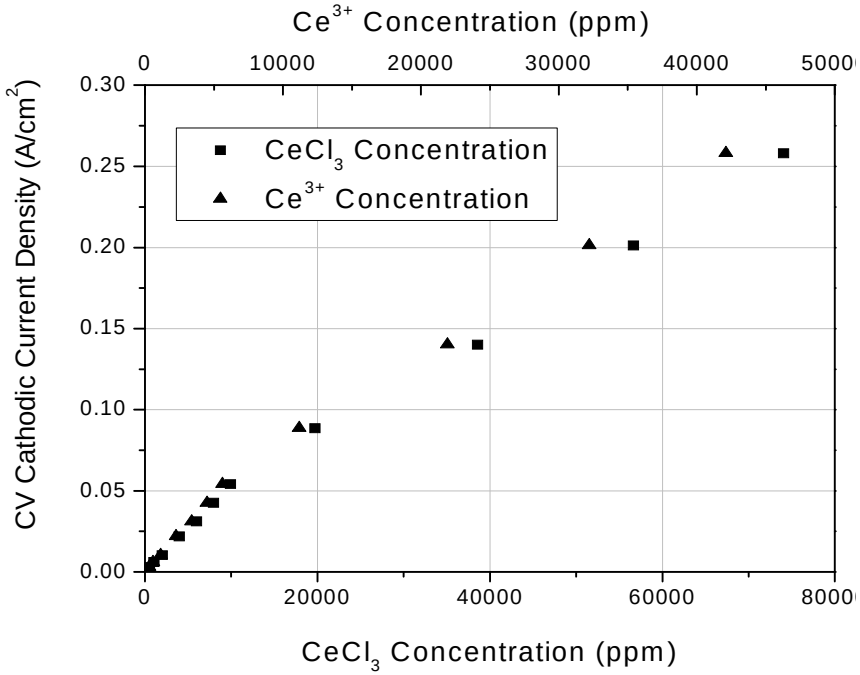
Ce3+ Concentration (ppm)
0
10000
20000
30000
40000
CV Cathodic Current Density (A/cm2)
0.30
0.25
0.20
0.15
0.10
0.05
0.00
CeCl3 Concentration
Ce3+ Concentration
0
20000
40000
60000
CeCl3 Concentration (ppm)

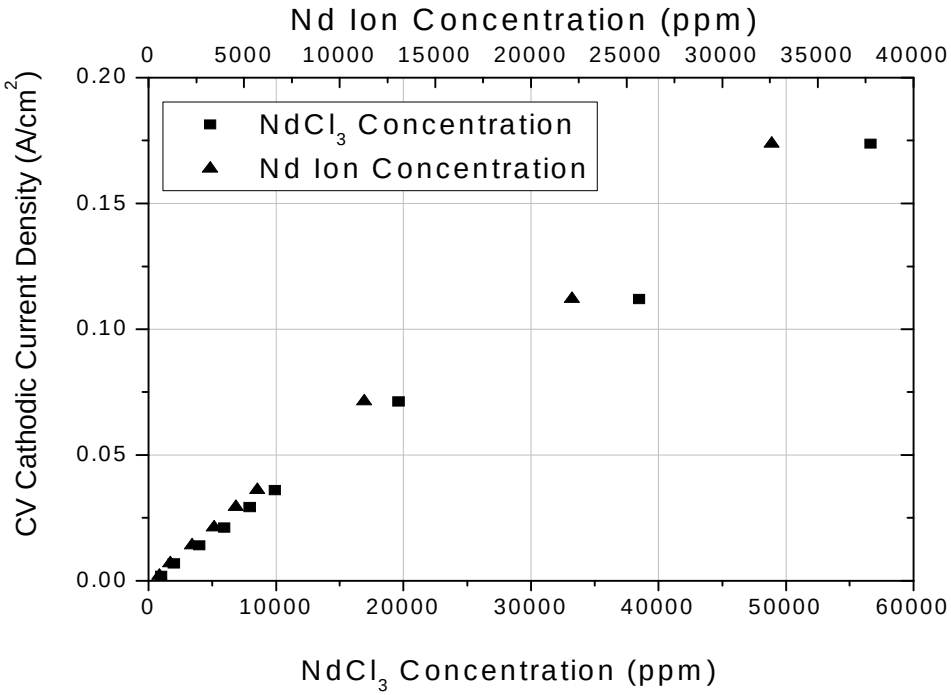
Nd Ion Concentration (ppm)
0
5000
10000
15000
20000
25000
30000
35000
40000
CV Cathodic Current Density (A/cm2)
0.20
0.15
0.10
0.05
0.00
NdCl3 Concentration
Nd Ion Concentration
0
10000
20000
30000
40000
50000
60000
NdCl3 Concentration (ppm)

Concentration Detection Methods

	Coefficient of Determination	
Element	Anodic	Cathodic
La	0.9414	0.9591
Ce	0.9506	0.9849
Nd	0.9666	0.9796
Dy	0.9295	0.9839
Average	0.9470	0.9769

- CV cathodic curve is most linear
- ASV best suited for low concentrations (< 1wt%)
  - Large amount of material plated onto WE complicates oxidation process at high concentrations

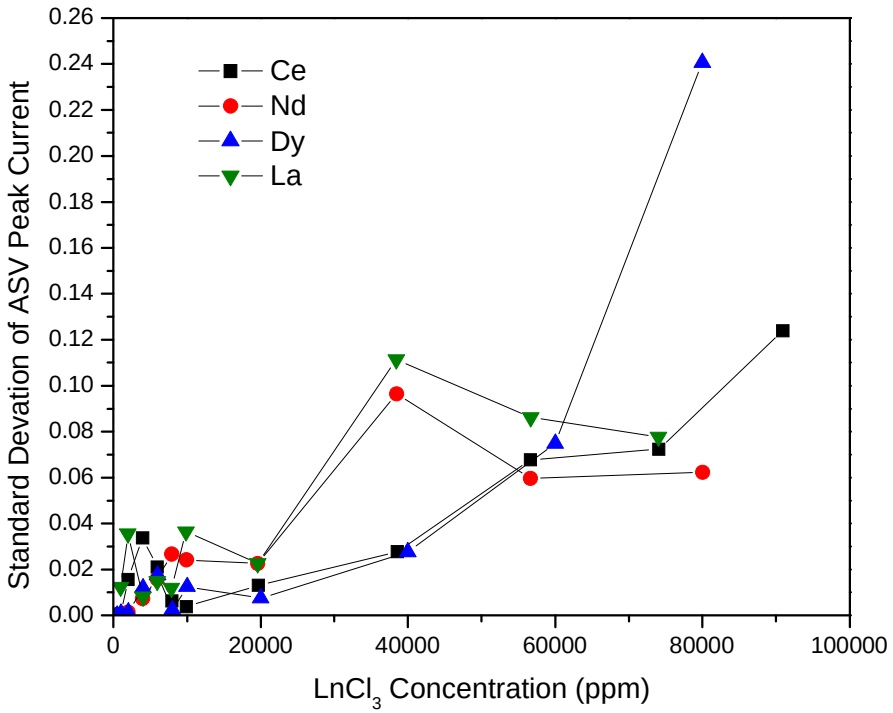

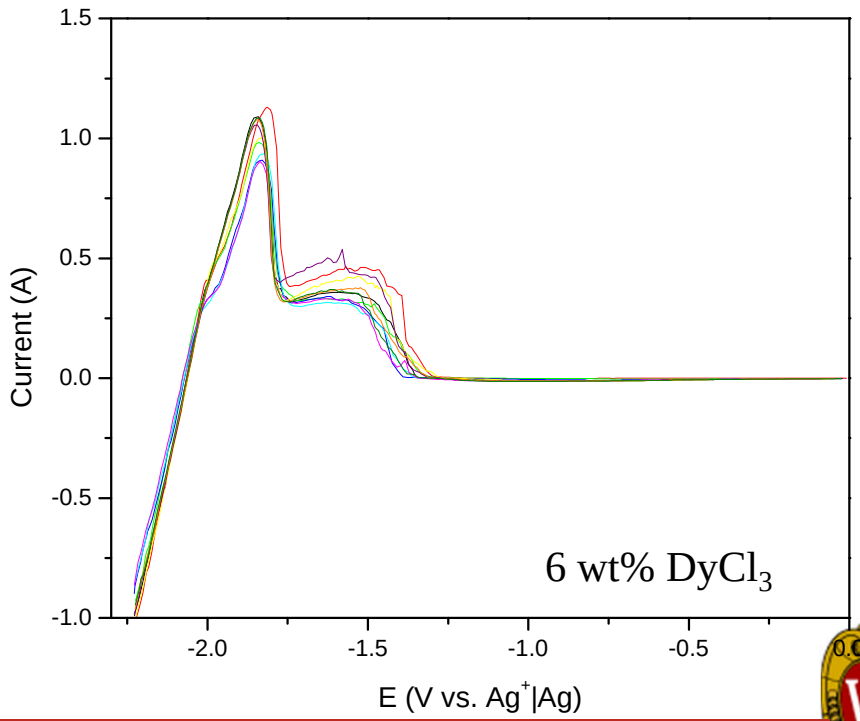

Differential Scanning Calorimetry (DSC)

Differential Scanning Calorimetry

- DSC measures the energy required to keep a sample and an inert reference material at the same temperature while subjecting them both to identical heating or cooling programs
- Heat-flux DSC
  - Sample and reference material located in the same heater connected by a high conductivity heating block
  - Thermal transitions in the sample cause the temperature of the sample to change relative to the reference
  - Temperature difference causes heat transfer between the sample and reference pans

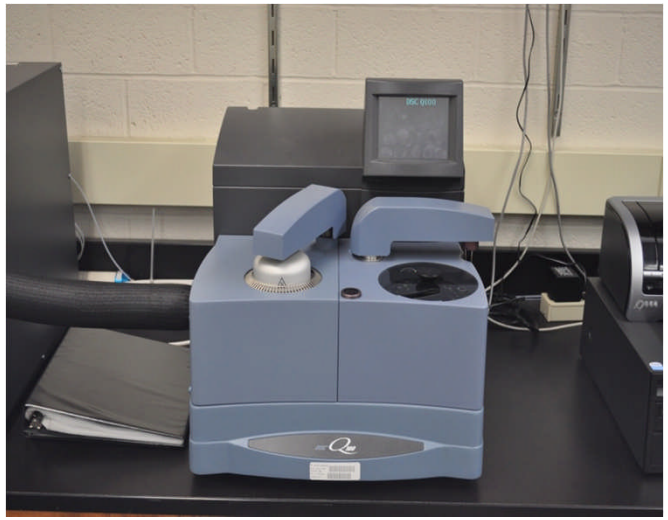

TA Instruments Q100 DSC

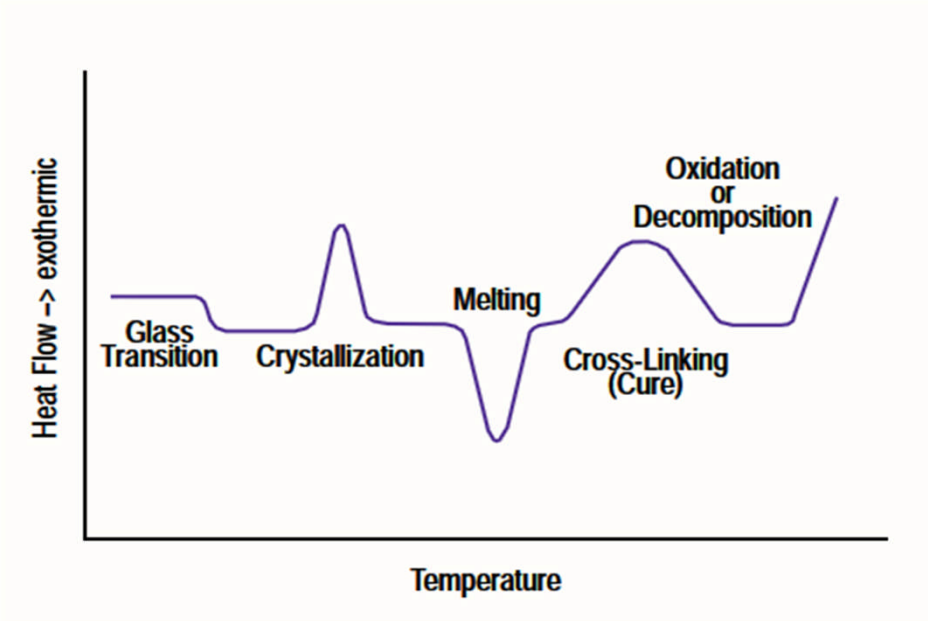

Q100 Modulated Differential Scanning Calorimeter (TA Instruments)

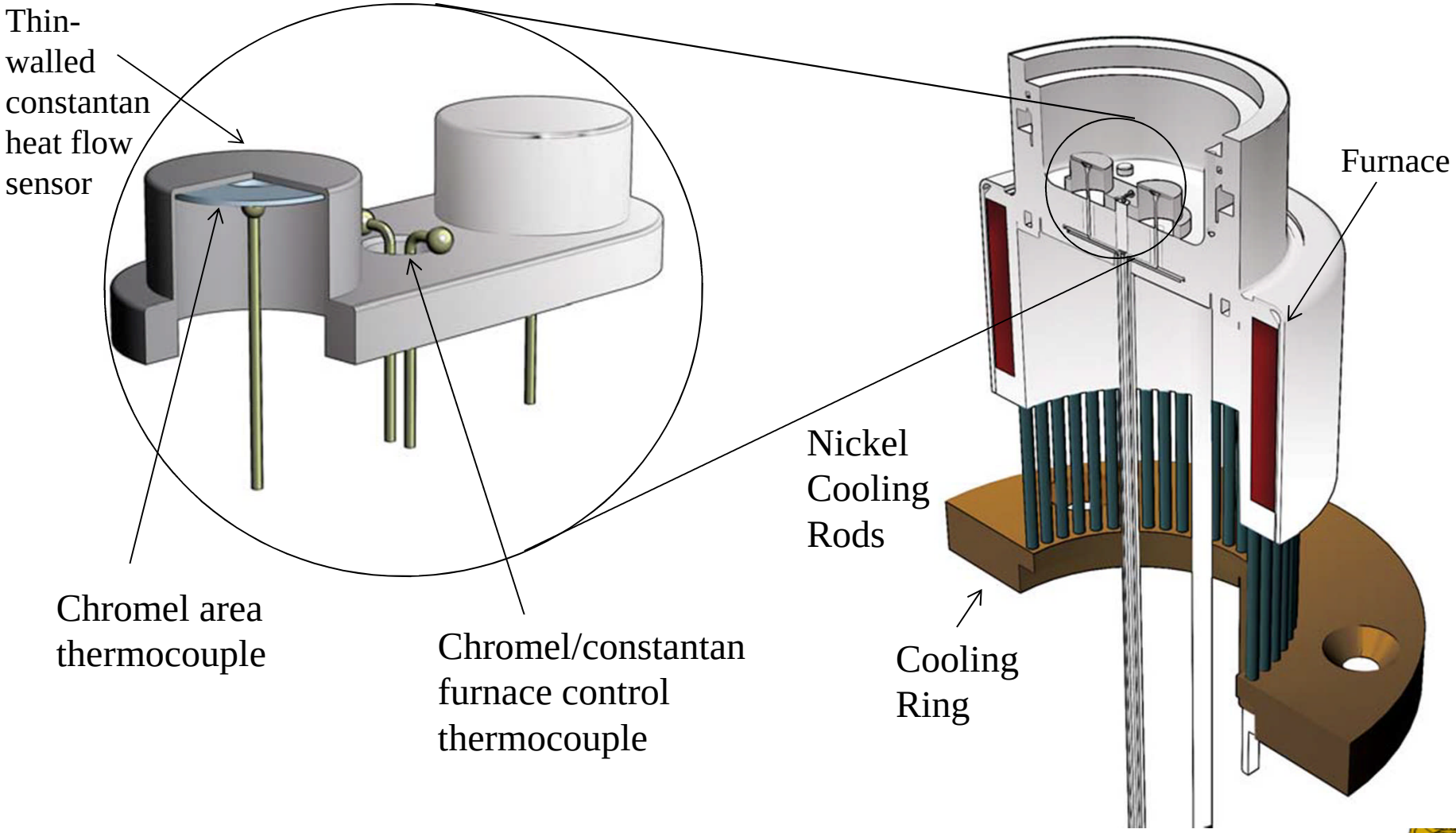

DSC Theory

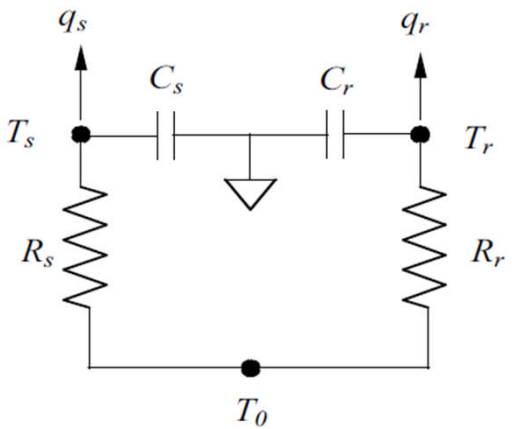

$$q_s^{\cdot} = \frac{\Delta T_0}{R_s} - C_s \frac{dT_s}{dt}$$

$$q_r^{\cdot} = \frac{\Delta T}{R_r} - C_r \frac{dT_r}{dt}$$

- Endothermic reaction
  - Sample temperature lags behind reference temperature and heat is transferred to the sample
- Exothermic reaction
  - Reference temperature lags behind sample temperature and heat is transferred away from the sample

Conventional heat flow

Accounts for the differences in heating rates of the two calorimeters

$$q^{\cdot} = \frac{\Delta T}{R_r} + \Delta T_0 \left(\frac{1}{R_s} - \frac{1}{R_r}\right) + (C_r - C_s)\frac{dT_s}{dt} - C_r \frac{d\Delta T}{dt}$$

Accounts for differences in thermal resistance of sample and reference calorimeters

Accounts for differences in heat capacities between the two calorimeters

LiCl-KCl (99+% Pure)

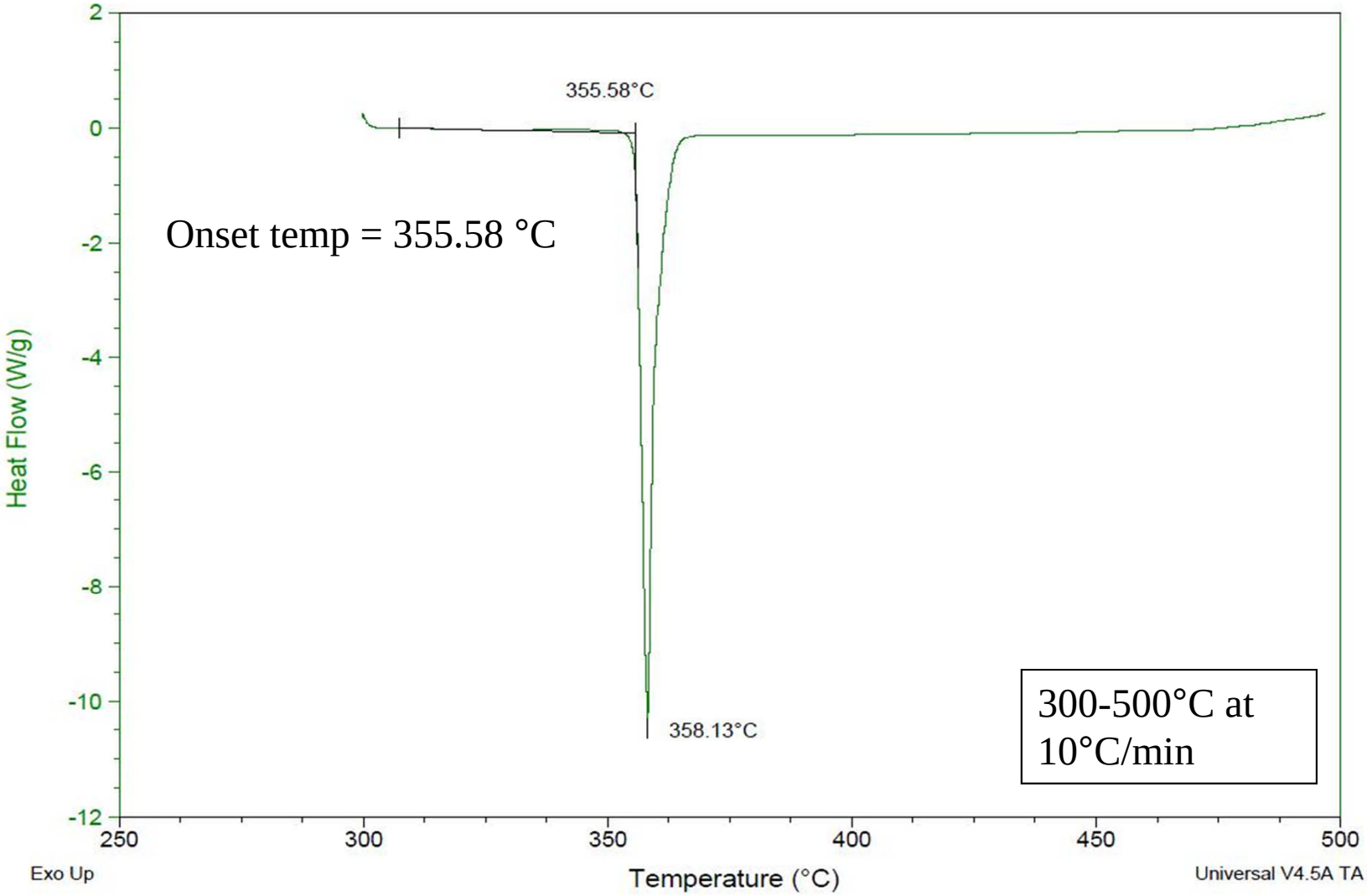

DSC: $CeCl_3$ Concentration Study

Parameters

- 300-500°C at 10°C/min
- Sample mass < 10 mg

Melting point of pure LiCl-KCl measured to be 355.58°C

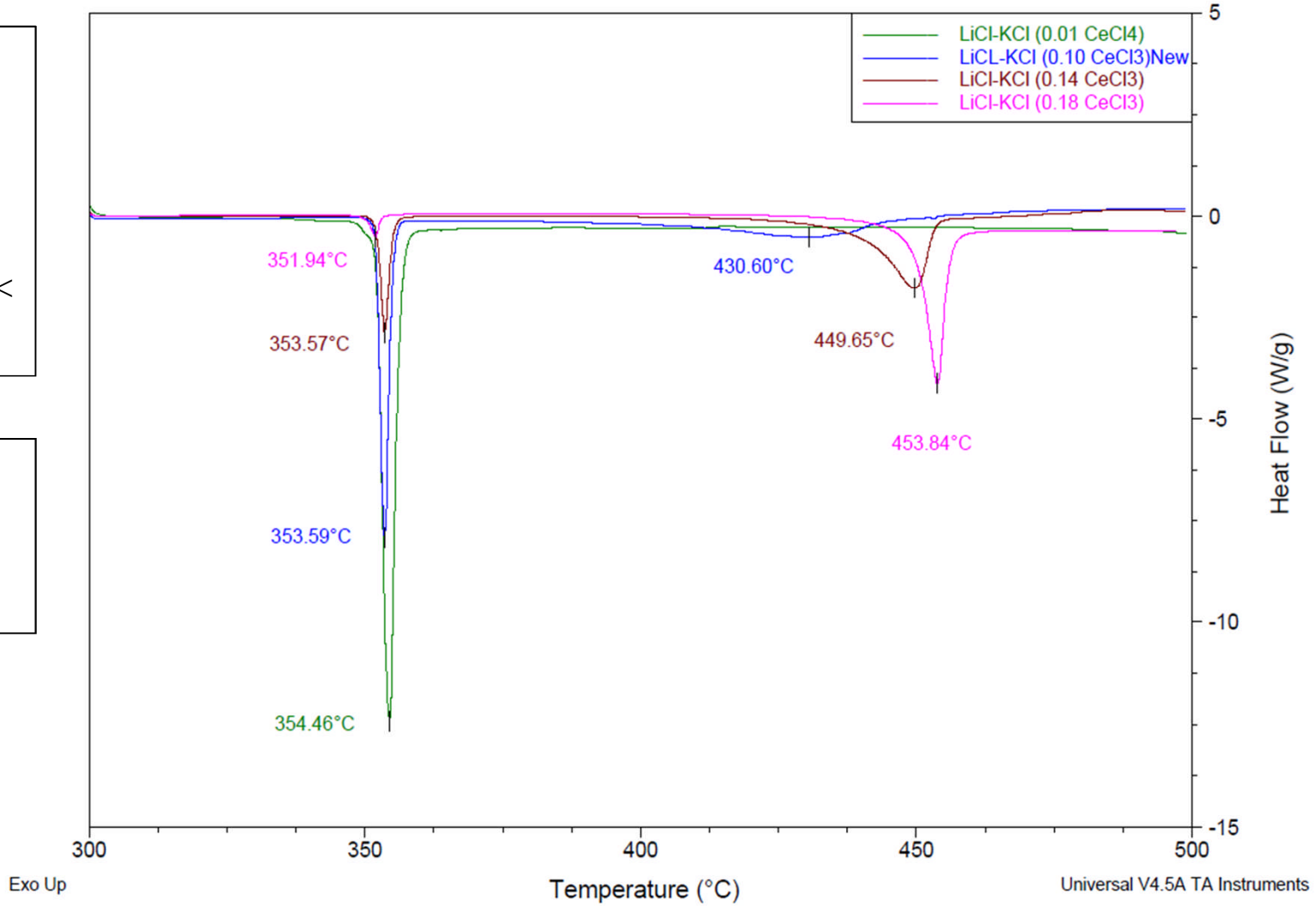

DSC Heating Curve

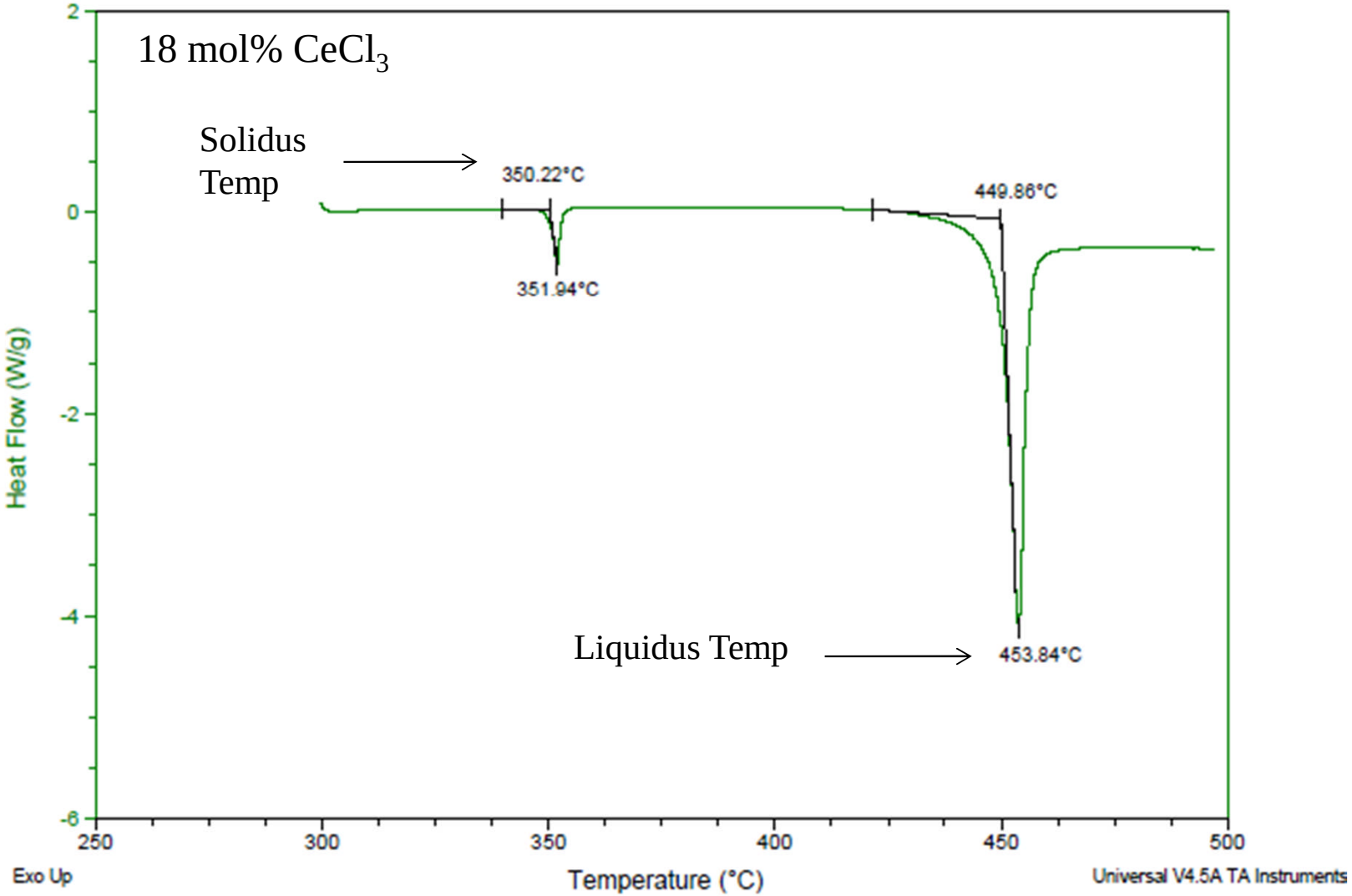

Pseudo-binary phase diagram: LiCl-KCl eutectic and $CeCl_3$

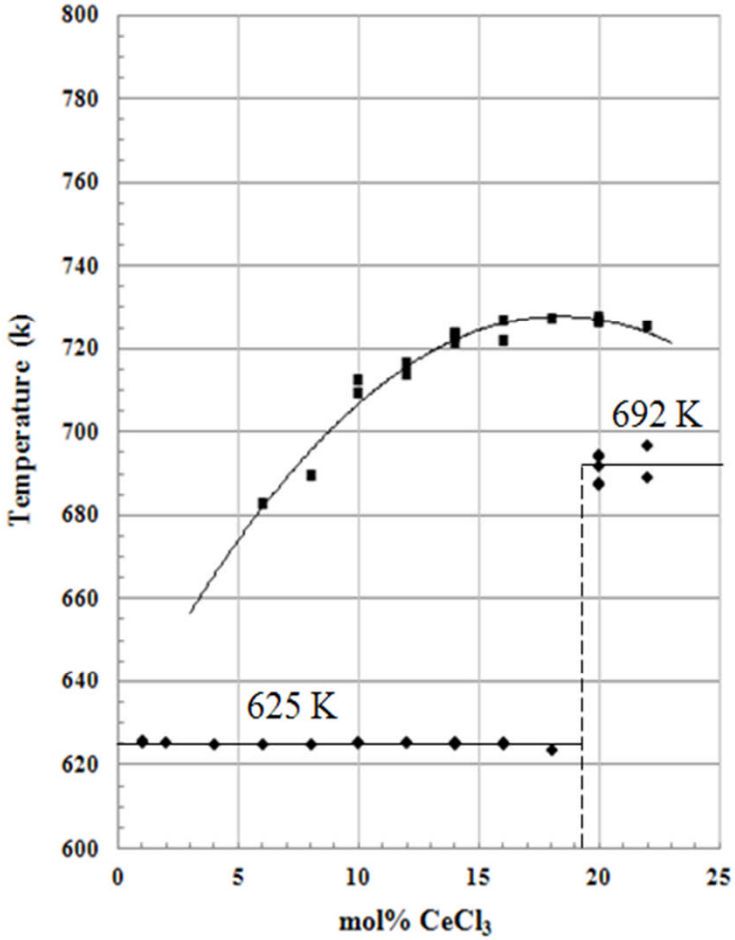

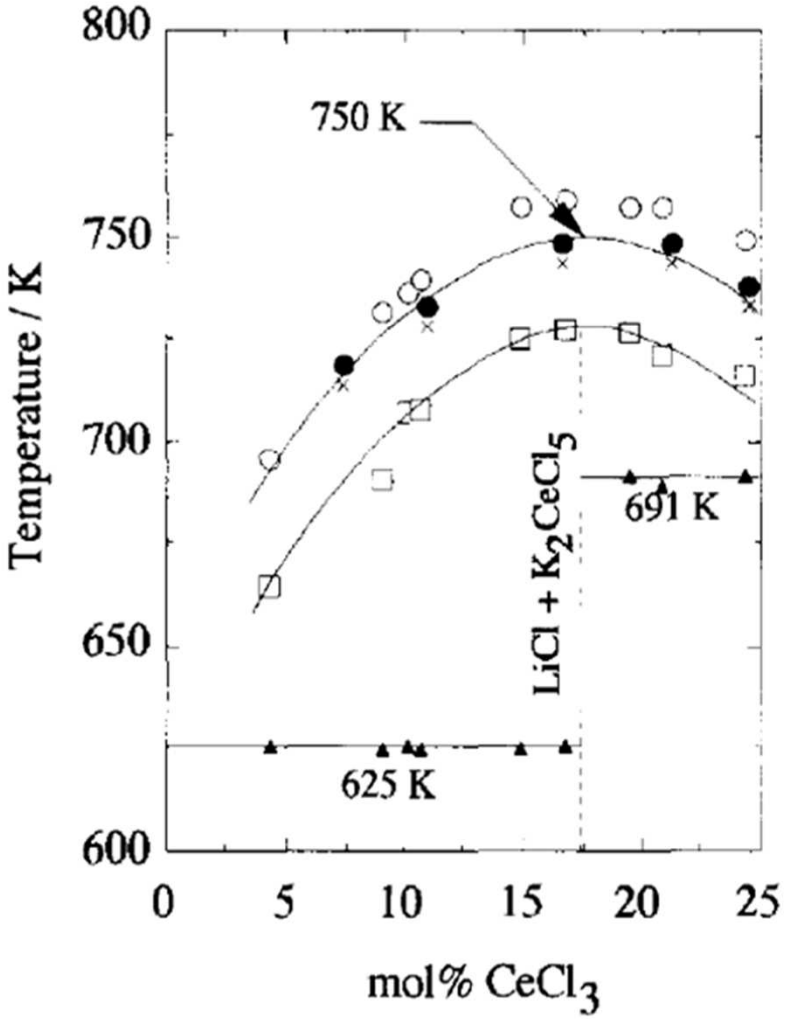

(Nakamura, K. 1994)

DSC: $LaCl_3$ Concentration Study

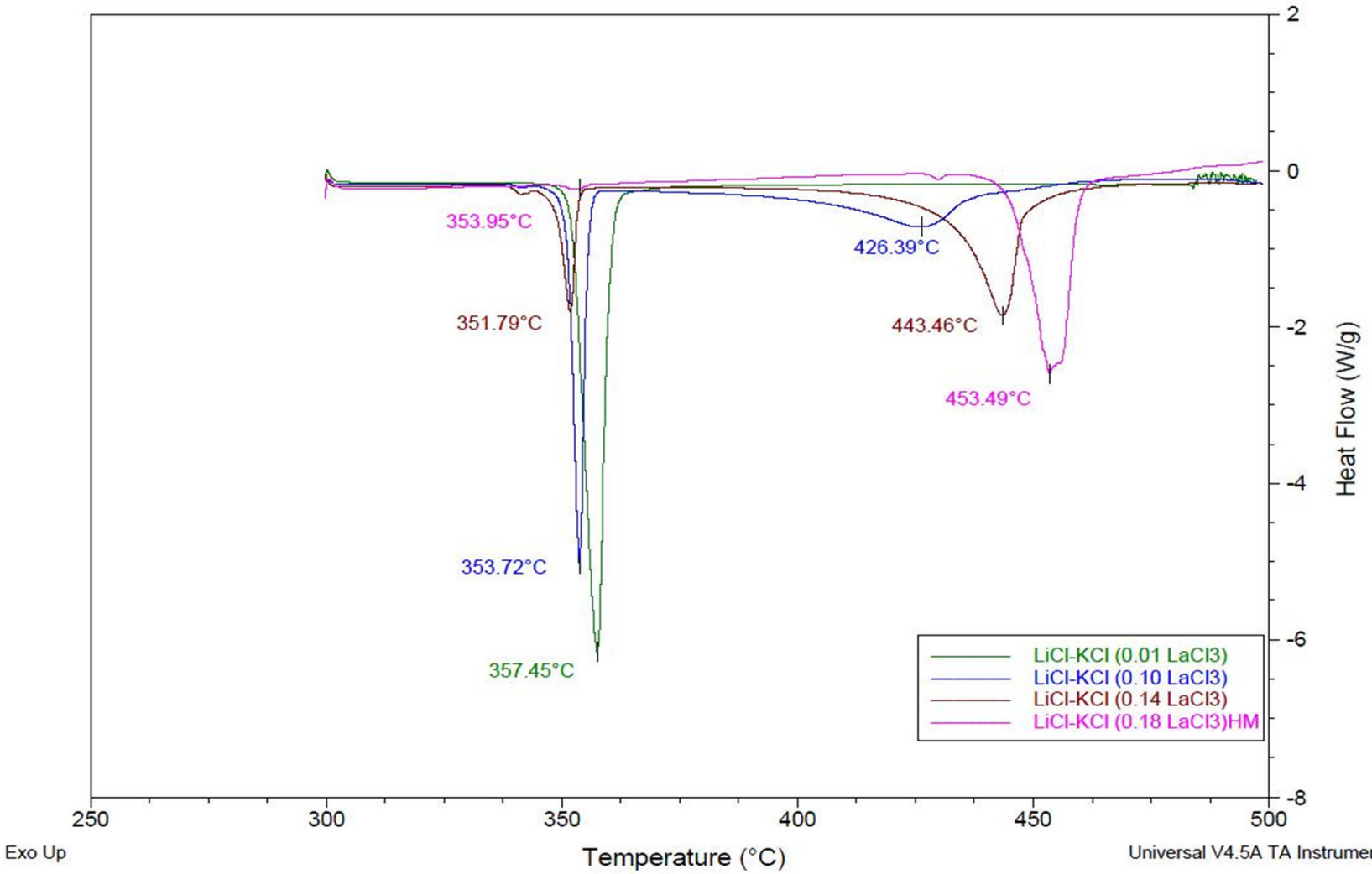

Pseudo-binary phase diagram: LiCl-KCl eutectic and $LaCl_3$

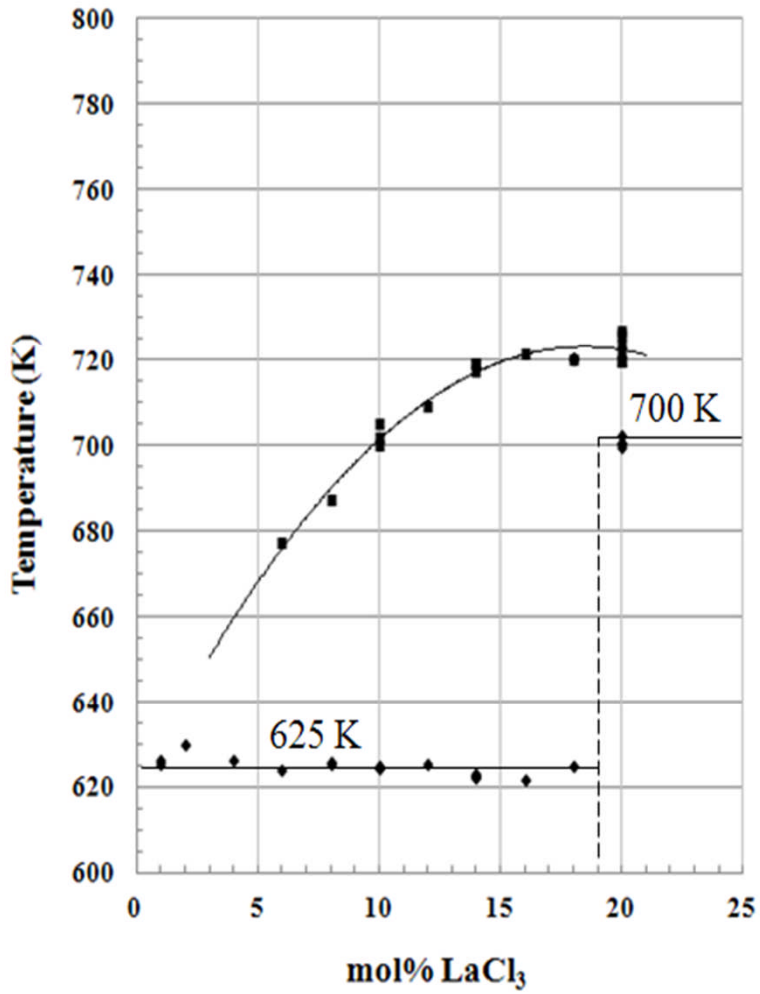

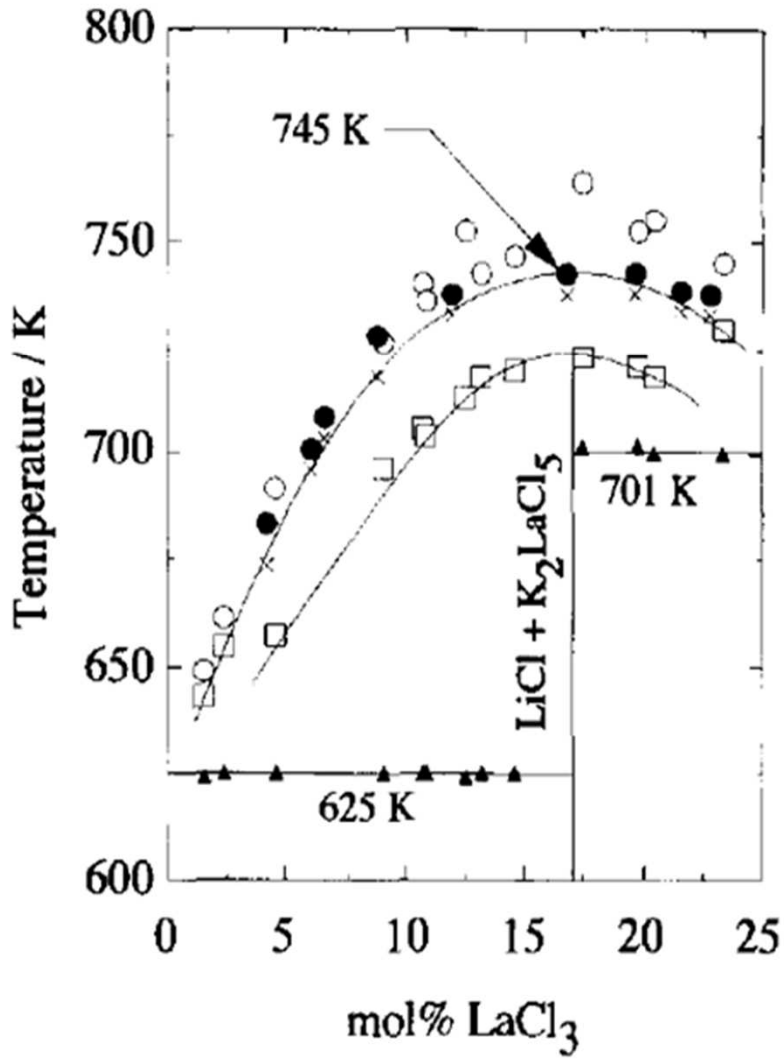

(Nakamura, K. 1994)

DSC: $NdCl_3$ Concentration Study

DEPARTMENT OF
Engineering Physics
College of Engineering
University of Wisconsin-Madison

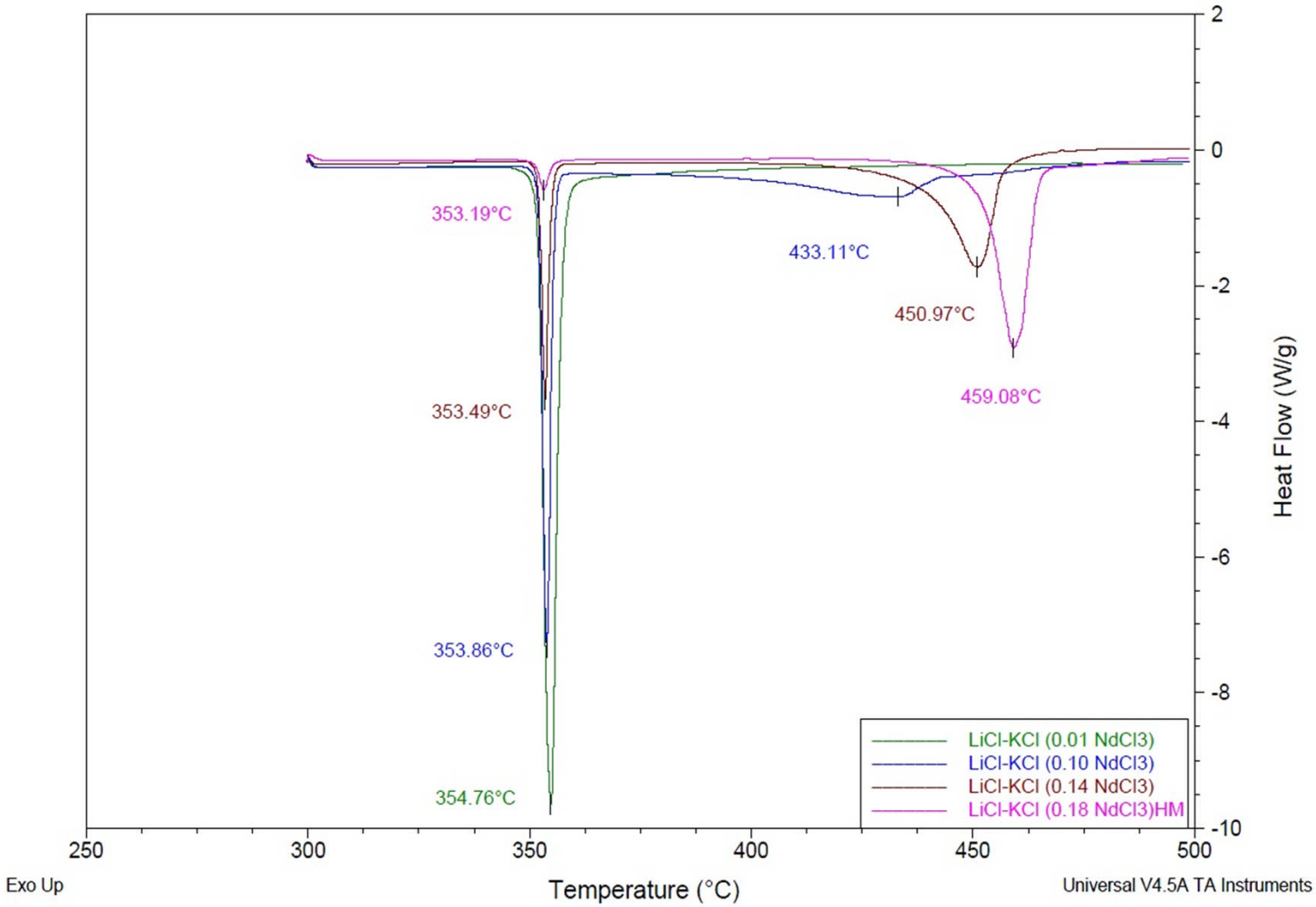

Pseudo-binary phase diagram: LiCl-KCl eutectic and $NdCl_3$

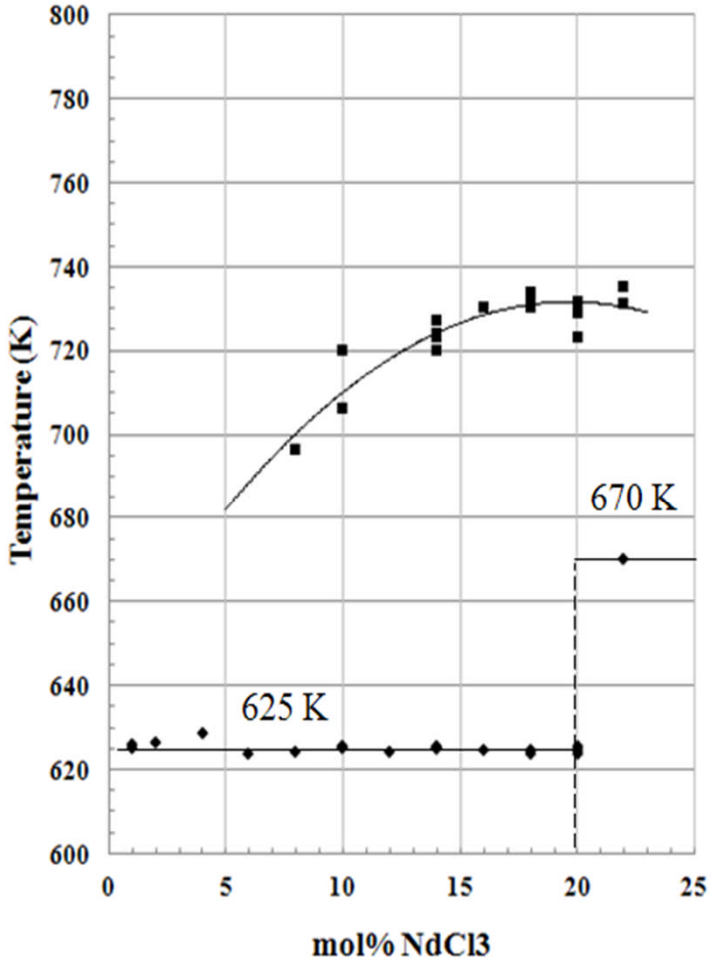

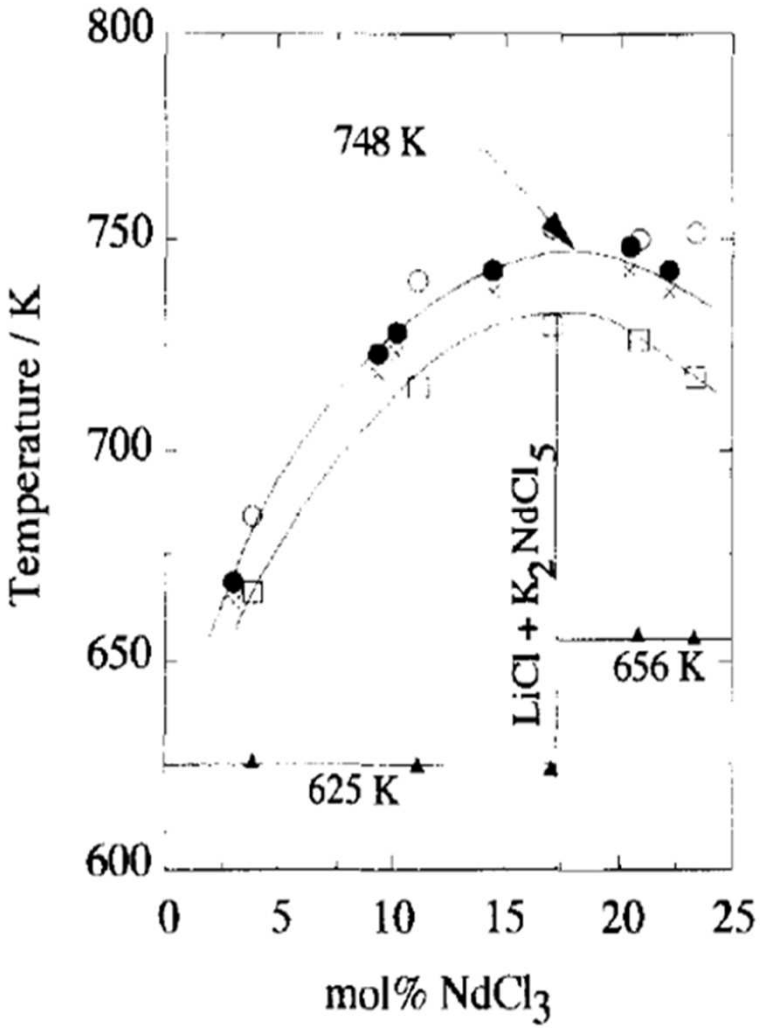

(Nakamura, K. 1994)

NaCl Concentration Study

- One clear endothermic peak on DSC scans of NaCl samples up to 30 mol%
- Visual inspection of melting process confirmed that this peak is the onset of melting
- More DSC analysis necessary to find thermal transition corresponding to liquidus temperature

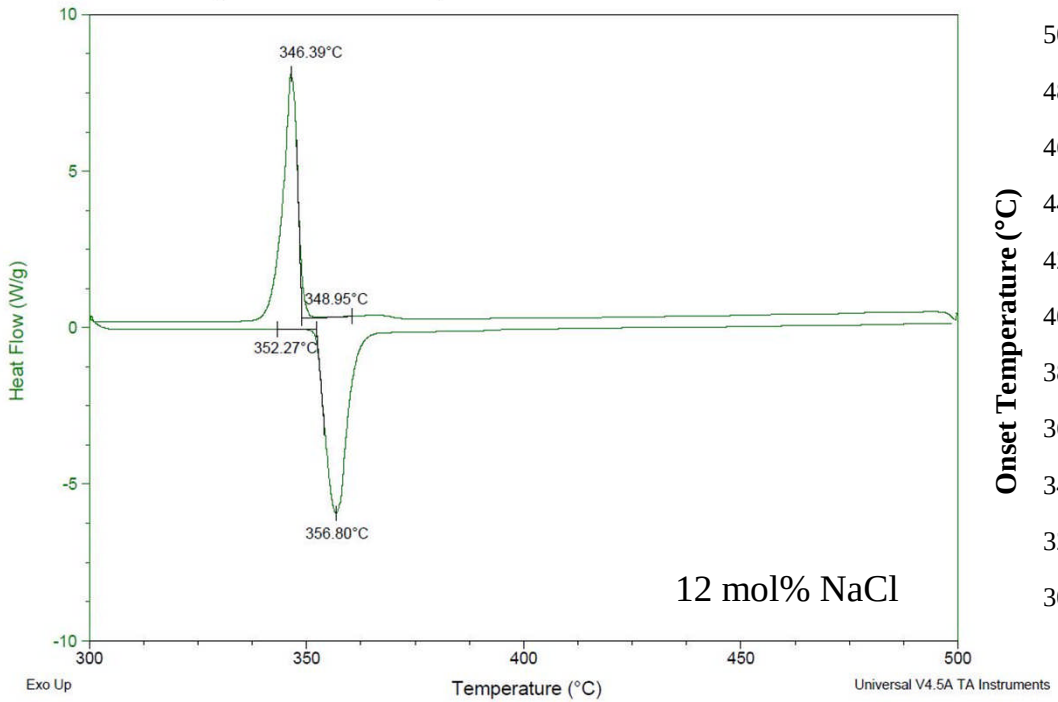

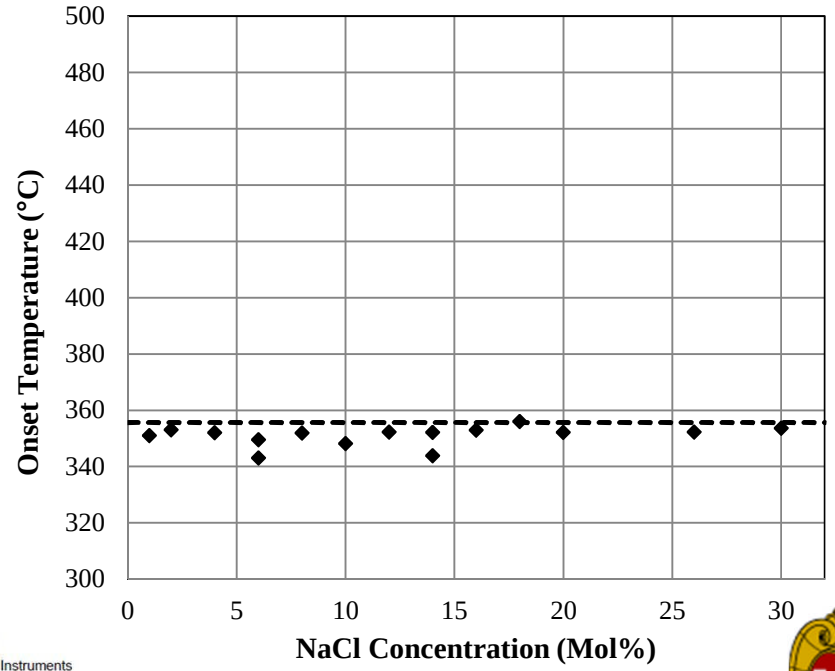

Density Measurements

Molten Salt Density Measurements

DEPARTMENT OF
Engineering Physics
College of Engineering
University of Wisconsin-Madison

- Based on Archimedean Principle
  - Buoyant force exerted on an immersed body is equal to the mass of the fluid displaced by the body

$$\rho = -\frac{\overbrace{(M_i - M_0)}^{\text{Mass of fluid}}}{V_b\underbrace{\{1 + 3C(T - T_0)\}}_{\text{Thermal expansion}}}$$

Volume of bob (displaced fluid)

Experimental Apparatus

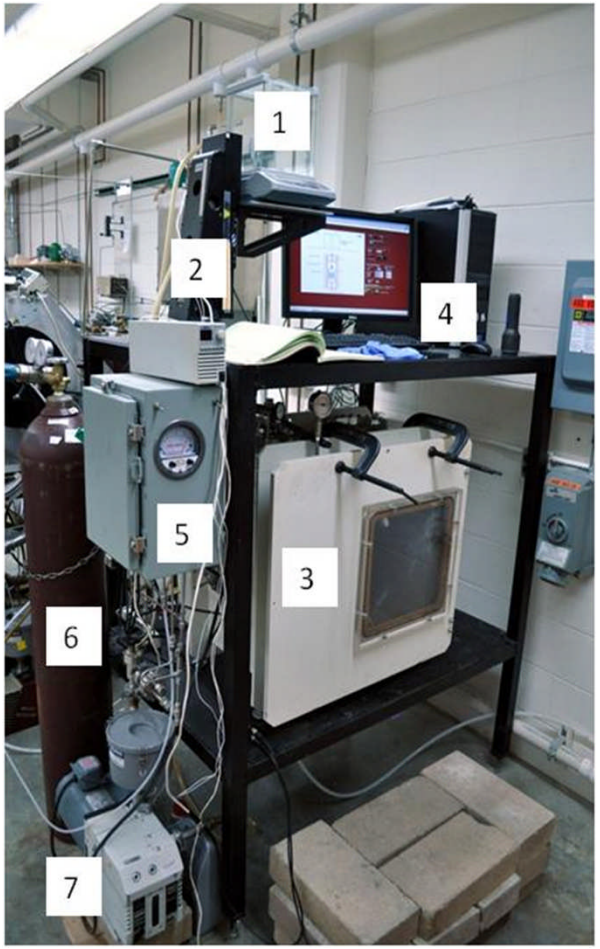

1. Analytical Balance
2. Adjustable platform
3. Sealable chamber
4. PC with LabView
5. Atmosphere control
6. Argon cylinder
7. Vacuum pump

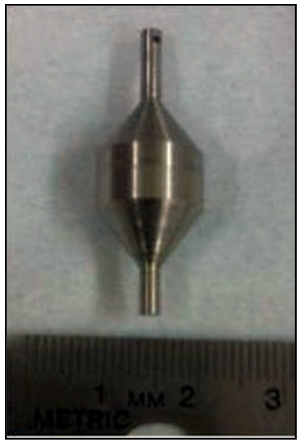

Nickel Bob

Experimental Apparatus

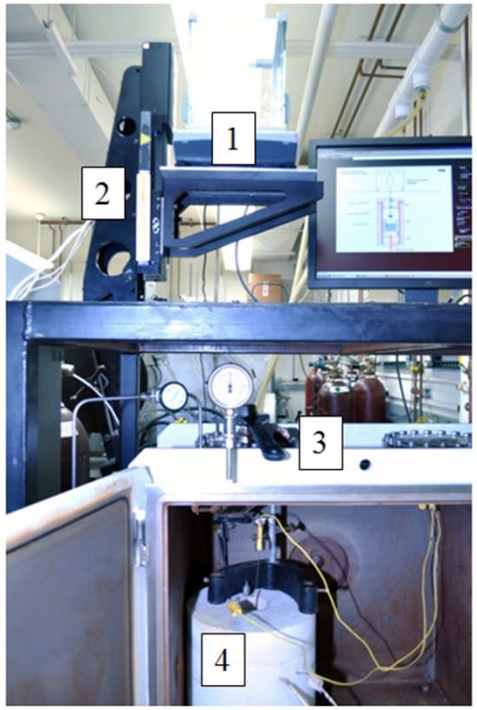

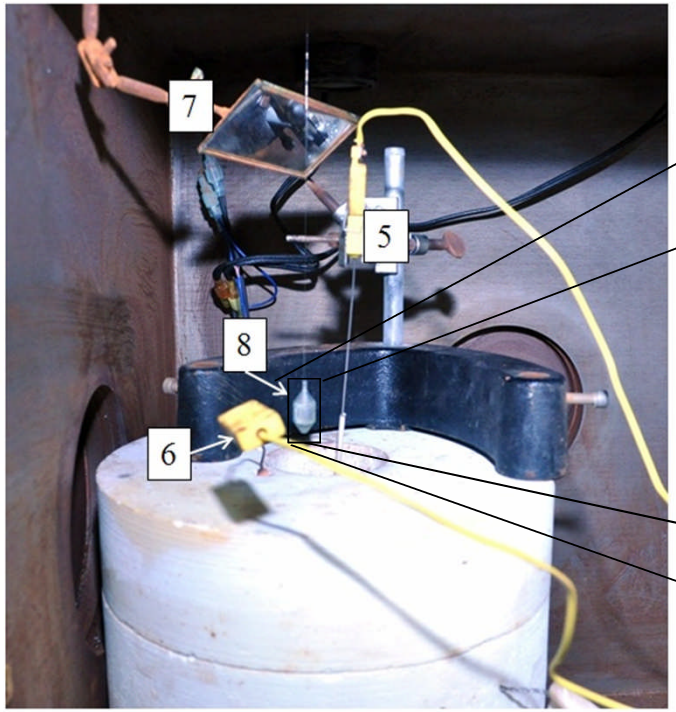

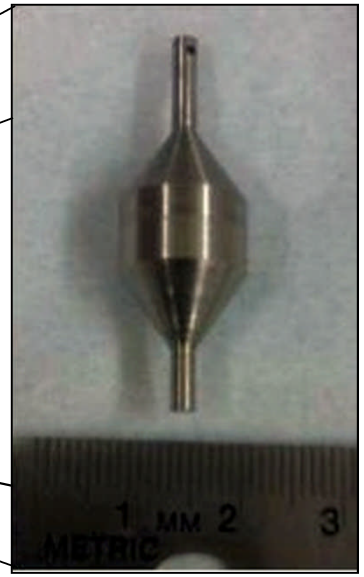

Nickel Bob

1. Analytical balance
2. Adjustable platform
3. Sealable Chamber
4. Furnace
5. Salt thermocouple
6. Heater wall thermocouple
7. Mirror
8. Nickel bob

Density Model

Theoretical density of a multi-component fluid:

$$\frac{1}{\rho_{calc}} = \sum \left(\frac{w_i}{\rho_i}\right) \longrightarrow \frac{1}{\rho_{salt,\ calc}} = \frac{w_{LiCl}}{\rho_{LiCl,500°C}} + \frac{w_{KCl}}{\rho_{KCl,\ 500°C}} + \frac{w_{LnCl_3}}{\rho_{LnCl_3,\ 500°C}}$$

Correction factor, k, applied to metal chloride densities: $\rho = kA + B(C + t)$

k = 0.99973 for monovalent chlorides

k = 0.82601 for trivalent chlorides

- k accounts for non-ideal behavior of metal chlorides in the salt (attractive and repulsive forces)
- Values determined based on measured UCl_3 data

Metal chloride	A	B	C	Density at 500°C (g/ml)
KCl	2.1359	-5.831E-04	273.15	1.6851
LiCl	1.8842	-4.328E-04	273.15	1.5496
$LaCl_3$	4.0895	7.774E-04	273.15	4.6905
$CeCl_3$	4.248	9.200E-04	273.15	4.9593
$NdCl_3$	5.0659	-1.522E-03	273.15	3.8891

Bob Volume Calibration and Initial Testing

$$\rho = -\frac{(M_i - M_0)}{V_b\{1 + 3C(T - T_0)\}}$$

- Nickel bob volume determined by weighing bob in three fluids of known density
  - DI water
  - Acetone
  - Carbon tetrachloride

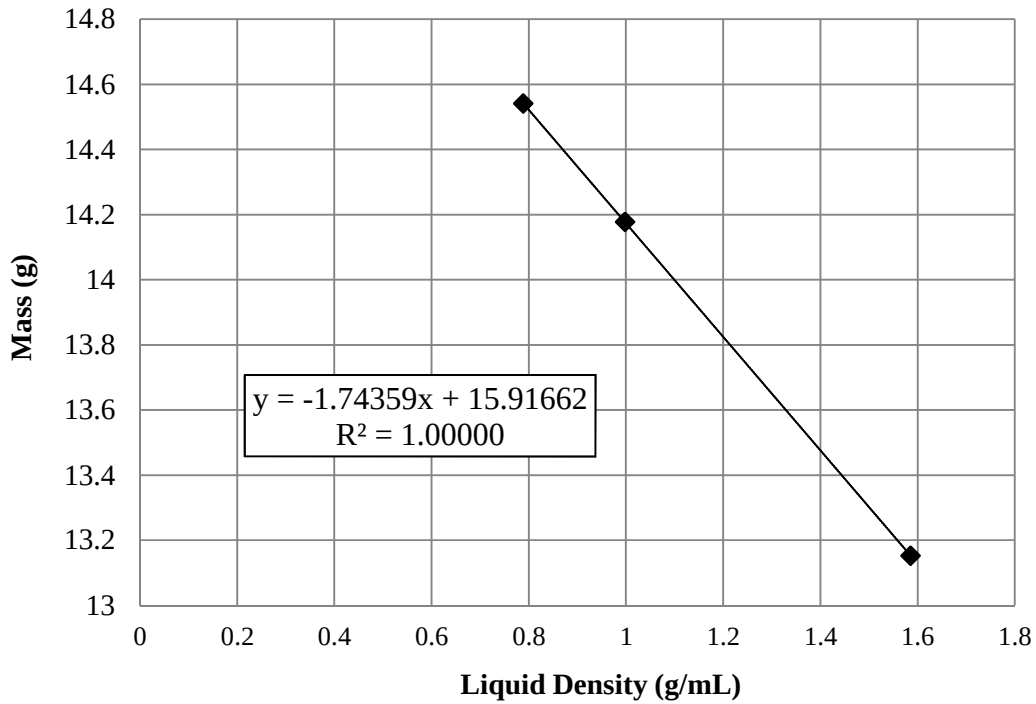

- Density of pure LiCl-KCl
  - Measured: 1.6130 g/cm^3
  - Literature: 1.6213 g/cm^3

Density Results

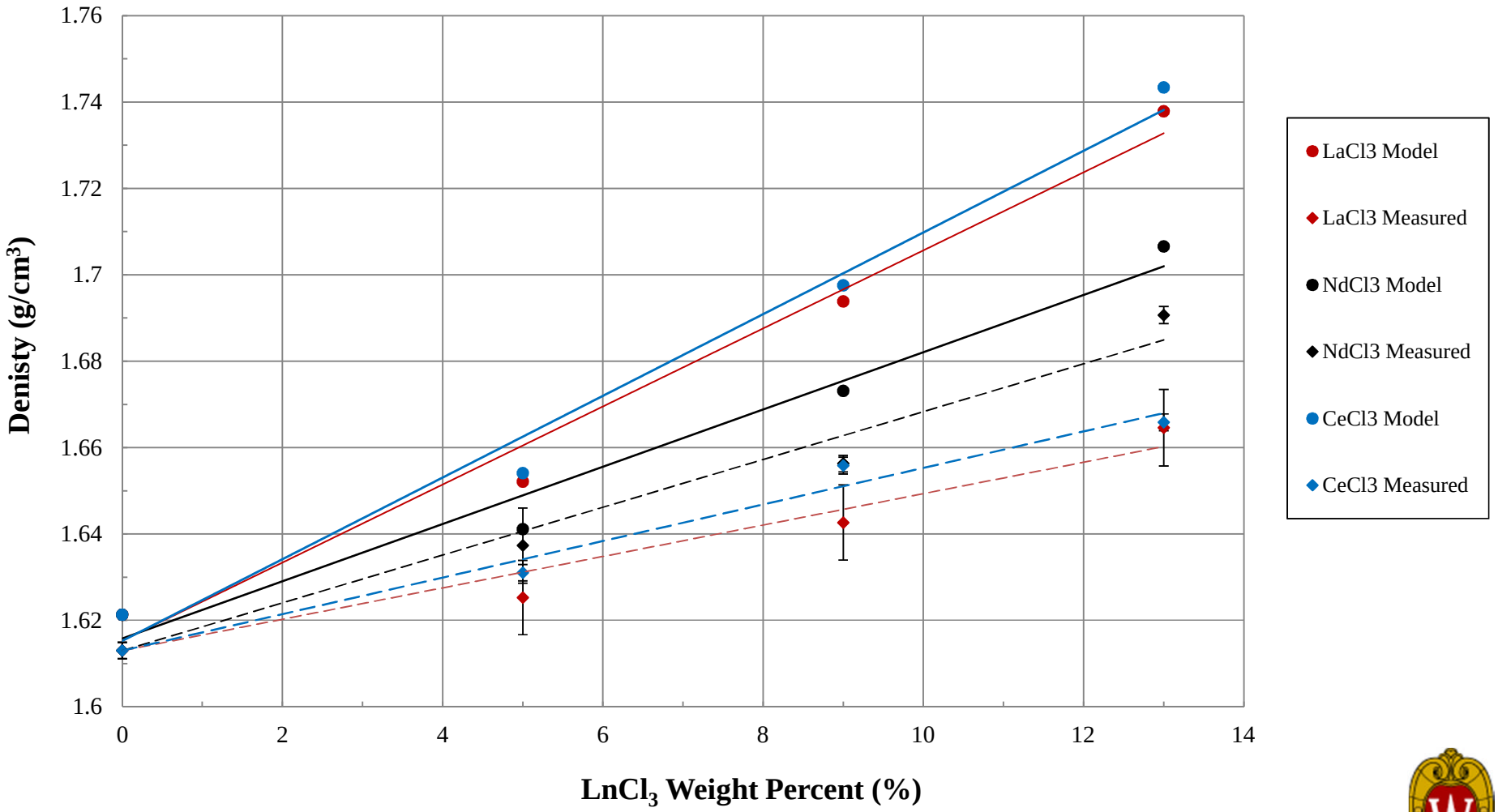

Density Results

- Measured values are within 5% of calculated values at all concentrations
- $LaCl_3$, $NdCl_3$, and $CeCl_3$ exhibit more non-ideal behavior than UCl_3 which was used to determine the k value for trivalent metal chlorides in the model

	Concentration (wt %)	Density (g/cm^3) model	Density (g/cm^3) measured	Percent Difference (%)	Measured Error (g/cm^3)
$LaCl_3$	0	1.6213	1.6130	0.51	0.0019
	5	1.6521	1.6253	1.63	0.0086
	9	1.6939	1.6427	3.02	0.0087
	13	1.7379	1.6646	4.22	0.0089
$NdCl_3$	0	1.6213	1.6130	0.51	0.0019
	5	1.6411	1.6373	0.23	0.0087
	9	1.6732	1.6563	1.01	0.0019
	13	1.7066	1.6907	0.93	0.0020
$CeCl_3$	0	1.6213	1.6130	0.51	0.0019
	5	1.6541	1.6310	1.40	0.0019
	9	1.6976	1.6558	2.46	0.0019
	13	1.7434	1.6659	4.45	0.0019

Conclusions

- Electrochemistry behavior of $DyCl_3$ and UCl_3 in LiCl-KCl
  - Characterized redox reaction mechanisms
  - Diffusion coefficient decreases as a function of metal chloride concentration
  - Added to the scientific basis for an *in situ* electrochemical probe to measure fission product buildup in the electrorefiner
  - Calculated apparent standard potentials and equilibrium potentials
- DSC analysis of LiCl-KCl-$LnCl_3$ (Ln = La, Ce, Nd) salts
  - Increases in melting point detectable at concentrations as low as ~6 mol%
  - Liquidus temperatures found to reach a maximum at approximately 20 mol%
  - The maximum liquidus temperatures for the La, Ce, and Nd phase diagrams were found to be 453, 454, and 462°C respectively
- Molten salt density measurements
  - Measured density values were less than theoretical values at all concentrations
  - Percent differences were less than 4.5% at all concentrations
  - Differences attributed to non-ideal mixing behavior

Acknowledgements

Thank you to Prof. Supathorn Phongikaroon, Robert Hoover, Michael Shaltry (University of Idaho), and other CAES staff for allowing the use of their facilities to support the uranium electrochemistry work.

This material is based upon work supported by Battelle Energy Alliance Subcontract No. 00088757 under DOE prime contract DE-AC07-05ID14517.

Thank you for your attention

Questions?

- Extra Slides Not Used after this point

$LnCl_x$ Concentration Determination: ASV Working Curve

DEPARTMENT OF Engineering Physics
College of Engineering University of Wisconsin-Madison

- Similar trends were observed with $CeCl_3$ and $NdCl_3$ additions
- Slope change seems to be less pronounced, or more continuous, for $NdCl_3$ additions

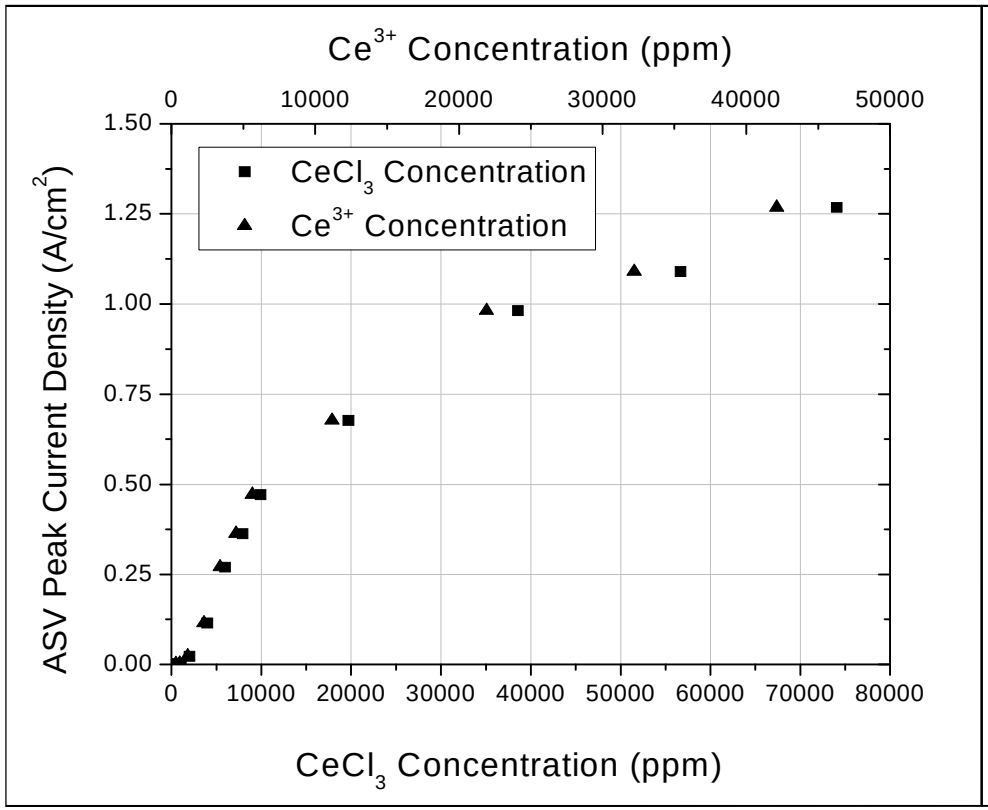

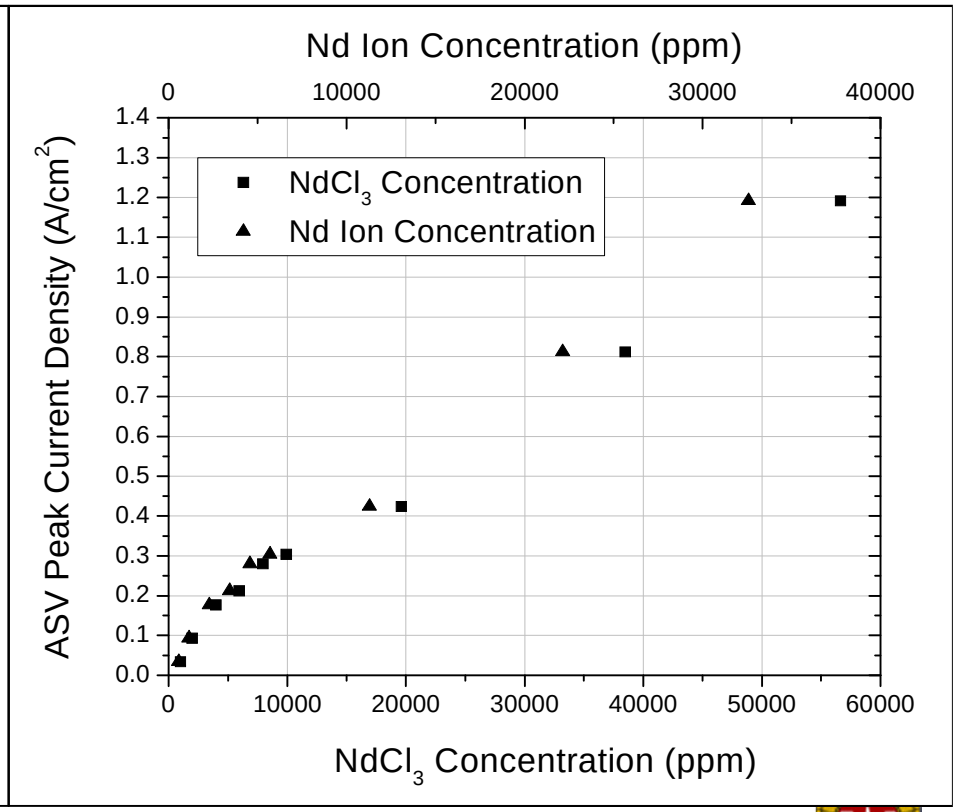

Standard Potential/Activity Coefficient of MCl_x in LiCl-KCl at 500°C

Compound	Reaction Mechanism	Apparent Standard Potential vs. $Cl^-\|Cl_2$	Comparison to literature
$LaCl_3$	$La(III) + 3e^- \leftrightarrow La$	-3.106	-3.146 (450°C)
$CeCl_3$	$Ce(III) + 3e^- \leftrightarrow Ce$	-3.066	-3.085
$NdCl_3$	$Nd(III) + e^- \leftrightarrow Nd(II)$ $Nd(II) + 2e^- \leftrightarrow Nd$	-3.081 (3→0) -2.946 (2→0)	-3.113 (450°C) -3.073 (450°C)

Compound	Activity Coefficient	Comparison to literature
$LaCl_3$	1.05×10^{-3}	5.7×10^{-3} (450°C)
$CeCl_3$	3.03×10^{-3}	1.18×10^{-2}
$NdCl_3$	3.55×10^{-4}	8.0×10^{-5} (450°C)

UCl_3 Cyclic Voltammetry

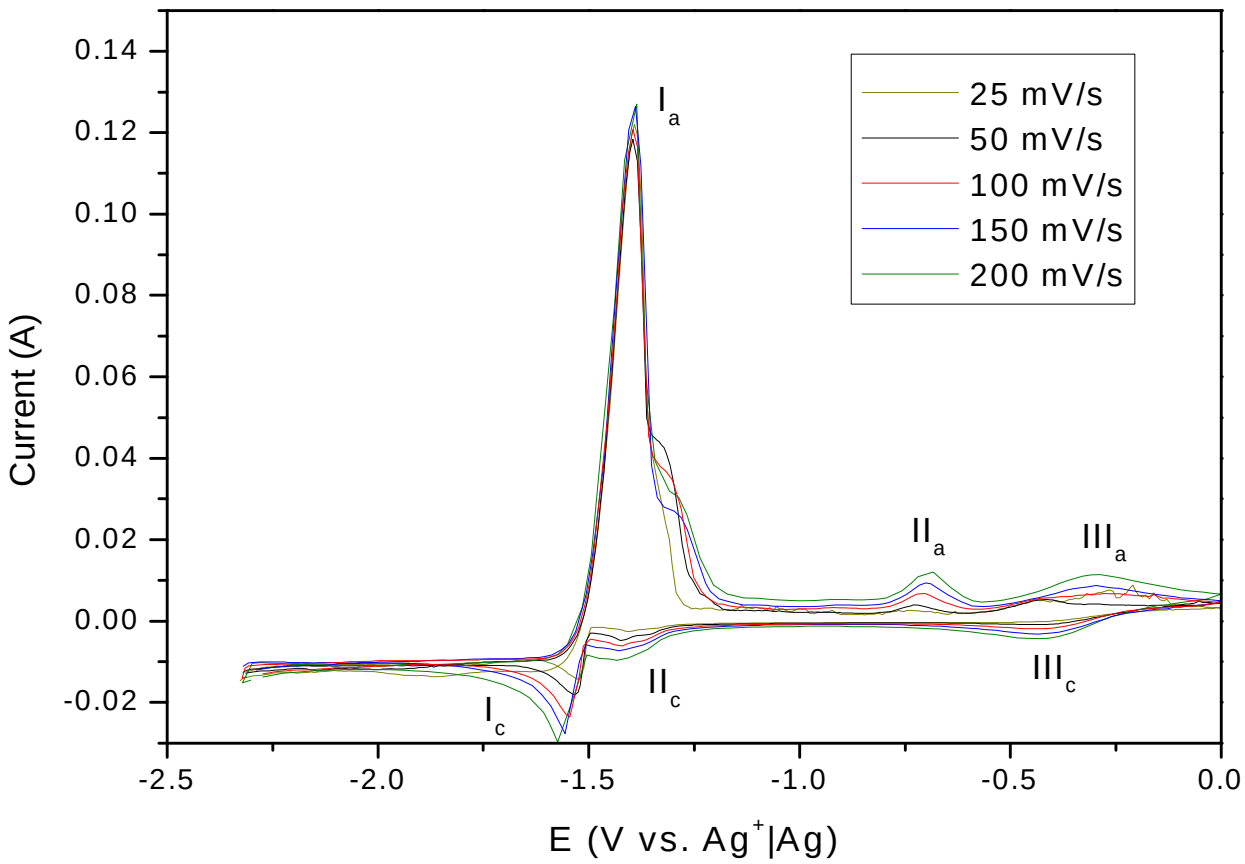

Cyclic voltammograms of LiCl-KCl eutectic containing 1 wt% UCl_3 at 500°C. -2.4V – 0V vs. 5 mol% Ag+|Ag reference

- I_c/I_a : $U^{3+} \leftrightarrow 0$
- II_c/II_a : adsorption and desorption of uranium monolayer on WE
- III_c/III_a :$U^{4+} \leftrightarrow U^{3+}$

UCl_3 CV: I_a/I_c Reversibility and Reaction Mechanism

DEPARTMENT OF
Engineering Physics
College of Engineering
University of Wisconsin-Madison

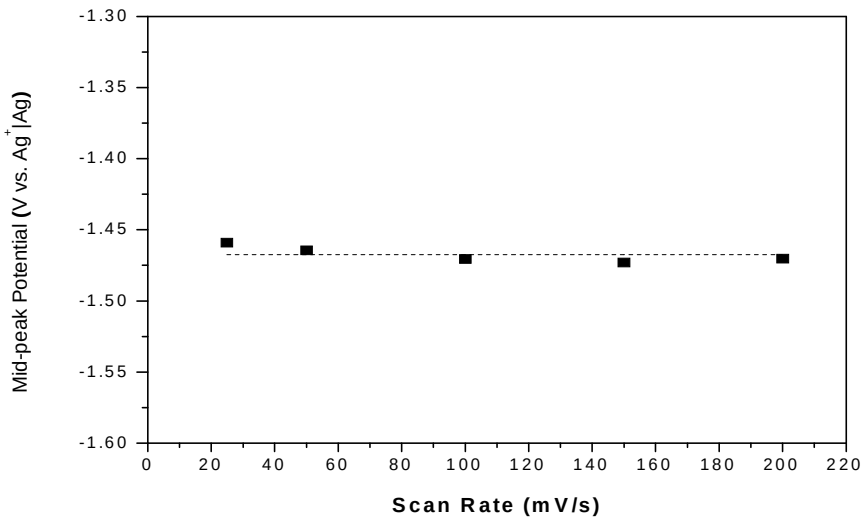

- Nonlinear relationship between anodic peak height and square root of scan rate
- Peak separation 2-3 times theoretical value
- $U^{3+} \leftrightarrow 0$ reaction is quasi-reversible

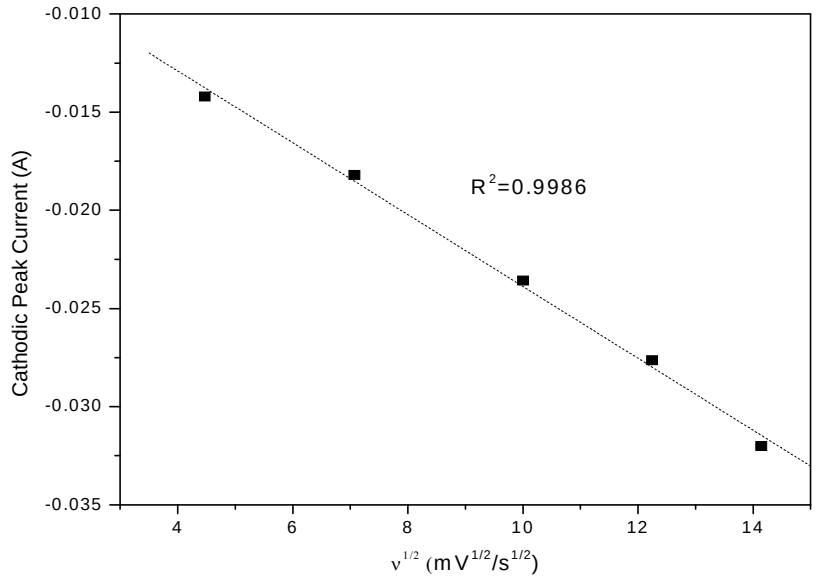

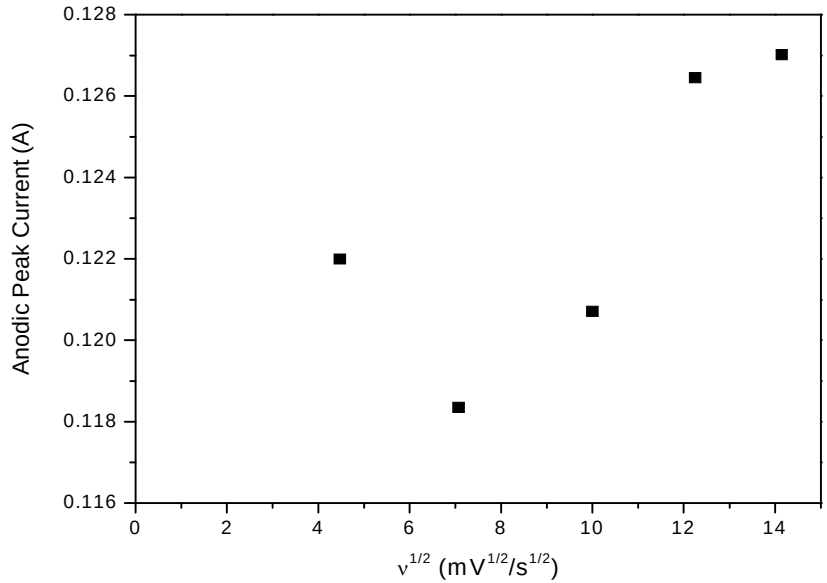

UCl_3 CV: II_a/II_c Reversibility and Reaction Mechanism

Peak separation voltage, ΔE, for peaks II_a and II_c at various scan rates.

	ΔE (V)	
Scan Rate (mV/s)	Measured	Calculated
25	0.135	0.051
50	0.139	0.051
100	0.150	0.051
150	0.168	0.051
200	0.167	0.051

- The peak separation voltage for a reversible redox process:
  - $\Delta E = 2.3\ RT/nF$
- Large peak separation indicates irreversible behavior
- Peaks II_a and II_c the results of adsorption and desorption of uranium monolayer on the tungsten WE

UCl_3 CV: III_a/III_c Reversibility and Reaction Mechanism

DEPARTMENT OF Engineering Physics
College of Engineering University of Wisconsin-Madison

- Linear relationship between anodic and cathodic peak height and square root of scan rate
- Little variation in mid-peak potential
- Peak separation values agree well with theoretical values
- n calculated to be 1.04
- U^{4+}/U^{3+} reaction is reversible

	ΔE (V)	
Scan Rate (mV/s)	Measured	Calculated
50	0.015	0.153
100	0.166	0.153
150	0.136	0.153
200	0.144	0.153

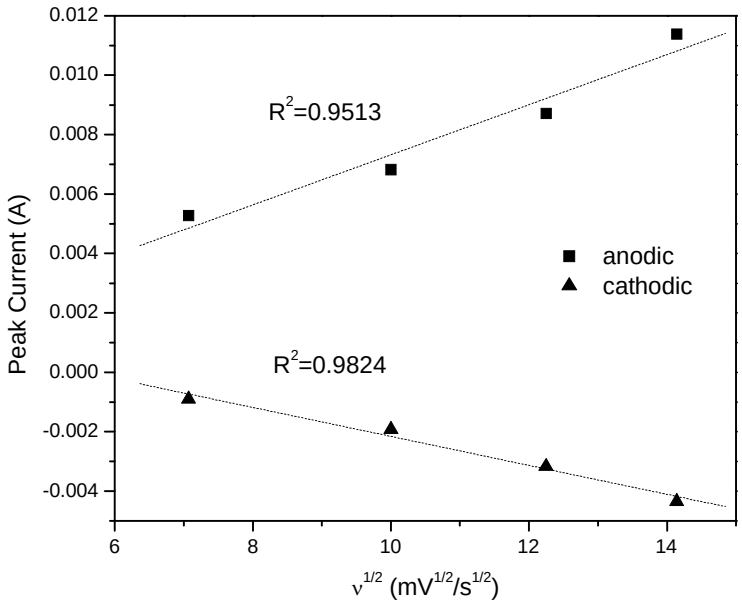

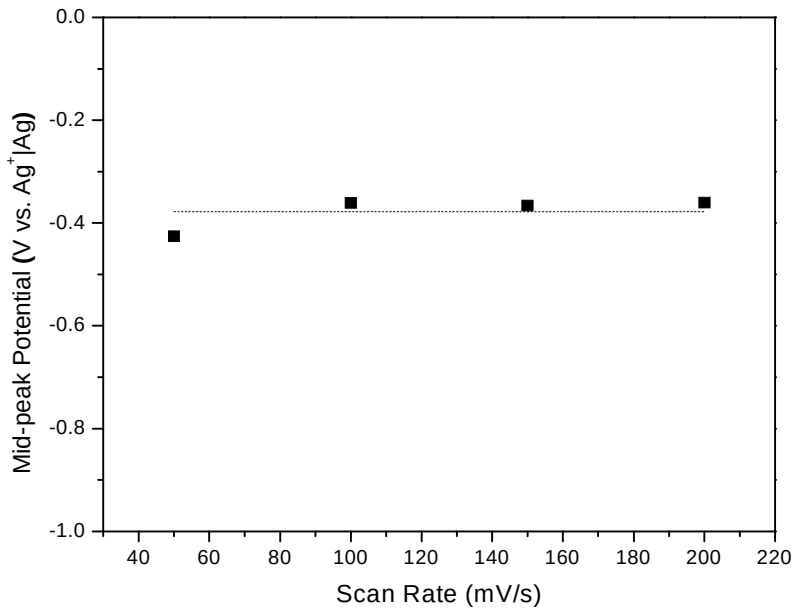

Ionic Diffusion Coefficients in LiCl-KCl at 500°C

DEPARTMENT OF
Engineering Physics
College of Engineering
University of Wisconsin-Madison

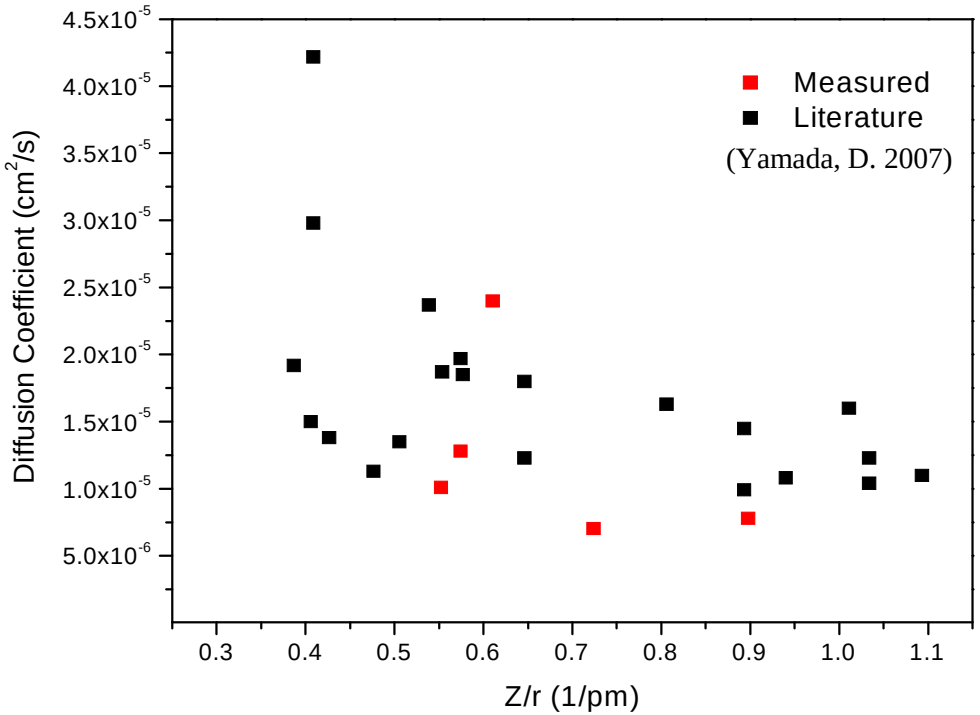

Element	Diffusion coefficient (cm^2/s)	Ionic radius, r (pm)	Z	Z/r (1/pm)
La(III)	1.01E-05	103.2	57	0.552
Ce(III)	1.28E-05	101	58	0.574
Nd(III)	2.40E-05	98.3	60	0.610
Dy(III)	7.03E-06	91.2	66	0.724
U(III)	7.79E-06	102.5	92	0.898

- Increased ionic interaction at high concentrations causes a decreases in diffusion coefficient
- Ionic potential, Z/r, quantifies how strongly an ion will interact with other ions
- Ions with higher potential have slightly lower diffusion coefficients

Anodic Stripping Voltammetry: Example

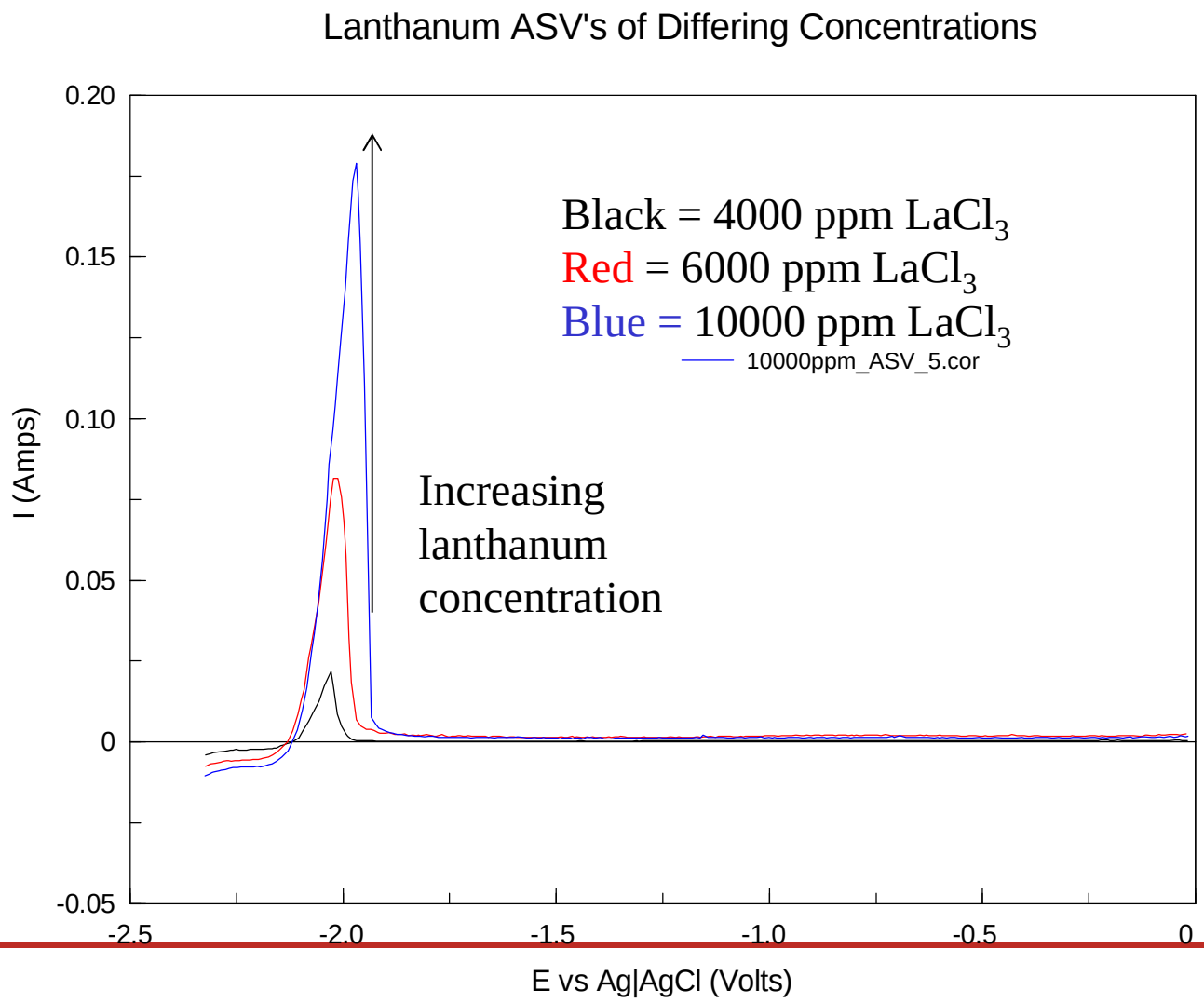

Chronopotentiometry: Example

For a reversible system: Sand Equation $$i\sqrt{\tau} = \frac{nF\,C_{M^{n+}}A\sqrt{\pi D_{M^{n+}}}}{2} = \text{Constant}$$

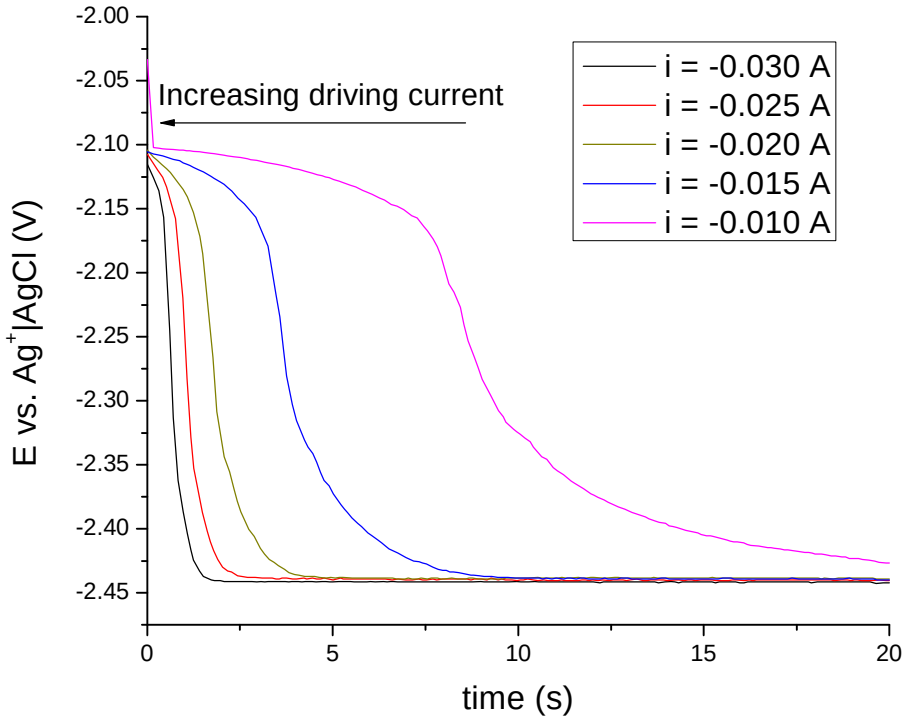

Typical chronopotentiograms of the $LaCl_3$-LiCl-KCl system. Data from $LaCl_3$-LiCl-KCl with $LaCl_3$ concentration of 0.59 wt% ($X_{LaCl3} = 1.36x10^{-3}$).

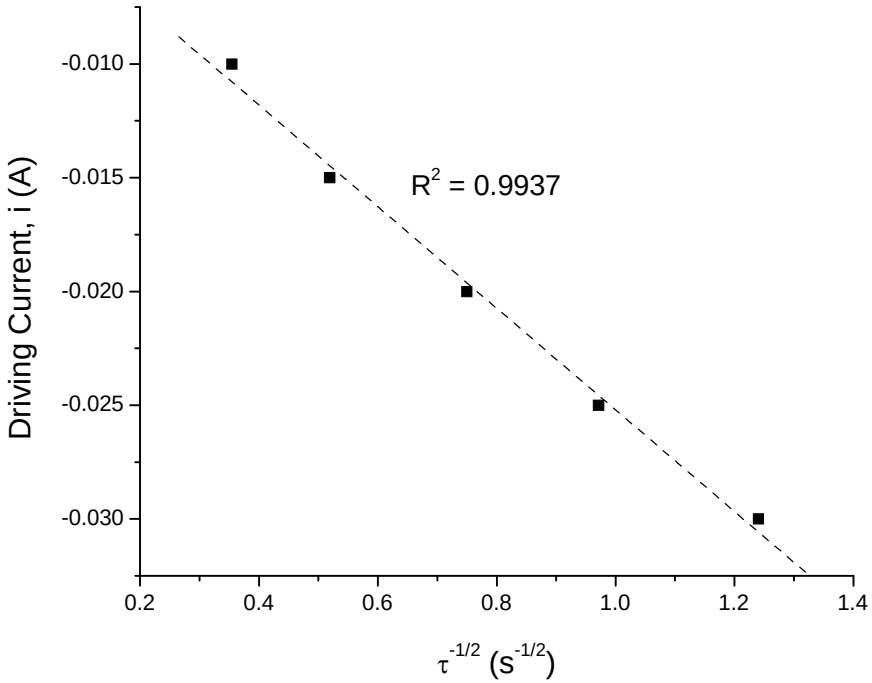

Linear dependency of driving current on $t^{-1/2}$ evidencing reversibility of $LaCl_3$-LiCl-KCl with $LaCl_3$ concentration of 0.59 wt% ($X_{LaCl3} = 1.36x10^{-3}$).

Diffusion Coefficient of $LnCl_x$ in LiCl-KCl at 500°C

DEPARTMENT OF
Engineering Physics
College of Engineering
University of Wisconsin-Madison

- Once again, similar trends were observed with $CeCl_3$ and $NdCl_3$ additions

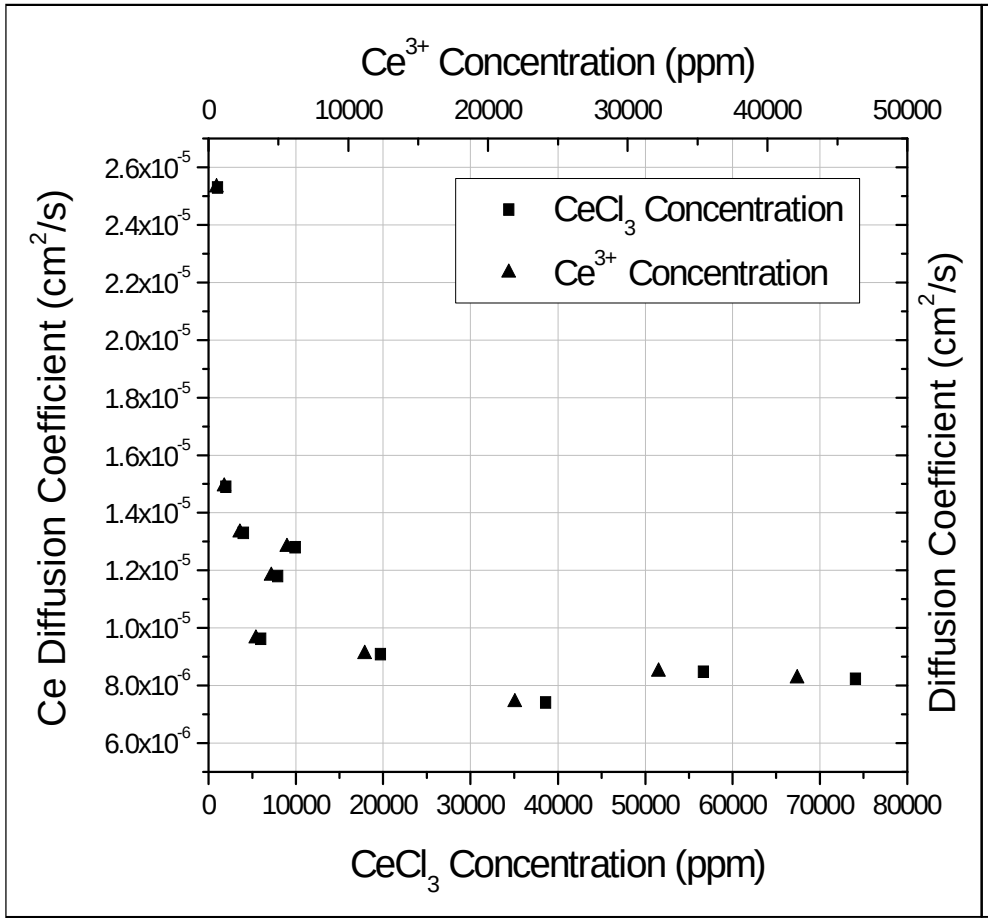

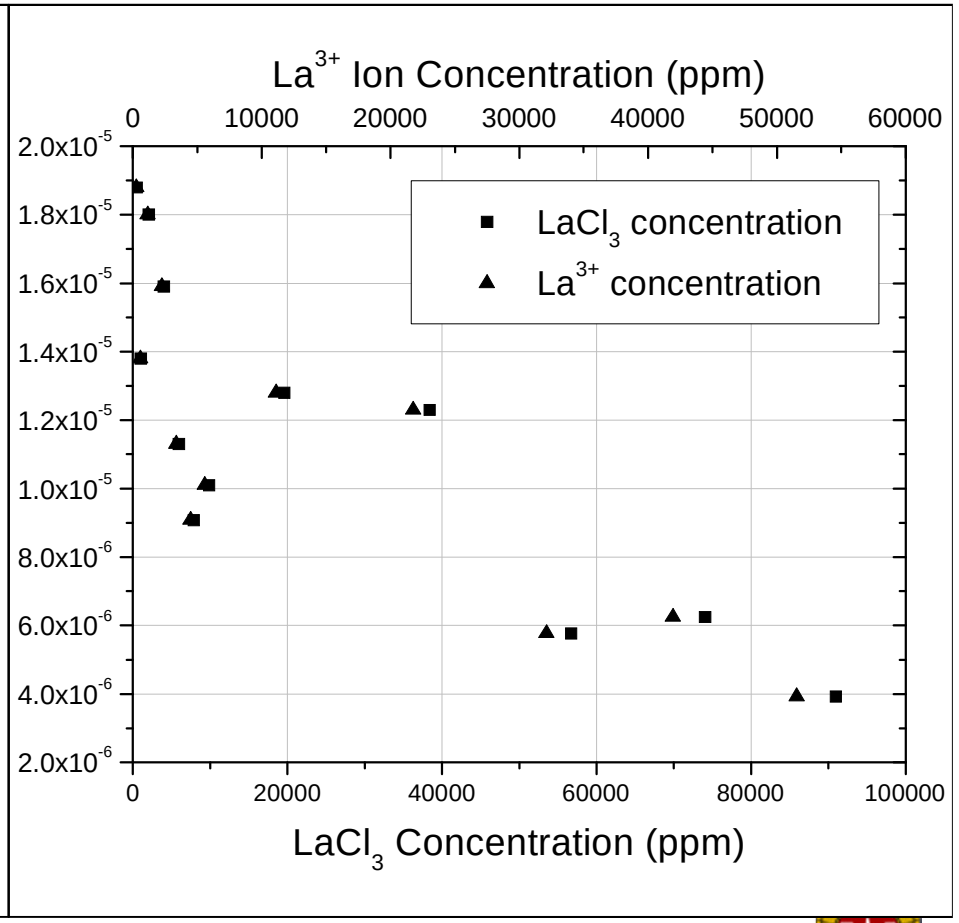

Diffusion Coefficient of $LnCl_x$ in LiCl-KCl at 500°C

- Parameters:
  - 20s @ I = 0A (Equilibrium)
  - 20s @ I = I_d
  - I_d varied for each concentration
  - Diffusion coefficient calculated with the Sand equation for each I_d
  - Average of these diffusion coefficients was plotted
- Diffusion coefficient drops off inversely with rare-earth chloride (and cation) concentration
- Possibly due to increasing cation interaction (like charges repelling)

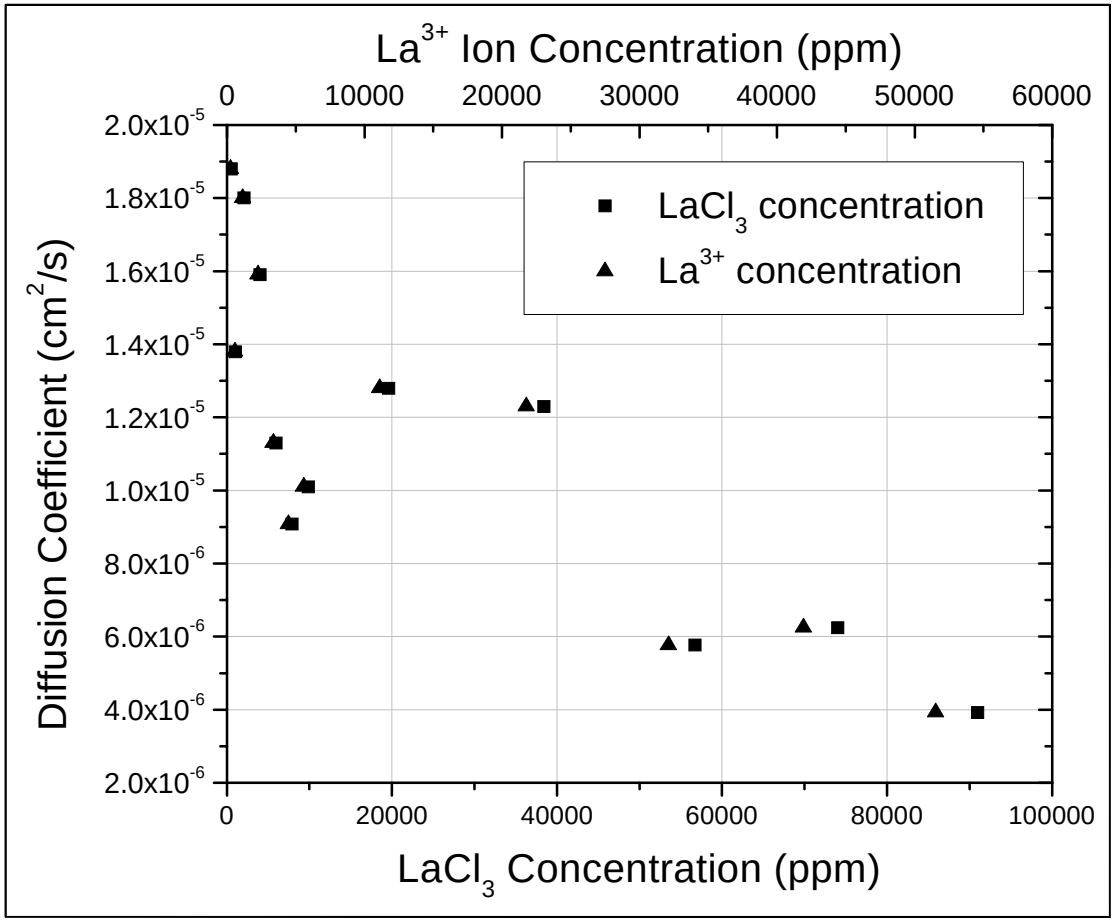

DSC Cooling Curve

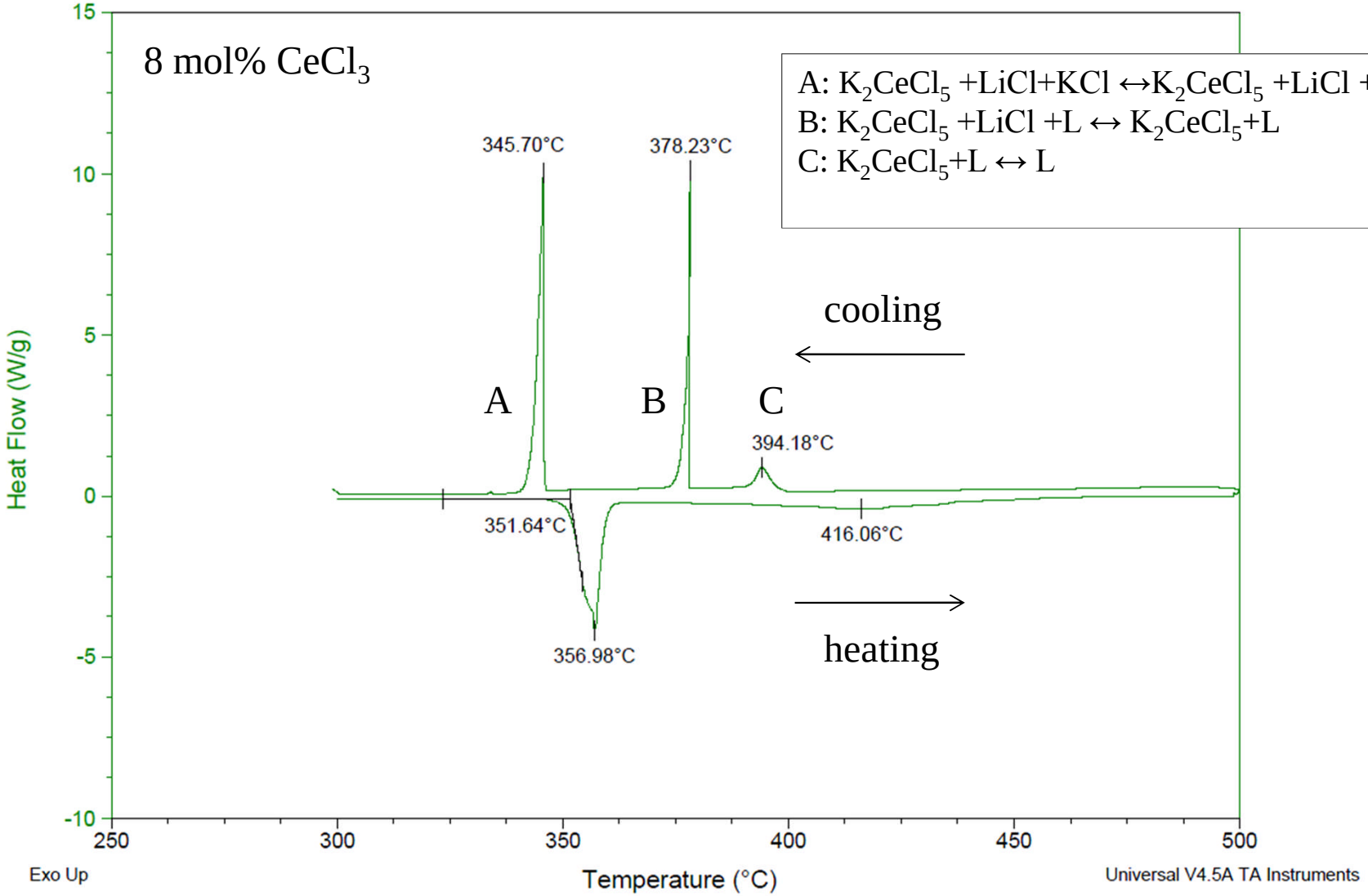

DSC – Initial Tests

- Melting point of pure LiCl-KCl found to be

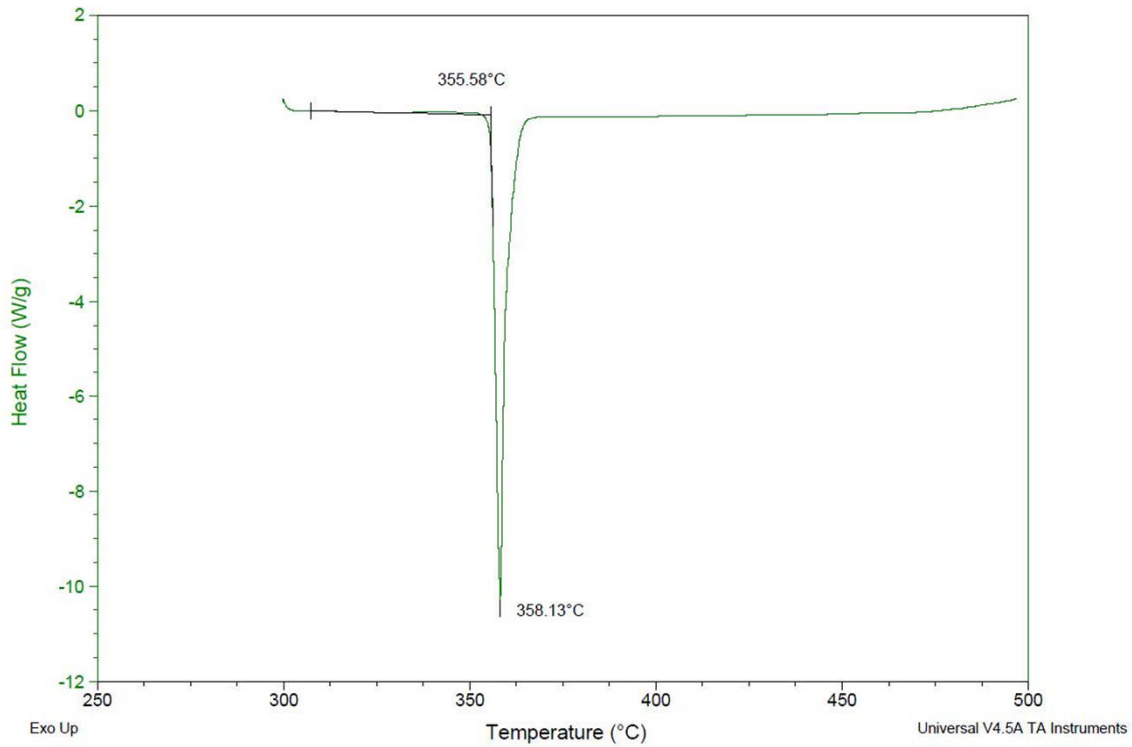

Reprocessing Motivation

- Spent fuel waste reduction
  - The nuclear industry has generated approximately 67,500 MTU of used fuel in its history
  - Long term geological waste storage has been put on hold (Yucca)
  - Increased scrutiny of spent fuel storage since Fukushima Daiichi

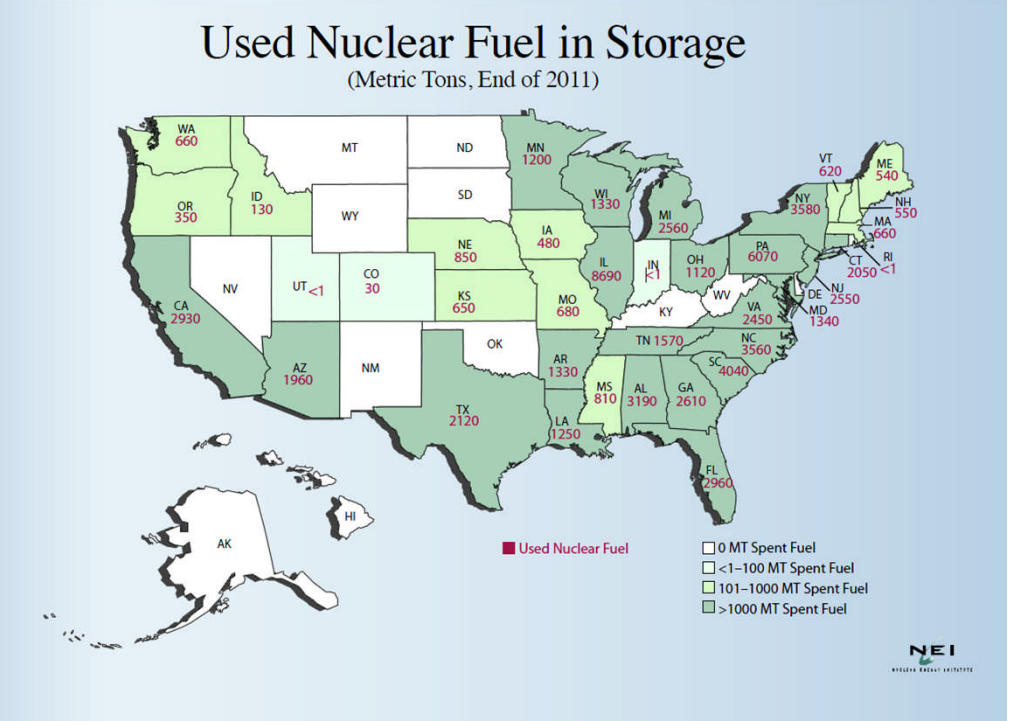

- Increased uranium utilization
  - Used fuel consists of (approximately): ~95% U^{238} , 1% U^{235}, 1 % Pu, 3% FP, with some other trace elements.
  - So about 97% of used fuel could be utilized for energy generation.

Pyroprocessing Overview

- Pyroprocessing is a method of reprocessing used nuclear fuel that involves electrochemically dissolving used fuel into LiCl-KCl eutectic, then uranium is selectively extracted using an electrodeposition process
  - Smaller waste streams and physical footprint than conventional PUREX process
  - Absence of pure plutonium stream reduces proliferation concerns

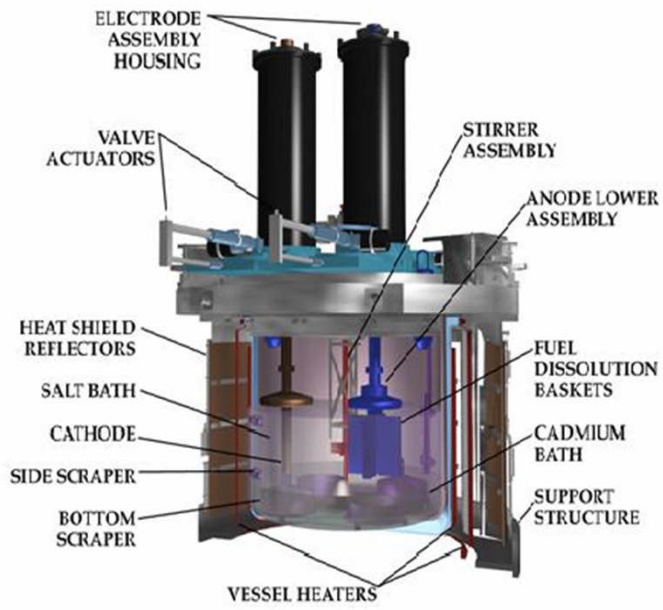

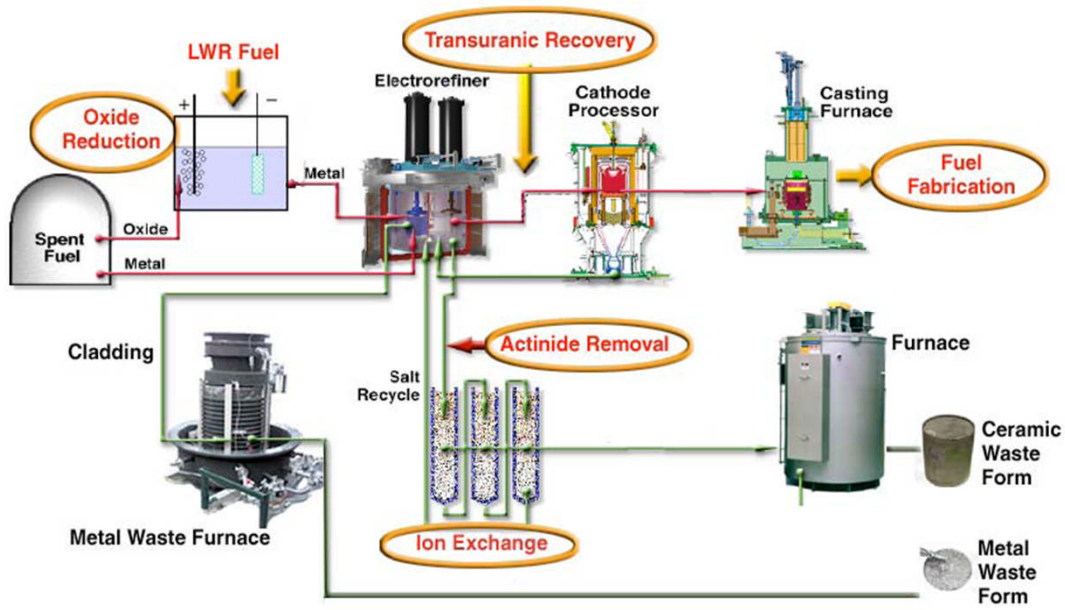

http://spectrum.ieee.org/image/37182

Mark IV Electrorefiner

- Pyroprocessing is used to process used EBR-II fuel at Idaho National Laboratory
- Chopped EBR-II driver fuel pins (U-Zr alloy in stainless steel cladding bonded with sodium) are placed in the anode dissolution basket
- Dissolved uranium is reduced onto a cylindrical steel cathode
- Fission products, lanthanides, and sodium accumulate in salt as electrorefining progress

Mark-IV Electrorefiner

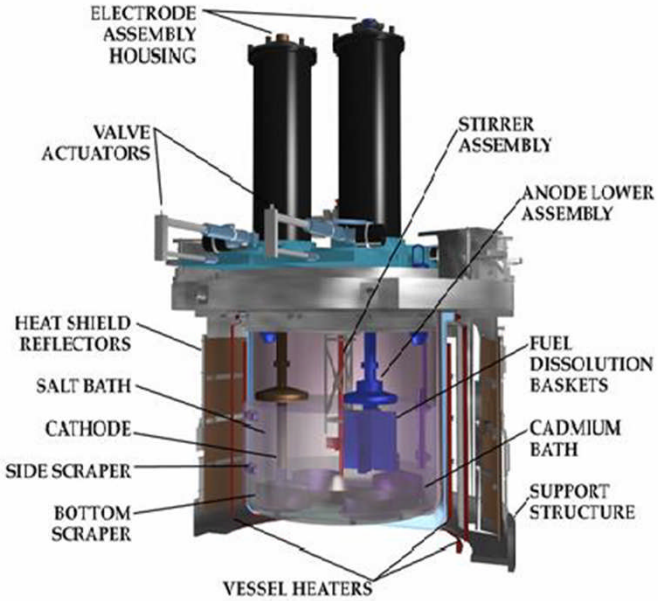

Mark-IV Electrorefiner schematic

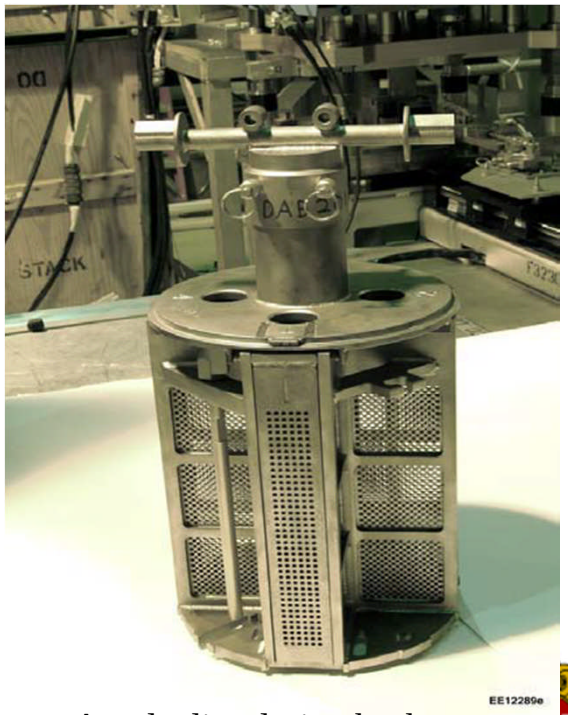

Anode dissolution basket

Electrochemical Cell

- Potentiostat
  - Capable of supplying and measuring voltage and current
  - Can force oxidation or reduction at the WE surface and measure the current or voltage response
- Cathode: electrode where reduction occurs
- Anode: reaction where oxidation occurs
- Redox reaction occurs at potential, E, defined by Nernst Equation

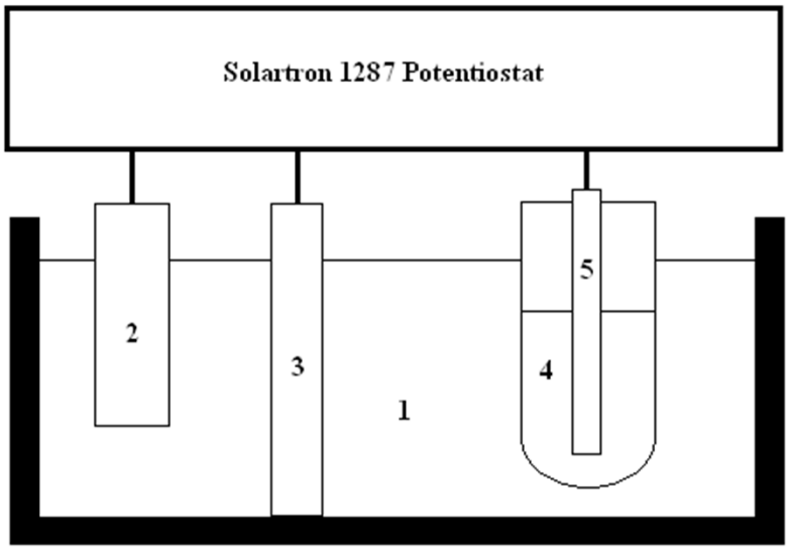

1. Molten LiCl-KCl
2. Tungsten WE
3. Glassy carbon CE
4. LiCl-KCl-AgCl (5 mol% AgCl)
5. Silver wire

Redox reaction: $O + ne^- \rightleftarrows R$

Nernst Equation: $E = E^{0\prime} - \frac{RT}{nF}\ln\left(\frac{O}{R}\right)$

Anodic Stripping Voltammetry (ASV)

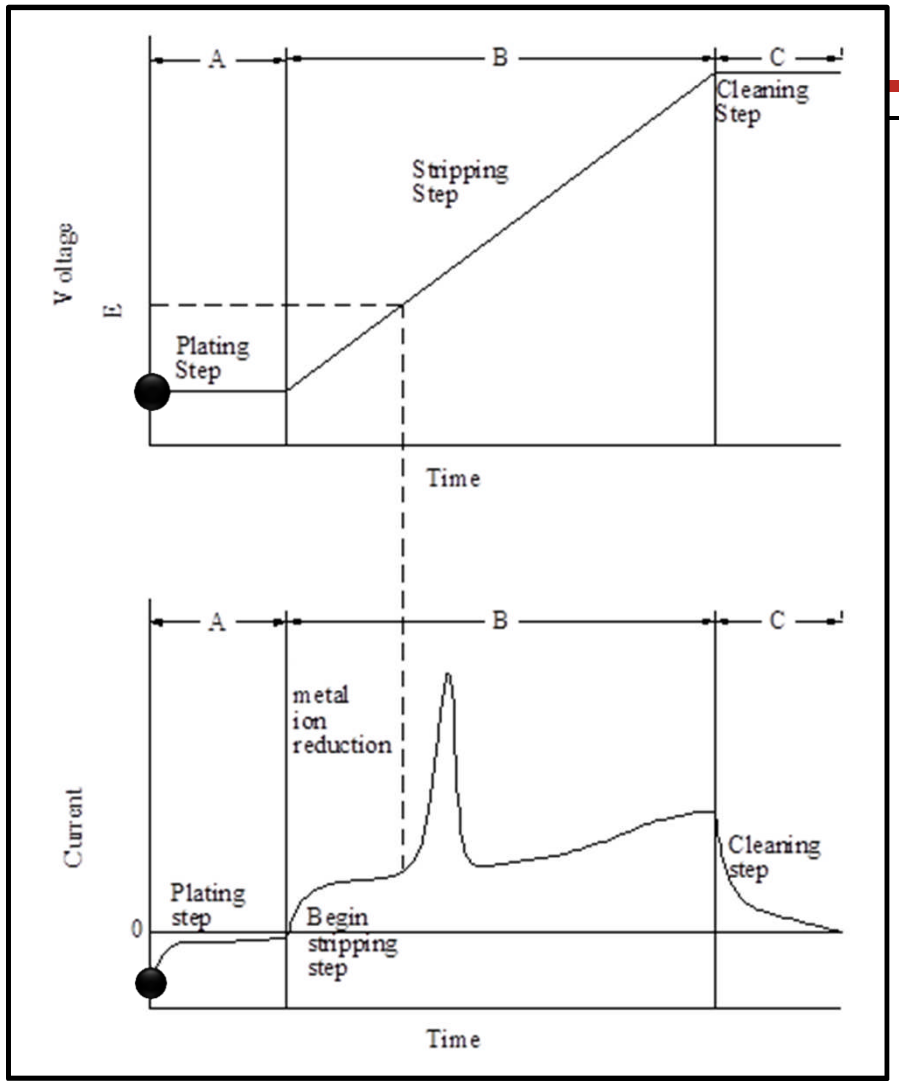

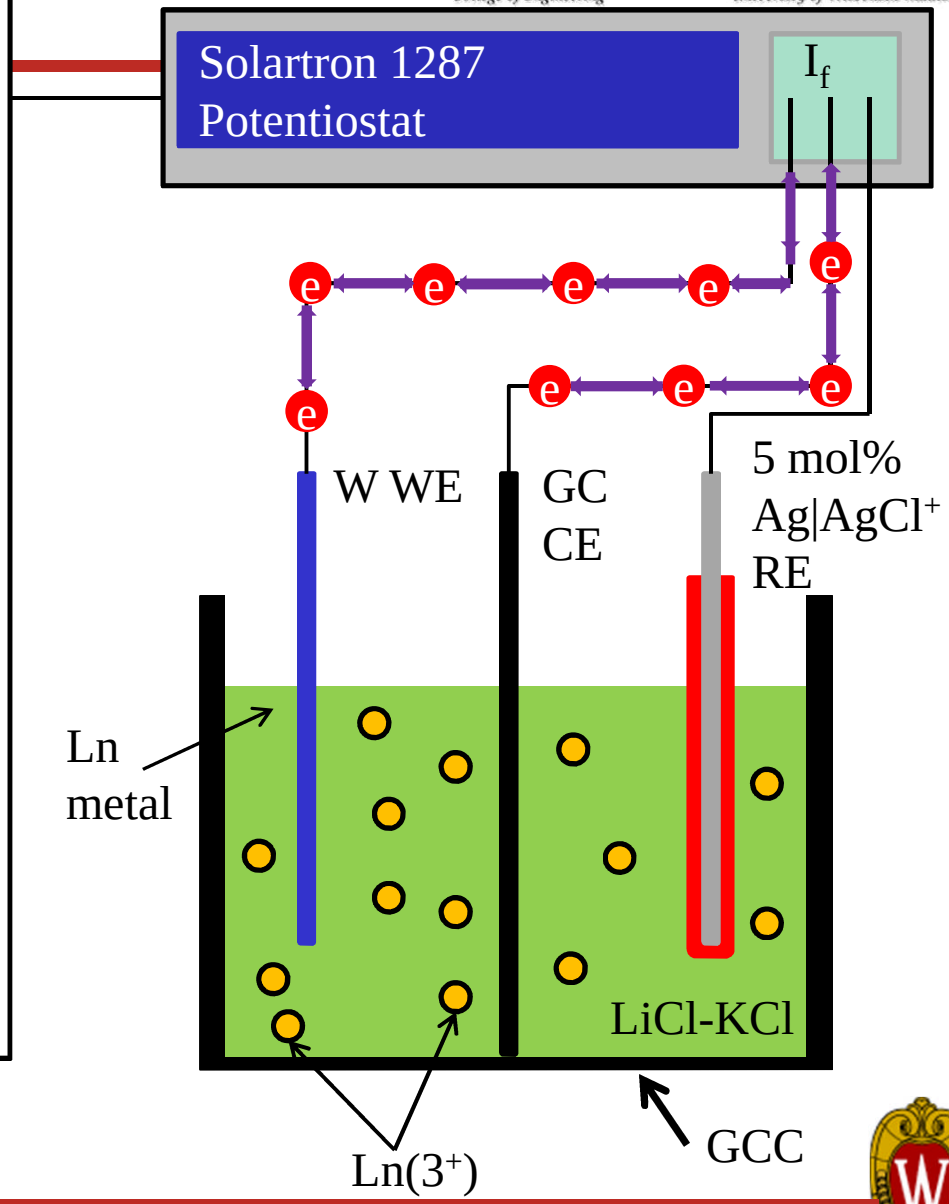

-2.3V – 0V @ 50 mV/s

Redox Reaction : $O + ne^- \leftrightarrow R$ at E_0

Cyclic Voltammetry (CV)

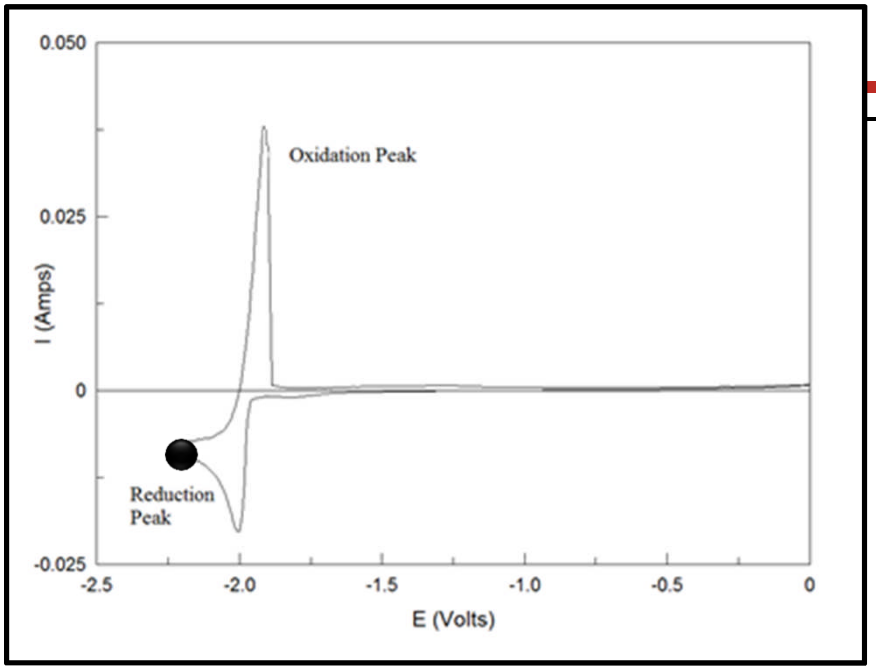

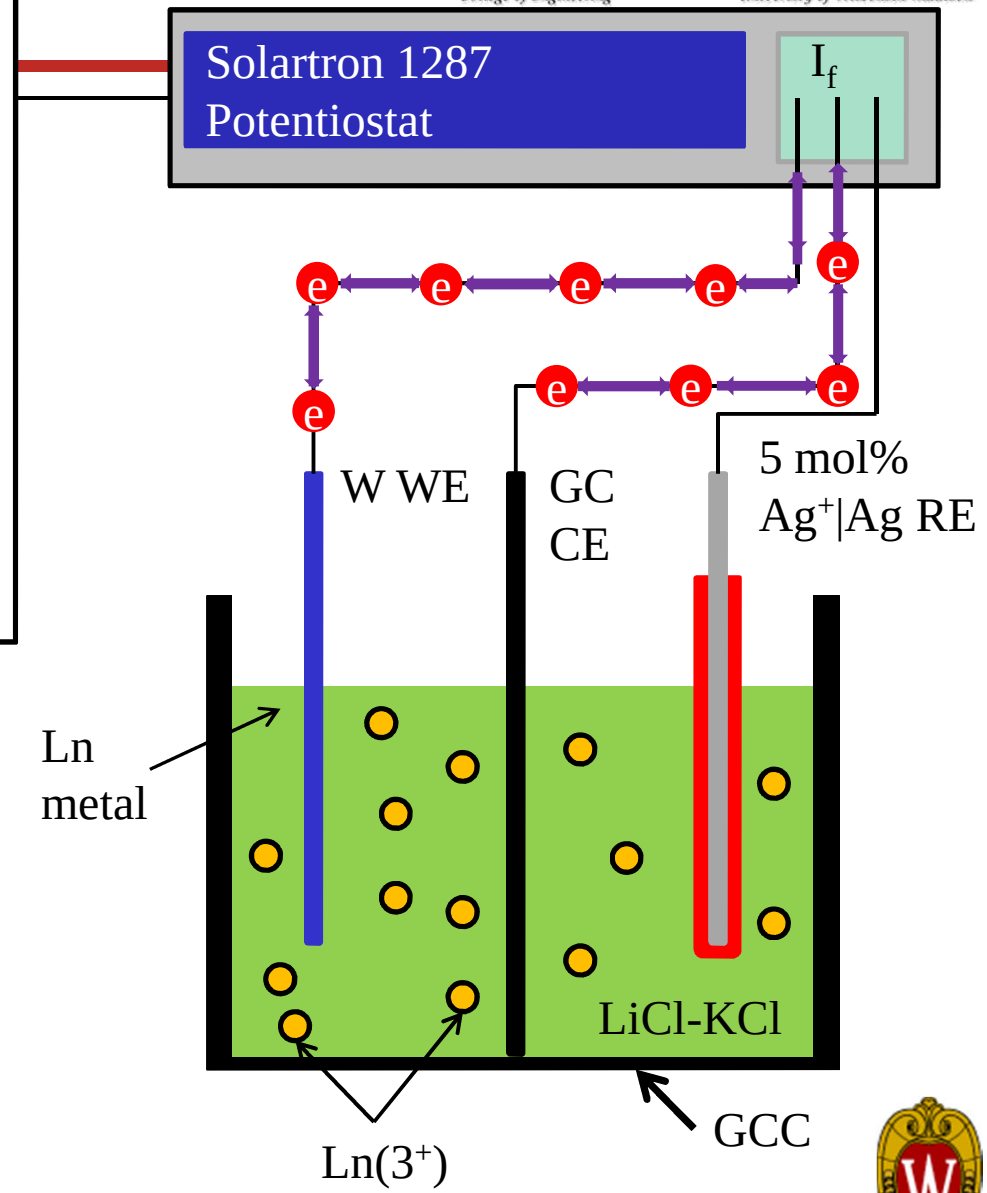

Randles-Sevcik Equation:

$$\frac{I_{p,c}}{\sqrt{v}} = 0.446(nF)^{\frac{3}{2}}(RT)^{-1/2}C_{M^{n+}}D^{1/2}S$$

I_p - Peak current (A)
n - Sweep rate (V/s)
N - Number of electrons transferred
F - Faraday constant (96485.3415 s-A/mol)
R - Universal gas constant (8.314 J/mol-K)
T - Temperature (K)
C - Concentration of the analyte in bulk solution (mol/m^3)
D - Diffusion coefficient (m^2/s)
S - Electrode surface area (m^2)

Chronopotentiometry (CP)

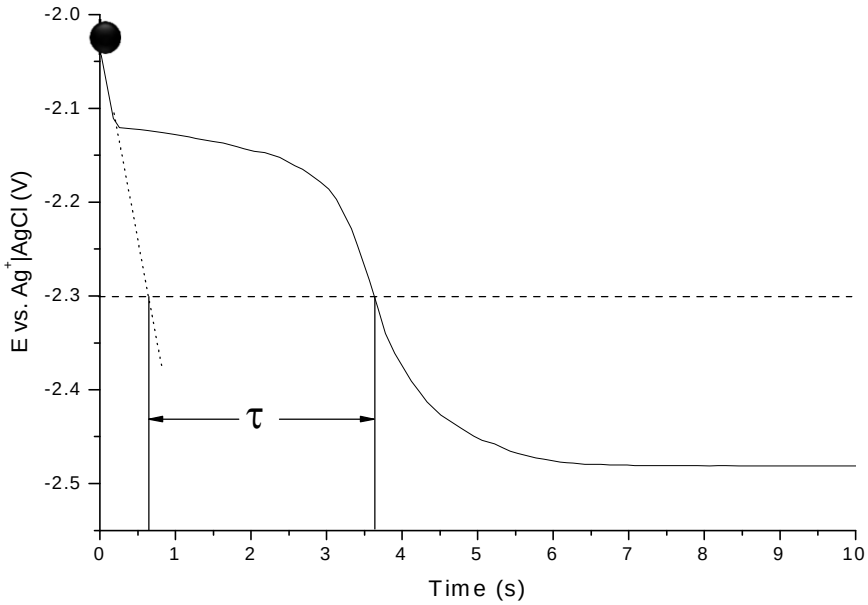

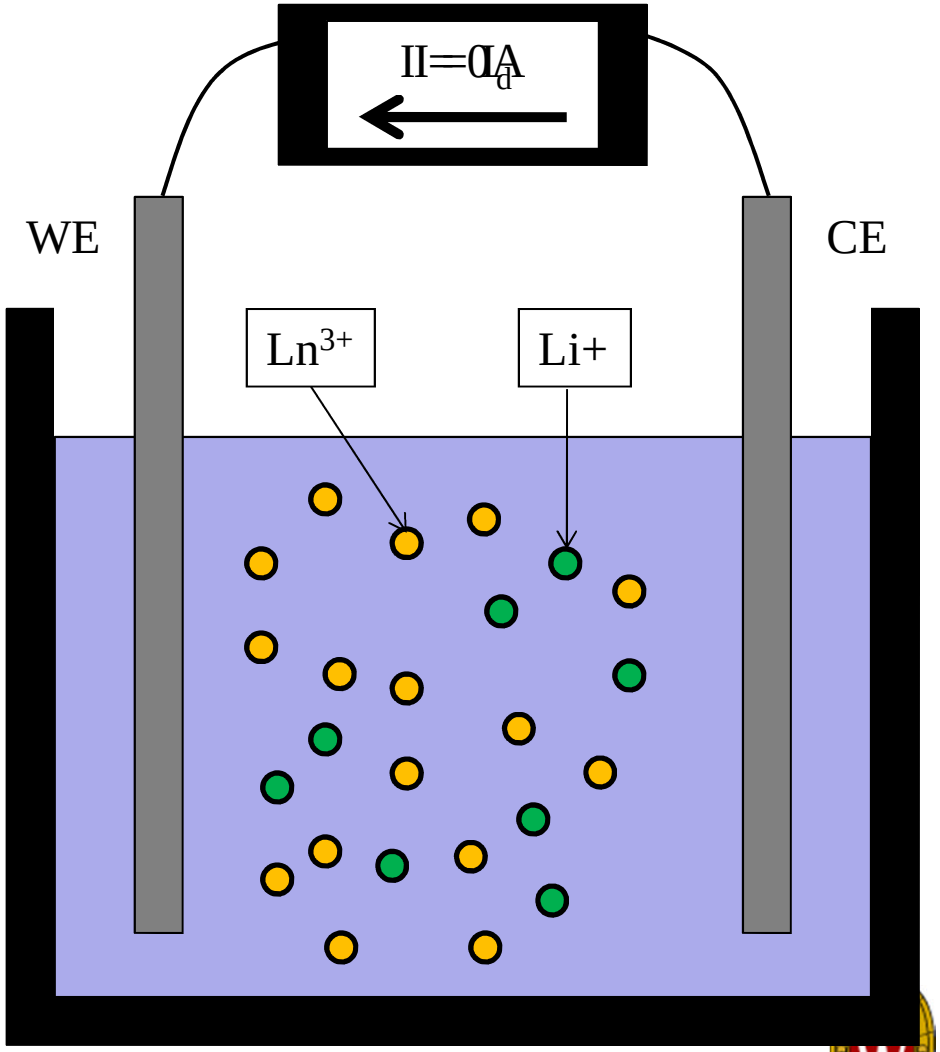

Sand equation: $$i\sqrt{\tau} = \frac{nF\,C_{M^{n+}}A\sqrt{\pi D_{M^{n+}}}}{2}$$

i – Driving current (A)
τ – Measured transition time (s)
F – Faraday constant (96485.3415 s-A/mol)
$C_{M}n+$ -- Concentration of the metal ion in the electrolyte (mol/cm^3)
A – Wetted area of the working electrode (cm^2)
D – Diffusion coefficient of the ionic metal in the bulk electrolyte (cm^2/s)
n – Numbers of electrons transferred in the redox reaction

$DyCl_3$: Confirmation of Reversibility

DEPARTMENT OF
Engineering Physics
College of Engineering
University of Wisconsin-Madison

$$\frac{I_{p,c}}{\sqrt{v}} = 0.446(nF)^{\frac{3}{2}}(RT)^{-1/2}C_{M^{n+}}D^{1/2}S$$

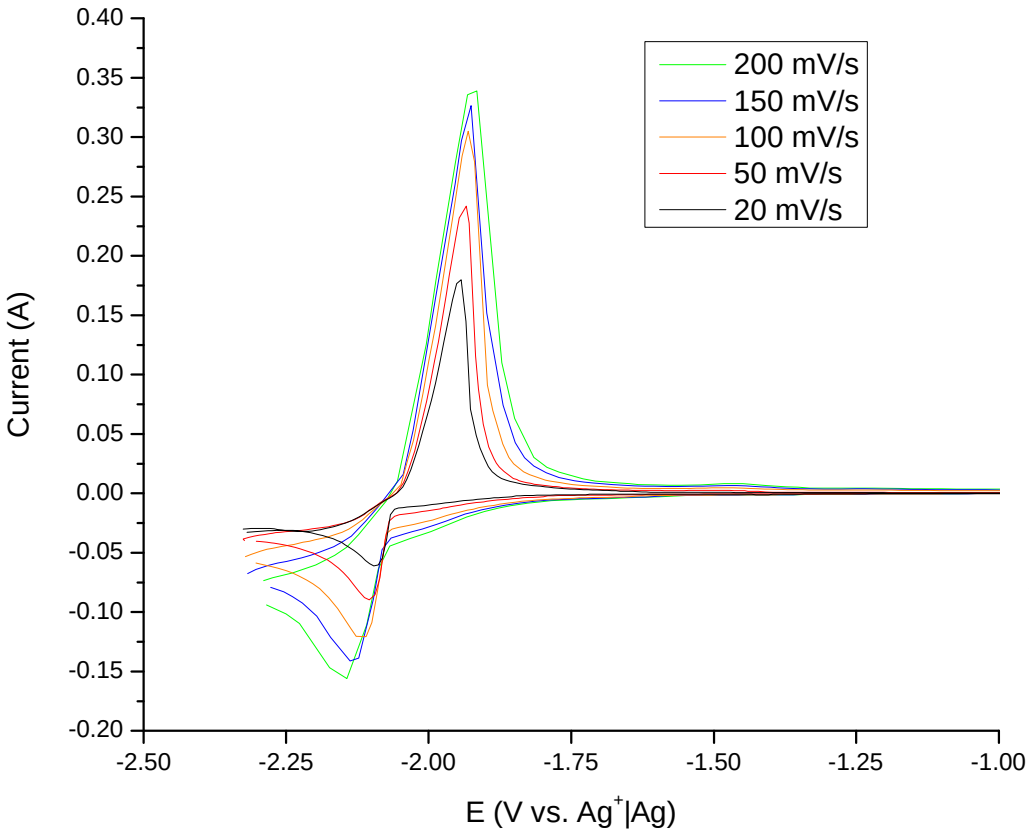

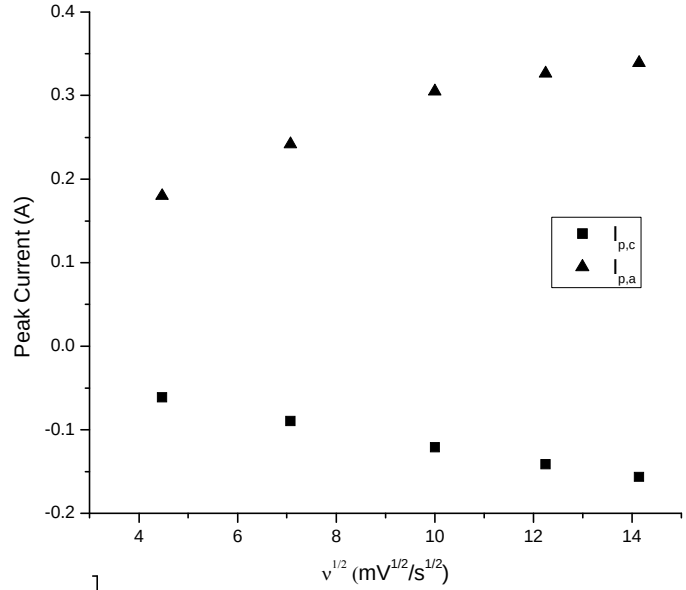

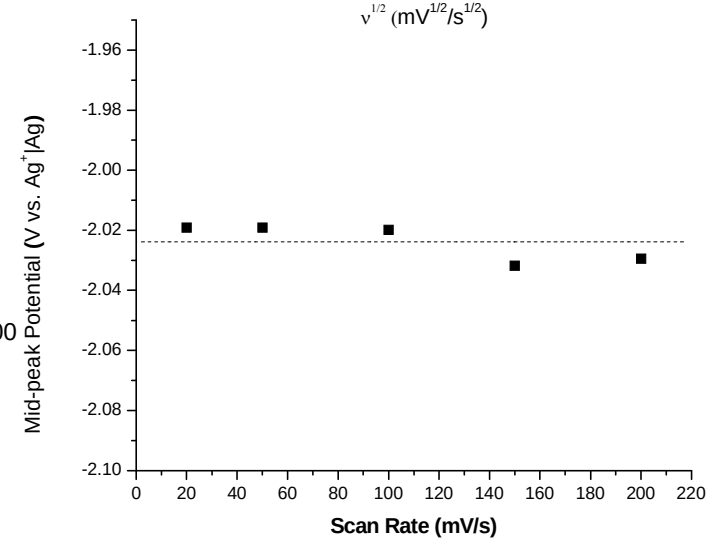

Cyclic voltammograms of 2 wt% $DyCl_3$ in LiCl-KCl at 500°C. -2.4V – 0V vs. 5 mol% $Ag^+|Ag$ RE